Drought Assessment for the Nile Basin using Meteosat Second Generation data with special emphasis on the upper Blue Nile Region

Beyene Ergogo Gadisso

March, 2007

Drought Assessment for the Nile Basin using Meteosat Second Generation data with special emphasis on the upper Blue Nile Region

By

Beyene Ergogo Gadisso

Thesis submitted to the International Institute for Geo-information Science and Earth Observation in partial fulfilment of the requirements for the degree of Master of Science in Geo-information Science and Earth Observation in Water Resources and Environmental Management Programme, Specialisation: Advanced use of Remote Sensing in Water Resources Management, Irrigation and Drainage.

Thesis Assessment Board

Chairman	Prof. Dr. Ing. W. Verhoef	WRS Department, ITC, Enshede
External Examiner	Dr. Yasir. A. Mohammed	IWMI, Nile Basin and East Africa Office
First Supervisor	Dr. B. H. P. Maathius	WRS Department, ITC, Enschede
Member	Ir. A. M. van Lieshout	WRS Department, ITC, Enschede

INTERNATIONAL INSTITUTE FOR GEO-INFORMATION SCIENCE AND EARTH OBSERVATION
ENSCHEDE, THE NETHERLANDS

Disclaimer

Abstract

Drought is considered by many to be the most complex but least understood of all natural hazards, making it difficult to predict and monitor. Because of the creeping nature of drought and its wider spatial extent, it is problematic to identify precisely the onset and severity of the event with a single indicator or index. The remedies for drought monitoring include first to identify its onset, its intensity and its change of direction, and this requires an understanding of the long-term conditions and a comparison with the current ones. Thus, large time records of remote sensing data is required.

Nile Basin is a region prone to extreme climate events such as drought and flood. Successive years of low and erratic rainfall have left large areas of the region in severe drought that resulted in crop failure, water shortage and has raised serious food security concerns for the region. Drought assessment and monitoring for the basin using conventional methods which rely on the availability of weather data are tiresome and time consuming. In contrast, the satellite-sensor data are consistently available, cost-effective and can be used to detect the onset of drought, its duration and magnitude. As timely information on the extent and severity of drought can limit impacts of drought-related losses, the near real time assessment through effective monitoring using Meteosat Second Generation (MSG) data plays a significant role in mitigating its adverse impacts.

A deviation of the current NDVI with the long-term mean NDVI, the Vegetation Condition Index (VCI) and the Temperature Condition Index (TCI) derived from the near real time MSG data were used in this study for drought detection, monitoring and predict trends of the agricultural production yield. The results clearly indicate that the temporal and spatial characteristics of drought in the Nile Basin can be detected and mapped by the DSI, VCI and TCI indices. These results were validated by in situ data, collected from part of the upper Blue Nile Basin in the so-called “Amhara” region, such as precipitation and agricultural crop yield. The validation result shows that there is a strong correlation between the satellite derived indices and the ground truth data, both precipitation and agricultural production yield for most of the districts, especially for the districts that entirely belong to the upper Blue Nile basin. Similar results could also be expected for other parts of the basin.

Key words: Drought, drought-monitoring indices, MSG-SEVIRI, near-real time monitoring, agricultural production yield and correlation.

Acknowledgements

Above all, I would like to thank the Almighty God without whose blessing, it would not have been possible all my wishes to come in to reality.

I would like to express my sincere gratitude to the Directorate of ITC for granting me this unique opportunity to study for a Master of Science degree. I am also grateful for my employer, Irrigation department of SNNPR for providing me this opportunity to pursue higher studies.

Very special thanks to my primary supervisor Dr. B.H.P. Maathius for his all-round support, excellent guidance and encouragement during my studies. His commitment all through my thesis work was overwhelming and above all, his critical comments and valuable advices helped me to take this research in the right direction. I really appreciate his keen interest and deep knowledge in the subject matter.

I am greatly indebted to my second supervisor Ir. G.N. Parodi for his help whenever I am in need of it. I appreciate his constructive comments and invaluable tips to improve my research work. It is also my immense pleasure to express my deep gratitude to Ir. Arno van Lieshout, Programme Director of Water Resources, for his support, encouragement and guidance he had been giving me during my stay in ITC.

I would like to extend my sincere gratitude to Dr. Yasir A. Mohammed from IWMI, Nile Basin and East Africa office for his critical comments which really helped me to improve my research work and all IWMI staffs for facilitating and providing me all the required supportive materials for my field campaign.

Acknowledgement is due to the EUMETSAT and RSG lab of ITC for providing me the MSG data. My appreciation goes to Mr. Worku Gashew, head of policy analysis department of the Amhara National Regional state, Bureau of Finance and Economic Development for providing the agricultural statistics data and allowing me to collect essential ancillary data from their Library. I am also indebted to the Ethiopian Meteorological Service Agency for giving me all the required weather data.

I would also like to express my appreciation to all WRS department staffs and ITC community who helped me directly or indirectly during my stay in ITC.

I would also like to extend my appreciation to all my course mates for their support, wonderful social atmosphere and lending hand for each other, especially the Ethiopian fellow friends for their encouragement in times of pressure and stress.

Last but not least, I wish to express my deep gratitude to all my family members for their continuous moral support and encouragement during my endeavour to complete this study.

Table of contents

List of figures

List of tables

Abbreviations & Acronyms

ARTEMIS	Africa Real Time Environmental Monitoring Information System
AVHRR	Advanced Very High Resolution Radiometer
AWC	Available Water Content
BT	Brightness Temperature
CCD	Cold Cloud Duration
CMI	Crop Moisture Index
DEVndvi	Deviation of NDVI
DMCN	Drought Monitoring Centre- Nairobi
DN	Digital Number
DSI	Drought Severity Index
DVB	Digital Video Broadcasting
EMS	Electromagnetic Spectrum
EMSA	Ethiopian Meteorological Service Agency
EOS	Earth Observation System
EROS	Earth Resources Observation System
ESA	European Satellite Agency
ET	Evapotranspiration
EUMETSAT	European Organization for Exploitation of Meteorological Satellites
FAO	Food and Agricultural Organization for United Nation
FEWS	Famine Early Warning Systems
GAC	Global Area Coverage
GDAL	Geospatial Data Abstraction Library
GIMMS	Global Inventory Monitoring and Modelling Studies
GIEWS	Global Information Early Warning System
GIS	Geographic Information Systems
GVI	Global Vegetation Index
HRV	High Resolution Visible
ILWIS	Integrated Land and Water Information System
ITC	International Institute for Geo-Information Science and Earth Observation
IWMI	International Water Management Institute
LAI	Leaf Area Index
MODIS	Moderate Resolution Imaging Spectroradiometer
MSG	Meteosat Second Generation
MVC	Maximum Value Composite
NASA	National Aeronautics and Space Administration
NDVI	Normalized Difference of Vegetation Index
NIR	Near Infra Red
NOAA	North Oceanic and Atmospheric Administration
PDSI	Palmer Drought Severity Index
SEVIRI	Spinning Enhanced Visible and Infrared Imager
SPI	Standard Precipitation Index

TCI	Temperature Condition Index
TIR	Thermal Infra Red
TOA	Top of Atmosphere
UTC	Coordinated Universal Time
UTM	Universal Transverse Mercator
VCI	Vegetation Condition Index
VGT-S10 products	10-day synthesis Vegetation products
WFP	World Food Programme
WMO	World Meteorological Organization
WSVI	Water Supply Vegetation Index

1. Introduction

1.1. Background

"Drought is an interval of time, generally of the order of months or years in duration, during which the actual moisture supply at a given place either falls short of the climatically expected or climatically appropriate moisture supply"(Palmer 1965, (IWMI 2006)). The severity of drought depends upon the degree of moisture deficiency, the duration and the size of the affected area. As there is no a precise and universally accepted definition of drought, there exists uncertainty in the occurrence of drought and its severity. This uncertainty often affects decisions on whether to take the remedial measure at the right time and place. Drought impacts may vary from region to region based upon the differences in social, economical and environmental characteristics at all levels.

According to World Meteorological Organizations, drought has been categorized as, Meteorological: a measure of departure of precipitation from normal. It basically originates from a deficiency of precipitation and is focused on the physical characteristics of drought, rather than on the impacts associated with shortage of precipitation in a region. Agricultural: refers to a situation where the amount of moisture in the soil no longer meets the needs of a particular crop. It is more closely associated with the deficiencies in the soil moisture than precipitation deficiencies. Because of this fact, agricultural drought lags the occurrence of meteorological drought. Hydrological: It is best defined by deficiencies in surface and subsurface water supplies, which lead to a lack of water availability to meet normal and specific demands; and Socio economic: refers to the situation that occurs when physical water shortages begin to affect people (McVicar and Jupp 1998).

Different types of drought require different drought indicators. Some indicators are more suited to monitor agricultural droughts, others to assess hydrological or meteorological drought. The assessment of socio-economic drought requires socioeconomic and nutrition-based indicators. To monitor agricultural drought, the most suitable indicators are those that are responsive to soil moisture status and are therefore based on the soil water balance. The reason is that the timing of soil moisture deficits in relation to crop water requirements and sensitivity to moisture stress is of major importance to assess the impact of drought on crops. At the same time, the indicators should be simple enough to allow straightforward interpretation.

Drought occurs in almost all climatic regimes. It occurs in high as well as low rainfall areas. It is a temporary anomaly and as such it differs from aridity, which is a permanent feature of climate in low rainfall areas (Wilhite 2000). Drought is considered by many to be the most complex but least understood of all natural hazards, making it hard to predict and monitor. Because of the creeping nature of drought and its wider spatial extent, it makes difficult to identify precisely the onset and severity of the event with a single indicator or index. The prescriptions for drought monitoring include first to identify its onset, its intensity and its change of direction, and this requires an understanding of the past conditions and a comparison with the present ones, thus, large historical datasets are required.

Unlike other natural hazards it is not possible to operationally identify when a drought has started or ended. Impacts are cumulative and the effects magnify when events continue from one season to the next. The economical impact occurs in agriculture and related sectors which depend on the surface and groundwater supplies. In addition to obvious losses in yields in both crop and livestock production, drought is associated with the increase in insect infestations, plant disease and wind erosion (Hounam 1975). The social impact is present in periods of extreme, persistent drought.

Nile Basin is a region prone to extreme climate events such as drought and flood. Successive years of low precipitation have left large areas of the region in severe drought that resulted in crop failure, water shortage and has raised serious food security concerns for the region. Drought is one of the major environmental disasters in the Nile Basin, generally characterized by abnormal soil water deficiency. It is mainly caused by natural climatic variability, such as precipitation shortage or increased evapotranspiration. Since these climatic factors have a large spatial and temporal variation, it is hard to monitor or predict drought events. Remote sensing, however, can help to do so due to its largest spatial scale and frequent coverages (Su and Roerink 2004).

Thus, remote sensing has become a standard tool in most food security systems, such as the Famine Early Warning Information System (FEWIS). This is mostly the result of decreasing costs of satellite data products and image analysis tools, large-area coverage, and significant correlations between soil moisture status or biomass productivity and parameters derived from spectral analysis like NDVI. Also, remote sensing offers a unique ability to integrate the effects of changing weather, vegetation, soil, and land use. Several low resolution satellite sensors are now available that can provide near real-time monitoring of vegetation and thus cover seasonal changes over large basins. In addition to NOAA-AVHRR sensor operated and archived since more than 20 years, new sensors became recently available for continental or global vegetation monitoring, like SPOT-VEGETATION (since 1998), EOS-MODIS (since 2000) or MSG-SEVIRI (since 2004). The SEVIRI sensor onboard the geostationary satellite Meteosat Second Generation, with improved temporal resolution has a potential for accurate assessment of NDVI, because the increased temporal resolution helps to overcome problems related cloud cover coupled with the distribution makes the MSG data well suited for early warning systems.

1.2. Drought situation in the upper Blue Nile basin (Amhara region)

In recent years, Ethiopia in general, the “Amhara” region in particular has suffered from a number of severe droughts and associated famines. Of the 105 woredas in the region, forty-eight are drought prone and chronically food-insecure. There has been no single year since 1950 where there was no drought in the eastern part of the region (Team 2000). Famines have been recorded as far back as biblical times. On the other hand, much of the western part of the region has good soils and adequate rainfall and typically produces agricultural surpluses.

Below-averaged belg, secondary rains (march-may) coupled with delayed and sporadic meher, or the main rains (June- September) have led to widespread food insecurity in the region. The lack of sufficient precipitation during the belg season failed to replenish water sources. In addition, given the poor performance of the meher (main season) rains, food insecurity continues to spread to agro-

pastoral and agricultural areas, particularly the lowlands and midlands of the region. USAID's Famine Early Warning systems Network (FEWS-NET) estimates that overall crop production will be 8-10% below average.

1.3. Research Problem

The total area of the Nile basin is over 300 million km^2 that represents 10.3 % of the area of the continent (www.fao.org). Major food production is almost completely dependent on rain-fed agriculture. The Blue Nile basin is characterized by arid climatic conditions and erratic rainfall, and often hit by recurring droughts. Frequent and severe drought has become a major climate disaster throughout the upper Blue Nile Basin. Recurrent drought events cause serious economic, social and environmental problems and are devastating particularly the agricultural economy. Drought assessment and monitoring for the basin using conventional methods which rely on the availability of weather data are tedious and time consuming. On the other hand, these weather data are often incomplete and limited in the basin. Moreover, it is not always available in good time to enable relatively accurate and timely large scale drought detection and monitoring. In contrast, the satellite-sensor data are consistently available, cost-effective and can be used to detect the onset of drought, its duration and magnitude. As timely information on the extent and severity of drought can limit impacts of drought-related losses, the near real time assessment through effective monitoring using Meteosat data plays a significant role in mitigating its adverse impacts.

1.4. Research Objective

Given the above stated problem, the following research objectives have been formulated to face the challenge:

1.4.1. General objective:

- To apply remote sensing data, particularly that obtained from the Meteosat Second Generation satellite for spatio-temporal drought monitoring and improves the uncertainties in the understanding of the drought dynamics.

1.4.2. Specific objectives:

- To investigate the effectiveness of satellite derived drought indices as an indicator for drought assessment.
- To investigate the nature of the relationship between satellite derived indices and agricultural production yield, and
- To apply the derived technique to assess the drought intensity over part of the upper Blue Nile basin (Amhara region) in Ethiopia from January, 2005 to December, 2006.

1.5. Research Questions

For the above-mentioned objectives to meet their targets, key research questions has to be addressed:

- What are the current possibilities and limitations of satellite derived indices in drought monitoring, especially focusing on the near real-time MSG data?
- Can drought indices derived from remote sensing data sufficiently identify and characterize droughts?
- Is the deviation of these indices with the long term-mean a good indicator for drought assessment and can it be used for monitoring?
- Are these indices complementary with one another and how do they correlate with trends of agricultural production?
- Is it possible to develop a toolbox based on MSG-indicators linked with agricultural statistics for drought prediction and loss of agricultural production as an early warning system?

1.6. Hypotheses

The research hypothesis formulated to achieve the research objectives are:

- The time series of MSG data and thematic information can be used as a tool for drought monitoring.
- The spatial and temporal characteristics of drought can be detected, tracked and mapped by satellite derived indices.
- The results obtained from the drought indices can be validated by in situ data such as agricultural crop yield.

1.7. Study Area

The study area covers the whole Nile basin which has an area of over 300 million square kilometres. About ten sub-Saharan African countries share this basin. The geographical location of the basin ranges from 4^0 S to 32^0 N, stretching over different geographical, climatological and topographical regions (Mohamed 2005). Its agro-ecological zones range from high rainfall plateau lands in Ethiopia to arid and semi-arid low lands. It also takes in globally significant swampland in Sudan's Sudd and the huge ecological diversity in freshwater ecosystems in the Great Lakes region. The total population of the 10 Nile countries is estimated to be 330 million people. Also it is estimated that 160-180 million of these people live within the Nile Basin. Nine of the 10 Nile countries are among the poorest in the world.

A part of the upper Blue Nile basin which is found in the North-west part of Ethiopia in the so-called Amhara region has given especial emphasis in this study and ground truth data, mainly agricultural yield production is collected for validation of the results of remotely sensed data. The region has an estimated total area of about 170, 000 square kilometres, which is 11% of the total area of the country. Most of the region is on the highland plateau and is characterized by rugged mountains, hills, plateaus, valleys and gorges. Hence, the region has varied landscapes composed of steep fault escarpments and adjoining lowland plains in the east, nearly flat plateaus and mountains in the centre, and eroded landforms in the north. Most of the region is a flat plain extending into the Sudan

lowlands. Topographically, the Amhara region is divided into highlands in the north and massive mountain ranges in the east and west, and lowlands in the north western including the low lying Nile Basin. The topographical features represent diversified elevations ranging from 700 meters above sea level (m.a.s.l) in the eastern edge to over 4600 m.a.s.l. in the northwest. Climatologically, the region is divided generally into Kola (hot zone), Woyina Dega (warm zone), and Dega (cold zone). Based on the moisture availability and thermal zones, ten major agro-ecological zones and 18 sub-zones have been identified in the region. The annual mean temperature of the region is between 15 to 21 degree centigrade. But in valleys and marginal areas the temperature exceeds 27 degree Celsius. This varied ecology lends itself to diversified agriculture. A little over 50% of the total area of the region is considered potentially arable for agricultural production activities. The economy of the region is dominated by agriculture. Most of the region is suitable for producing cereals and pulses. The low levels of agriculture productivity, land-holding sub-division due to rural population increase and recurrent drought in parts of the region combined to leave almost a quarter of the population food insecure. Cereals account for more than 80 percent of cultivated land and 85 percent of total crop production. The principal cereal crops in the Amhara region are teff, barley, wheat, maize, sorghum and finger millet. Pulses and oil crops are the major categories of field crops.

The population of the Amhara region is approximately 15 million people of whom 89% live in rural, agricultural households. A population growth rate of 3 percent a year is leading to a doubling of human population every 25 years. This rapid population growth rate has led to severe land shortages and rapid natural resource degradation. In the Amhara region, 94 percent of households have insufficient land to meet their food needs (Team 2000). Rural households are compelled to clear and cultivate marginal lands on steep hillsides. Only one to three percent of the Amhara region remains forested. Overgrazing further denudes the land of vegetative cover.

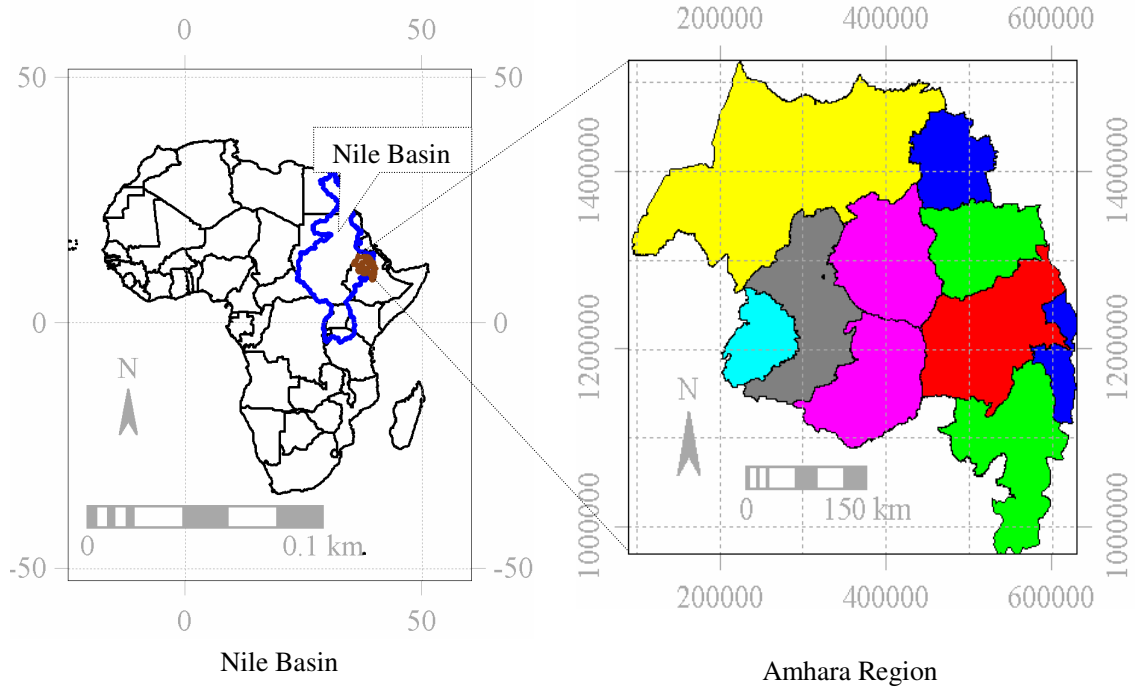

Figure 1-1: Location of the study area.

1.8. Structure of the thesis

The content of this paper is outlined hereunder as follows:

Chapter 1 deals with an introduction which comprises background, problem statement, objectives of the study, research questions, hypothesis for the study and description of the study area.

Chapter 2 contains literature review on the main concept of drought related theories. In this section different drought indices which are used for detecting the on-set and severity of drought has been thoroughly discussed. Also previous works on the subject matter has been reviewed briefly in order to compare and contrast the results obtained in this study.

Chapter 3 explains the materials used and the selected methodology adopted for the research. Here field data results and acquisition of satellite images and its processing has been discussed briefly.

Chapter 4 discusses the results of satellite data and its processing. In this part computational analysis of different drought indices derived from remote sensing data has been given and also attempts have been made to show the implication of the results obtained from satellite data.

Chapter 5 addresses the discussion and analysis of the results, which includes validation of the results of remotely sensed data with the ground truth data which has been obtained from part of the study area, the so-called “Amhara” region which is found in the North-West part of Ethiopia.

Chapter 6 gives conclusions and recommendations of the research and possibilities towards developing a real time early warning system.

2. Literature Review

2.1. The concept of Drought

Drought is a normal, recurrent feature of climate, although it is erroneously considered as a rare and random event. It differs from aridity, which is restricted to low rainfall regions and is a permanent feature of climate. Drought should be considered relative to some long-term average conditions of the balance between precipitation and evapotranspiration in a particular area. It is also related to the timing and the effectiveness of the rains.

Drought has many facets in any single region and it always starts with the lack of precipitation, but may affect soil moisture, streams, groundwater and human beings. This leads to the identification of different drought, which reflects the perspectives of different sector on water shortages. The deficiency of rainfall starts a drought. The longer and the more spatially extensive this deficiency, the more likely the occurrence of droughts.

Because drought is a recurring phenomenon and typical for the majority of world zones, the most productive lands of all continents can lose millions of tons production annually. Social, physical, and economic impacts of drought can be overwhelming, especially in the developing countries. The immediate consequences of drought include water supply shortages, destruction of ecological sources, and losses of agricultural production, resulting in famine, human suffering, death, and desertion of whole geographic regions.

Drought can be defined as abnormally dry weather sufficiently prolonged to cause serious hydrological imbalances. By definition drought can vary in time and space, depending on area's water budget. Components of the water budget are separated into inputs and outputs. Inputs include precipitation in the form of rain. The primary output is evapotranspiration. Other important factors include water stored in the soil and that which runs over land. All of these components of a water budget influence the timing and magnitude of droughts.

Drought definitions vary from region to region and may depend upon the dominating perception and the task for which it is defined. In general, there are two main definitions of drought: conceptual and operational. Conceptual definitions help people to understand the concept of drought. Also it is important in establishing drought policy. An operational definition of drought helps people to identify the beginning, end and degree of severity of a drought. It is usually made by comparing the current situation to the historical average, often based on a 30-year period of record (according to World Meteorological Organization recommendations). Operational definitions can also be used to analyze drought frequency, severity, and duration for a given historical period. Operational definitions are formulated in terms of drought indices. It is often region specific and is based on scientific reasoning, which follows the analysis of certain amounts of hydrometerlogical information.

All the definitions are related to the impacts of a dry spell on human activities. The impacts of drought may be environmental, economical and social. The environmental impact is the result of damages to plant and animal species, wildlife habitat, air and water quality, degradation of landscape quality and soil erosion. The economic impact occurs in agriculture and related sectors, which depend on the surface and ground water supplies. The social impact is present in periods of extreme persistent drought.

The severity of drought can be measured climatically, socially and economically. A fundamental problem is determining the severity of a drought. To make measurements of drought more meaningful indices have been used which examine the state and development of relevant meteorological and hydrological conditions.

2.2. The Role of Remote Sensing in drought monitoring

Remote sensing is the acquisition of digital data in the reflective, thermal or microwave portion of the electromagnetic spectrum (EMS). Measurements of the EMS are be made either from satellite, aircraft or ground-based systems, but characteristically at a distance from the target. Remotely sensed images are recorded digitally by sensors on board of the satellites. The satellites with appropriate swath width to monitor large areas vary in height above the earth's surface from approximately 700km, which orbit the earth, to some 36,000km, which are geostationary above the equator. The images can be manipulated by computers to highlight features of soils, vegetation and clouds. Each pixel contributing to the images is a measurement of a particular wavelength of electromagnetic radiation at a particular spatial scale for a particular location at a specific time.

Remote sensing techniques make possible to obtain and distribute information rapidly over large areas by means of sensors operating in several spectral bands, mounted on aircraft or satellites. A satellite, which orbits the earth, is able to explore the whole surface in a few days and repeat the survey of the same area at regular intervals. Rapid developments in computer technology and the Geographic Information Systems (GIS) help to process remote sensing observation from satellites in spatial format of maps. The integration of information derived from remote sensing techniques with other datasets provides tremendous potential for identification, monitoring and assessment of droughts.

Recent advances in operational space technology have improved our ability to address many issues of early warning and efficient monitoring. Weather satellites were first designed to help weather forecasts, but were found to be useful for addressing vegetation issues. Since the late 1980's they have also been used for drought detection, monitoring and impact assessment in agriculture (Kogan 1997). Use of environmental satellites enables us to detect drought 4-6 weeks earlier than before and delineated more accurately, and its impacts on agriculture can be diagnosed far in advance of harvest, which is the most vital need for global food security (Kogan 2000). Spectral radiances have been combined into indices and used as proxies for estimation of the entire spectrum of vegetation health (condition) from excellent to stressed (Kogan 1997).

Since drought covers large areas, it is difficult to monitor them using conventional systems. Timely information about the onset of drought, its extent, intensity, duration, and impacts can limit drought-

related losses of life, minimize human suffering, and reduce damage to the economy and environment (Kogan 1997). Weather data is a fairly good source of information that can be used for drought assessment. However, the scarcity of weather stations in some areas make drought monitoring a daunting task. Lack of information about a drought becomes especially acute in areas where the weather station networks is limited (e.g. sub-Saharan Africa). Furthermore, the data is often incomplete for the few available weather stations and/or not available early enough to enable timely drought detection and impact assessment. Use of satellite data avoids most of these problems. Moreover, observations from space provide permanent data archive and extra visual information. Also it is cost effective and enables one to have a regular and repetitive view of nearly the earth's entire surface (Kogan 1997).

The ability to use satellite data in drought detection and mapping is based upon the fact that moisture-stressed vegetation has a higher reflectance than green, healthy, and photosynthethically active vegetation in the visible spectral band and a lower reflectance in the near-infrared band (Unganai and Kogan 1998). Surfaces such as water, snow, and clouds tend to have higher reflectance in the visible region compared to near-IR and consequently NDVI assumes negative values for these features. Bare soil and rocks exhibit similar reflectance in both the visible and near-infrared regions, thus the NDVI values tend to zero. Once calibrated with the ground truth, satellite data can be used to monitor the onset of drought, the vegetation's response to drought, and its recovery from the resulting stress (Unganai and Kogan 1998).

The main limitation of remote sensing data for drought monitoring is that the most common satellite-derived drought indicators like NDVI are difficult for interpretation. As NDVI provides only a very rough measure of crop growing conditions or vegetation vigour, high NDVI values do not necessarily reflect the condition of food crops. Also since the vegetation indices represent the condition of the overall vegetation cover and do not allow for the differentiation of cereal and other food crops, a sudden increase in the vegetation at the beginning of the rainy season does not always indicate the presence of that particular crop. Furthermore, the NDVI images can not be used to determine which crops have reached maturity or harvested. Hence, to properly interpret NDVI it is essential to know the actual crop calendar.

2.3. Previous works on drought monitoring and analysis.

Since launching of the Africa Real Time Environmental Monitoring Information System (ARTEMIS) by FAO in 1988 (Mazzanti 1996), it is possible to obtain a routinely every 10-days vegetation Index (NDVI) imagery covering Africa based on the data obtained from the Meteosat and NOAA series of satellites. A temporal profile can be constructed for each pixel and an image of a certain month or decades are compared with the average of that period. Hence, the FAO ARTEMIS database provides a good view of the behaviour of the vegetation index over a season.

The Global Information and Early Warning System (GIEWS) has been utilising low resolution satellite remote sensing data to monitor vegetation and rainfall development over large areas in real time. Satellites images are often the only information available in near real-time for many parts of the world. Also, they provide a "snapshot" of the vegetation and meteorological conditions through the

growing season. Furthermore, satellite images from the current growing season can be compared with the historical archive containing images dating back as early 1980s for Africa. Since the late 1980s, the images have been provided by the Advanced Real Time Environmental Monitoring Information System (ARTEMIS) of the FAO in aim to provide policy analysts and decision makers with the most up-to-date and accurate information available on all aspects of food supply and demand. The main reasons for the selection of these low spatial but high temporal resolution satellites are area coverage, observation frequency and cost. High resolution satellite systems would provide a more detailed view of agricultural or affected areas concerned, but do not permit weekly or decadal monitoring, which is necessary for timely early warning and interventions.

The GIEWS makes extensive use of two types of satellite derived data: Cold Cloud Duration (CCD) and Normalised Difference Vegetation Index (NDVI) images for drought and food insecurity monitoring. Decadal and monthly images of Africa indicating rainfall estimates in millimetre, estimated number of rainy days, and CCD are processed from the METEOSAT data that the ARTEMIS receives directly and daily from the European satellite through a primary data user station. However, the NDVI imagery used by the GIEWS comes from the two sources. The first is from a 7.6km resolution Global Area Coverage (GAC) NDVI images for Africa from the data collected by the Advanced Very High Resolution Radiometer (AVHRR) sensor on board the polar orbiting NOAA satellite. Besides, since 1998 the ARTEMIS has been acquiring the NDVI data derived from the VEGETATION (VGT) instrument on board the SPOT-4 and 5 satellites every 10-days covering the entire landmass of the globe.

Increased demand for information and prediction services prompted the establishment of a specialized institution, Drought Monitoring Centre-Nairobi (DMCN) for the east African countries. Its main objective is to timely provide climate information and prediction services for enhanced application of such products to reduce climate and weather-related risks to food security for sustainable development of the horn of Africa. The DMCN produces and disseminates two types of products on routinely basis, decadal (10-days) and monthly products.

Several studies have been conducted in sub-Saharan African countries. Most of them use vegetation indices for monitoring of drought in the region. Among them, one is a method developed by Kogan (Kogan 1997) which is based on the relationship of the Vegetation Condition Index and Temperature Condition Index (VCI-TCI) indices for drought detection and monitoring. The method follows the consideration that the absolute maximum and minimum of NDVI and Brightness Temperature (BT) calculated from several years of data that contain the extreme weather events (drought and non-drought years) can be used as criteria for quantifying the extreme conditions (Kogan 1995). Accordingly the maximum and minimum NDVI and brightness temperature (BT) values were calculated from the long term records of remote sensing data for each of the weeks in the year and for each pixel. The result presented in this method shows the high potential VCI-TCI indices have for maintaining a global drought watch.

The method has been validated in many parts of the region using agricultural production yield anomaly with encouraging results. For example, the tool was tested in two African countries, Zimbabwe in Southern Africa and Ethiopia in Eastern Africa. The agriculture of these countries is very important for food self-sufficiency, and food production is highly dependant on drought. To test

the indices as a tool for drought monitoring, the method used averaging the weekly VCI-TCI values over each districts of the selected administrative provinces of a country to correlate with 9-yr corn anomalies (departure from the mean). Weather conditions in these years were varied from favourable to extremely unfavourable. Correlation obtained between corn yield and weekly indices, when the weather is critical for crop growth, was very strong. However, the correlation degrades in regions where corn area is small and/or environmental resources are very limited for successful farming. Thus, the method suggests that when crop yield is used as a validation tool in marginal areas, VCI-TCI spatial aggregation should be done only for the areas of intensive farming.

The validation results clearly indicate the utility of VCI-TCI as a sole source of information about vegetation stress and consequently drought as a major cause of the stress. Moreover, this study concludes as they were also useful for real-time assessments and diagnosis of vegetation condition and weather impact on vegetation. However, the TCI derived from the thermal channel need to be treated with caution since the information content of composited TIR measurements is uncertain, as TIR emissions from the earth change rapidly with time of day and atmospheric conditions. Moreover, existing algorithms have limitations in accounting and correcting for factors such as emmissivity variations in space, time, different wavelengths and view angle.

The other method makes use of the relationship between NDVI and rainfall for drought monitoring in the Sudan (Kassa 1999). This study explores the use of NDVI, since it has been widely used in drought monitoring, and is one of the most reliable and widely available of indices. In this study, regression techniques were used to verify whether there is a correlation between NDVI and rainfall data in Sudan, between 1982-1993.Then after establishing a positive correlation, the NDVI values over a twelve-year period were used to classify ecological areas in Sudan and produce a drought risk classification map. The result showed that there is a strong positive relationship of NDVI to rainfall in Sudan within each year, regression coefficients obtained for each year ranges between 0.74 to 0.8.

Also, in order to see the trend over 10 years, the annual rainfall was plotted against the cumulative annual NDVI values and it appeared that the NDVI values corresponded to the rainfall, but with a time lag of one year. This study comes up with a hypothesis that there is a time lag between the rainfall and the NDVI response. The results obtained in this method were compared with two other methods, the relationship between NDVI and rainfall during the plant-growing season and with the method using the relationship of NDVI with rainfall and surface temperatures. The former characterises the dynamics of the vegetation development via its growing season's parameters on consistent spatial scale and the second method is based on the relationship of the Global Vegetation Index (GVI) and the Temperature Condition Index (TCI) with rainfall.

Another approach utilizes the relationship between NDVI and crop yield production to analyse the crop yield reduction in the state of Kansas, located in the heart of the central Great Plains region of the North America. The method examined correlations between NDVI and annual corn and wheat production based on masks that delineate landscape patterns where these crops are produced in Kansas. The relationship were analysed using NDVI integrated over all combination of continuous time intervals (based on starting date and duration). The crop mask was created based on the characteristic that the crop produces high NDVI in the maturing time of the cropping season and low NDVI in the time after harvest. The result showed that annual corn production was more strongly

correlated with NDVI integrated over the maturing period of the growing season. Thus, the method suggests that the NDVI can serve as a reliable predictor of crop yield (Wang, M.Rich et al. 2005). Moreover, it has been shown that there exists a good correlation between NDVI anomaly and food grain anomaly in drought risk assessment study for Gujarat, India (Chopra 2006).

In another study (EKLUNDH 1997), the possibility of using NDVI data for crop and natural vegetation monitoring has been analysed by measuring the cross-correlation between time series of NDVI and vegetation indicators such as rainfall for areas where rainfall is a limiting factor. The result showed there is a fairly good correlation between NDVI and rainfall with coefficients of correlation between 0.7 and 0.9, and NDVI is found to lag behind rainfall by between one and three months. The study concludes if it is assumed that the rainfall data can be used as indicator for vegetation development over the season, there are limitations with the capability of NDVI for monitoring temporal variations in vegetation.

2.4. Drought Indices

Drought indices can be used to quantify the moisture condition of a region and thereby detect the onset and measure the severity of drought events; and to quantify the spatial extent of a drought event thereby allowing a comparison of moisture supply condition between regions (Quiring and Papakryiakou 2003). They are normally continuous functions of rainfall and/or temperature, river discharge or other measurable variable. Rainfall data are widely used to calculate drought indices; because of the long-term rainfall records are often available. Moreover, drought indices integrate various hydrological and meteorological parameters like rainfall, evapotranspiration (ET), runoff and other water supply indicators into a single number and gives a comprehensive picture for decision making (Narasimhan and Srinivasan 2005). There are several indices that measure how much precipitation for a given period of time has deviated from historically established norms. Although none of the major indices is inherently superior to the rest in all circumstances, some indices are better suited than others for certain uses.

2.5. Drought indices derived from hydro meteorological data

Palmer (1965) developed a soil moisture algorithm which uses precipitation, temperature data and local Available Water Content (AWC) of the soil. AWC is effectively a "model parameter", which has to be set at the start of calculations. Calculations result in an index (PDSI), which indicates standardized moisture conditions and allows comparison to be made between locations and between months. PDSI varies roughly between -6.0 and +6.0. More wet conditions are indicated by positive values of PDSI, and more dry by negative values. The thresholds for the classification of different wetness are arbitrary. PDSI values between -2 and +2 would normally indicate normal conditions, although the sub-range of -1 to -2 could also be treated as a mild drought. PDSI values are normally calculated on monthly basis. Further interpretation of monthly PDSI allows drought duration to be taken into account as well. PDSI values may lag behind emerging droughts by several months. This limits its application in areas of frequent climatic extremes.

The crop moisture index (CMI), also developed by Palmer (1968) and is a complement to the PDSI. It measures the degree to which crop moisture requirements are met, is more responsive to short-term changes in moisture conditions and is not intended to assess long-term droughts. CMI is normally calculated with a weekly basis, is based on the mean temperature, total precipitation for each week and the CMI value from the previous week. A number of other indices, which focus on water availability for crops, have been developed. As a rule, these methods calculate soil moisture balance with a 1, 5, 7 or 10-day time step and the degree to which the crop water requirement have been met.
The understanding that a deficit of precipitation has different impacts on the ground water, reservoir storage, soil moisture, snow pack and stream flow led McKee et al. (1993) to develop the Standardized Precipitation Index (SPI). Precipitation is the main factor which controls the formation and persistence of drought. The SPI was designed to quantify the precipitation deficiency for multiple time scales. These time scales reflect the impact of drought on the availability of the different water resources. SPI is based just on precipitation and, therefore, requires less input data and calculation effort than PDSI. A long-term precipitation record at the desired station is fitted to a probability distribution, which is then transformed into a standardized normal distribution so that the mean SPI is zero. SPI may be computed with different time steps and is reported to be able to identify emerging droughts sooner than the Palmer Index. Positive SPI values indicate greater than the mean precipitation and negative values indicate less than the mean precipitation. The SPI calculation for any location is based on the long-term precipitation record for a desired period and it is calculated using the following equation, written as:

$$(X_i - X_m) / \sigma$$

Where, X_i is the seasonal precipitation of station, X_m is its long-term mean and σ is the standard deviation of the long-term record. The drought categories defined by SPI values are listed below.

SPI Values	Drought categories
≥2.0	Extreme wet
1.5 to 1.99	Very wet
0 to -0.99	Mild drought
-1.0 to -1.49	Moderate drought
-1.5 to -1.99	Severe drought
≤-2.0	Extreme drought

Table 2-1: Classification of SPI values

2.6. Drought indices derived from remote sensing data

Several indices, which could be used amongst the others for drought monitoring, have been developed over the past few decades using remote sensing data. They are calculated from the reflectance and brighteness temperature in different bands and may be obtained for each pixel (the size of the pixel depends upon the resolution of a sensor). These indices have a few advantages over conventional climate data related indices, as they cover large areas and may show how drought is progressing over

the area. They have to be calibrated against ground climate data. Most commonly applied indices are discussed below.

2.6.1.1. Normalized Difference Vegetation Index (NDVI)

The Normalized Difference Vegetation Index (NDVI) is related to the proportion of photosynthetically absorbed radiation. Many natural surfaces are about equally as bright in the visible red and near-infrared part of the spectrum with the notable exception of green vegetation. Red light is strongly absorbed by photosynthetic pigments (such as chlorophyll) found in green leaves, while near-infrared light either passes through or is reflected by life leaf tissues, regardless of their color. This means that areas of bare soil having little or no green plant material will appear similar in both the red and near-infrared wavelengths, while areas with much green vegetation will be very bright in the near-infrared and very dark in the red part of the spectrum. In other words, for healthy living vegetation, this ratio will be high due to the inverse relationship between vegetation brightness in the red and infrared regions of the spectrum. The Normalized Difference Vegetation Index (NDVI) provides a measure of the amount and vigor of vegetation at the land surface. The magnitude of NDVI is related to the level of photosynthetic activity in the observed vegetation. In general, higher values of NDVI indicate greater vigor and amounts of vegetation. So, the normalized difference vegetation index (NDVI) provides us with an indication of how much green vegetation exists at a particular place on the ground. The NDVI values range from -1 to +1 with most values ranging from 0 to 0.6. Healthy green vegetation has a high NDVI value because more near-infrared light is reflected than red light. For bare soil on the other hand, both near-infrared and red light are strongly reflected so the NDVI would be near zero. Water and ice reflect a little more red than near-infrared light so those values tend to be slightly negative. Two characteristics of the NDVI that make it ideal for vegetation monitoring are that no other surface exhibits higher NDVI values than vegetated surfaces and that, when vegetation vigor changes due to the nature of vegetation growth and development or environmental induced stress such as drought, the NDVI also changes (Tucker 1987). Therefore, the NDVI does have potential in drought detection and climate impact assessment.

NDVI is calculated from two channels sensor, the near-infrared (NIR) and visible (VIS) wavelengths, using the following algorithm:

$$NDVI = (NIR - VIS) / (NIR + VIS)$$

Where λ_{NIR} and λ_{red} is the reflectance in the near infra-red and red bands respectively. NDVI ranges from -1 to +1.NDVI is a nonlinear function that varies between –1 and +1 (undefined when NIR and VIS are zero). Values of NDVI for vegetated land generally range from about 0.1 to 0.7, with values greater than 0.5 indicating healthy vegetation.

NDVI by itself does not reflect drought or non-drought conditions. But the severity of drought may be defined as NDVI deviation from its long-term mean (DEV_{NDVI}). This deviation is calculated as the difference between the NDVI for the current month and a long term mean for this month (IWMI 2006).

$$\boldsymbol{DEV_{NDVI}} = NDVI_i - NDVI_{mean,\ i}$$

Where $NDVI_i$ is the current NDVI for month I and NDVImean, i is the long term mean NDVI for a calendar month, i. When DEV_{NDVI} is negative, it indicates the below-normal vegetation condition and, therefore, suggests a prevailing drought situation. The greater the negative departure the greater the magnitude of a drought. In general, the departure from the long-term mean can be used effectively as drought indicator as it would reflect the conditions of healthy vegetation in normal and wet years. Its limitations are that the deviation from the mean does not take into account the standard deviation, and can be misinterpreted when the variability in vegetation conditions in a region is fluctuate in any given year(Thenkabail 2004).

2.6.1.2. Water Supply Vegetation Index (WSVI)

Water supply vegetation index is based on the fact that, in drought conditions, the Normalized Difference Vegetation Index (NDVI) values derived from satellite data will fall below normal. At the same time, the crop canopy temperature as seen by the same satellite will rise above normal. Both effects are related to available water supply, and by combining both effects in one index, a sensitive measure of drought conditions can be obtained. When crops are suffering from drought, their stomata openings are partly closed in order to reduce the loss of water. It causes an increase of temperature of the leaf surface. For initial and advance stage of a drought, the higher the temperature of the leaf surface is the more stress. At the same time, the growth of crops is affected by drought, resulting in the decrease of leaf area index (LAI). Besides, leaves will also be wither under high air temperature. All of these may result in reduction of NDVI. The smaller WSVI is the more severe drought is.

WSVI is given by:

$$WSVI=NDVI/Tb$$

Where Tb is the brightness temperature. When vegetation suffers from drought, the NDVI decreases and the temperature of the canopy increases. So, WSVI decreases (Jiren and Musul 2002).

2.6.1.3. Vegetation Condition Index (VCI)

Although the NDVI has been extensively used in the past for vegetation monitoring, it is often very difficult to interpret in relation to vegetation condition, especially when comparing different ecosystems. Vegetation condition index was first suggested by Kogan (1995). It shows, effectively, how close the current month's NDVI is to the minimum NDVI calculated from the long-term record of RS images. VCI enables to separate the short-term signal from the ecological signal.

$$VCI_j = \frac{(NDVI_j - NDVI_{min})*100}{(NDVI_{max} - NDVI_{min})}$$

Where, $NDVI_{max}$ and $NDVI_{min}$ are calculated from the long-term record for that month, and j is the index of the current month. NDVI values are calculated using the formula above. The condition of the ground vegetation presented by the VCI is measured in percent. The VCI values around 50% reflect fair vegetation conditions. The VCI values between 50 and 100% indicate optimal or above normal

conditions. At the VCI value of 100%, the NDVI value for selected month (week) is equal to NDVImax, which indicates optimal condition of vegetation. Different degrees of drought severity are indicated by VCI values below 50% Kogan (1995) illustrated that a VCI threshold of 35% may be used to identify extreme drought conditions and suggested that further research is necessary to categorize the VCI by its severity in the range between 0 and 35% (Thenkabail 2004). The VCI value close zero percent reflects an extremely dry month, when the NDVI value is close to its long term minimum. Low VCI values over several consecutive time intervals indicate to drought development.

The VCI captures rainfall dynamics better than the NDVI particularly in geographically non homogeneous areas. The VCI not only permits the description of land cover and spatial and temporal vegetation change but also allows quantifying the impact of weather on vegetation. Also the VCI makes it possible for one to compare the weather impact in areas with different ecological and economical resources. VCI values indicate easily how much the vegetation has advanced or deteriorated in response to weather and how far vegetation development is from the potential maximum and minimum defined by ecological limits.

2.6.1.4. Temperature Condition Index (TCI)

During the rainy season, it is common for overcast conditions to prevail for long periods of time. If this period lasts more than 3 weeks, the weekly NDVI values tends to be depressed giving the false impression of water stress or drought conditions. To remove the effects of cloud contamination in satellite assessment of vegetation condition, Kogan (1995, 1997) suggested Temperature condition index (TCI) and is calculated similarly to VCI but its formulation was modified to reflect vegetation's response to temperature (the higher the temperature the more extreme the drought). TCI is based on brightness temperature and represents the deviation of the current month's value from the recorded maximum. That makes it necessary to use TCI as tool to verify drought conditions. However, in contrast to the VCI, the TCI includes the deviation of the current month's value from the recorded maximum. In combination with meteorological observations, the relationship between surface temperature and the moisture regime on the ground will detect drought-affected areas before biomass degradation occurs. Hence, TCI can play an important role in drought monitoring.

$$TCI_j = \frac{(BT_{max} - BT_j)*100}{(BT_{max} - BT_{min})}$$

Where BT is the brightness temperature. The maximum and minimum values of BT are calculated from the long term records of Remote Sensing images (www.iwmi.cgiar.org).

2.7. The role of Meteosat Second Generation (MSG) in drought monitoring.

Meteosat Second Generation (MSG) is a joint project between ESA and the European Organization for Exploitation of Meteorological Satellites (EUMETSAT) and follows up the success of the first generation Meteosat weather satellite series with a higher performance. The first in a planned series of MSG Satellites was launched in 2002, entering into service with EUMETSAT in early 2004 and was renamed Meteosat-8. MSG transmits raw data to EUMETSAT control and processing centre to the

primary ground station for processing. The MSG satellites produce SEVIRI image data in the form of both High and Low rate SEVIRI image data. These real-time data are processed and are corrected for radiometric and geometric non-linearity before onward distribution to the user. The raw data consists of mainly images generated by the Spinning Enhanced Visible and Infrared Imager (SEVIRI) instrument, which is used for collection of image data with a very high temporal resolution for meteorological and other applications and Geostationary Earth Radiation Budget Experiment on board satellite, for monitoring the Earth's radiation budget at the top of the atmosphere for short-and long-wave radiation calculations, and understanding the Earth's climate balance. Once processed, the data is sent to a communication satellite for broadcasting to users.

MSG is a spin-stabilized satellite, and imaging is performed by combining satellite spin and rotation of the scan mirror. The Meteosat Second Generation satellite provides a large step to observe the earth from geostationary orbit. The primary mission of MSG data is the continuous observation of part of the earth's full disk. MSG takes one full image every 15 minutes. Image dimensions are 3712 by 3712 pixels in channels 1 to 11, and 5568 by 11136 pixels in channel 12. Nominal coverage includes the whole of Europe, all of Africa and locations at which the elevation to the satellite is greater than or equal to 10 degree. The various channels provide measurements with a resolution of 3 km at the sub satellite point. The High Resolution Visible (HRV) channel provides measurements with a resolution of 1 km. The earth is observed with a nominal repeat cycle of 15 minutes. This high temporal frequency enhances the observation scenes available, thus increases the chance of obtaining cloud free images, which open up for a new vegetation scheme and makes the MSG data well suited for an early warning system in particular for the African continent over which MSG is located (Fensholt, Sandholt et al. 2005).

MSG data are easily accessible to users in real time through low cost receiving systems. Also many local receiving systems have been installed in meteorological offices in African continent. Further more, new procedures are developed based on open software to process data and extract daily parameters like NDVI and surface temperatures. Besides, a study conducted by (Lacaze and Berges 2005) showed decadal synthesis of MSG SEVIRI NDVI are of better quality than those of SPOT-VEGETATION, because of improved removal of cloud-contaminated pixels. Moreover, in most areas it is suggested that MSG SEVIRI can provide NDVI synthesis of good quality for periods of 5 days or less. Thus, all these mentioned advantages make the availability of MSG data to contribute to improve early warning systems. Furthermore, its greater number of channels will make MSG more practical for many kind of land surface monitoring activities and so useful for a wider variety of environmental purposes. The only limiting factor is its coarse spatial resolution.

3. Materials and Methods

3.1. Data and Acqusition methods

3.1.1. Agricultural production yield data

The characteristics of satellite derived indices must be validated by ground truth data. The ground data intended to be used mainly in this study is agricultural production yield. As agricultural yields are sensitive to weather fluctuations, it will reduce abruptly during severe drought periods. Therefore, "average yield of grain crops for country's administrative regions can be used for validation of satellite-derived droughts" (Kogan 1997). For this study the ground data will be collected from part of the Blue-Nile Basin which is found in the North-West part of Ethiopia in the so-called "Amhara" region for validation purpose. The agricultural yield production statistics has been taken for most of the "Amhara region" which belongs to the upper Blue Nile basin. These data has been collected from the Amhara regional state, Bureau of finance and economic development through the policy analysis department. Agricultural production yield data is obtained for eight years starting from 1998 to 2005. To check the reliability of the statistical data, correlation between cultivated land in hectare and production yield obtained in tons has been made for each district (zones). The result showed that there is a high correlation for most of the districts except the so-called Wag-Hamra zone, which has a negative correlation.

Table 3-1 shows the agricultural statistics data of all the districts for eight years (1998-2005). The table summarizes total production yield and cultivated land over the main cropping season; and Figure 3-1 shows the correlation between the agricultural yields and cultivated land for West Gojam district. Similar graphs for the other districts are given in appendix A.

Year	Districts							
	West Gojam		East Gojam		North Gondar		South Gondar	
	Cultiv. land(ha)	Prod. (Quintal)	Cultiv. land(ha)	Prod. (Quintal)	Cultiv. land(ha)	Prod. (Quintal)	Cultiv. land(ha)	Prod. (Quintal)
1998	550455	7173549	548079	6524959	800215	6877208	818428	4642042
1999	568833	9195455	575309	7978174	835903	8097862	821858	6140784
2000	578029	9437080	573144	8605175	843797	7935839	586505	6487056
2001	78624	1041232	614257	8856071	716977	7847587	587853	4469455
2002	408340	5929767	431725	5650957	485009	5263940	370912	3857770
2003	392763	4481215	397966	3617575	472208	2704661	403552	3122056
2004	409023	5361453	278735	5065554	523527	4859031	412007	3208232
2005	491842	5667375	457515	5751625	560435	6888517	465598	3253113

Year	Districts					
	North Wollow		South Wollow		North Shoa	
	Cultivated land(ha)	Production (Quintal)	Cultivated land(ha)	Production (Quintal)	Cultivated land(ha)	Production (Quintal)
1998	203364	859683	376486	2511800	542031	4377533
1999	201891	1497946	406767	3475426	538823	5308730
2000	228094	1282015	478877	3780384	531239	4993977
2001	229498	1809229	470363	3223848	548506	5608172
2002	204917	2442211	356139	3836259	353597	3938673
2003	193420	1388573	331122	2461770	375073	2512286
2004	217294	2735107	382490	4733845	374207	4655269
2005	232528	2452466	428473	5396082	390871	5018611

Year	Districts					
	Awi		Wag Hamra		Oromyia	
	Cultivated land(ha)	Production (Quintal)	Cultivated land(ha)	Production (Quintal)	Cultivated land(ha)	Production (Quintal)
1998	294258	3689258	110365	186784	79196	239052
1999	304779	400129	84156	735363	4450253	47056316
2000	302547	3907335	106498	395628	84161	595630
2001	326881	4373839	117260	322698	83178	705803
2002	184740	2554974	67103	489648	44526	500102
2003	152166	1665913	74260	402505	59330	390031
2004	190986	1972649	79000	572776	55771	553448
2005	195225	2060810	95241	515650	56525	619221

Table 3-1: Agricultural production yield of all the districts in the region.

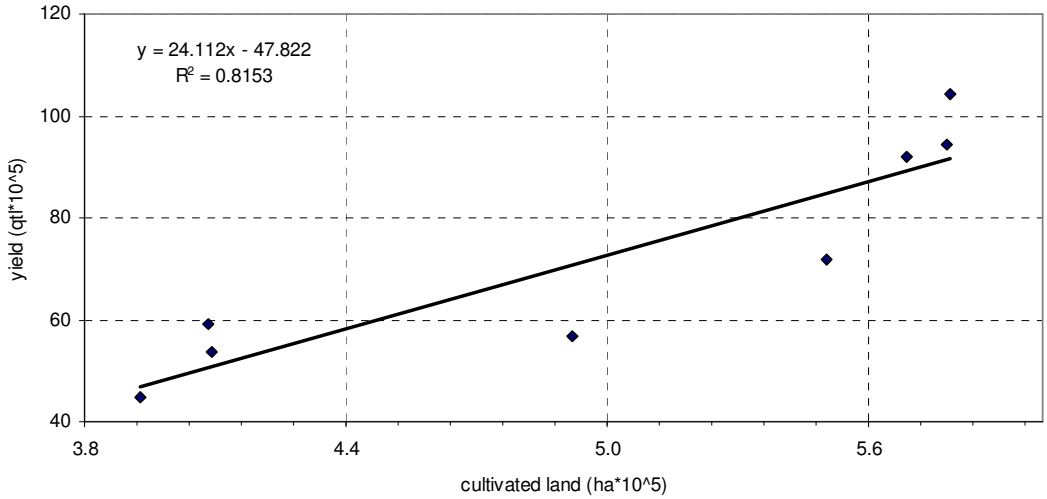

Figure 3-1: Graph showing the correlation between agricultural production yield and cultivated land for West Gojam district

3.1.2. Meteorological data

Apart from the agricultural production yield data, rainfall data has been collected from 18 stations on decadal basis to see the relation of NDVI with variability of rainfall. The stations are distributed over the districts. The data source is the Ethiopian Meteorological Service Agency (EMSA).

Meteorological data has been used to get the response of NDVI with the variability of rainfall in all the districts of the region. Use of inverse distance method was made for distributing the influence of each station over the entire region.

Figure 3-2: Rainfall stations in Amhara region.

3.1.3. Remotely sensed data

3.1.3.1. NOAA-AVHRR data

Long-term mean (1982-2004) of decadal composite NOAA pathfinder NDVI values encompassing the continent Africa were downloaded from the Famine Early Warning System (FEWS-NET) archive website: http://earlywarning.cr.usgs.gov/adds/datatheme.php; and Decadal Long-term NDVI values

are extracted for the Nile Basin only. NDVI is derived from data collected by the National Oceanic and Atmospheric Administration (NOAA) satellites, and processed by the Global Inventory Monitoring and Modeling Studies group (GIMMS) at the National Aeronautical and Space Administration (NASA). The data set was generated from original 1.1km^2 NOAA-AVHRR data as 10-day maximum value composites (MVC) aggregated to an 8km × 8km pixel resolution. EROS processes and archives a decadal (i.e., ~ 10-days, 36/year) Africa NDVI product from NASA GIMMS group. The data is inter-calibrated with SPOT Vegetation NDVI, and uses NOAA-17 since January 2004. The NOAA-17 NDVI data have also been inter-calibrated with NOAA-16 and previous products.

No correction has been applied to correct for atmospheric effects due to water vapour, Rayleigh scattering or stratospheric ozone. Artefacts in NDVI due to satellite drift has been corrected using empirical mode decomposition, which is especially important in tropical regions(Pinzon 2004). NDVI is archived as byte data files, and once imported, is referred to as 'raw data'. In order to recover the -1 to +1 range of NDVI values, the following formula has been used and water pixels are masked (Tucker 2005).

$$NDVI= raw/250$$

3.1.3.2. Meteosat Second Generation (MSG) data

MSG transmits the raw data to the Eumetsat control and processing centre in Darmstadt, via the primary ground station, for processing. The raw data consists mainly of images generated by the camera (Spinning Enhanced Visible and Infrared Imager) and the Geostationary Earth Radiation Budget Experiment on board the satellite. After the SEVIRI data are received from MSG-1 by EUMETSAT at Darmstadt (Germany), will be processed there at the ground station and will be sent to a communication satellite for broadcasting to users.

From its geostationary orbit at 0^0N, 0^0 W, Meteosat-8 continuously scans the Earth surface and transmits the data to the primary ground station. The data received is processed and rectified in to a so called Level 1.5 data-format. To handle the enormous amount of data, software tools are developed facilitating storage, easy import and radiometric-geometric calibration of the images. Stationed over Africa the MSG satellite provides a continuous observation and from the recordings provided the relevant (dynamic) meteorological and hydrological variables can be retrieved to assess the actual conditions of the natural resources (Maathuis, Gieske et al. 2006).

The images can be received using a low cost ground receiving station like the one installed at ITC. At ITC, using a satellite dish directed towards the Hotbird-6 satellite, the DVB (digital video broadcasting) signal can be received. The images are then archived in compressed format on external devices linked to the ITC network, and accessible through ordinary PCs. The problem with MSG data is that the file format is not standard. None of the commonly used remote sensing packages is able to open or process the raw compressed images. As a solution a driver for reading the images in Geospatial Data Abstraction Library (GDAL) was implemented (Maathuis, Gieske et al. 2006). GDAL is a translation library for raster geospatial data formats that is released under an open source license.

A sub-image covering the study area (Nile Basin) has been selected and a time series images on daily basis, starting from January 2005 to December 2006 are downloaded using MSG Data Retriever, software developed at ITC for efficient extraction of an image time series which is both geocoded and radiometrically corrected. In the example provided in Figure 3-3, for the specific region in East Africa comprising the study area, the visible 006 and 008 channels; and the 10.8 micron channel are retrieved for 11:00 hr UTC image. Then, The raw data are converted into reflectances and brightness temperature by selecting these options in the MSG data retriever windows(Gieske, Hendrikse et al. 2005) and exported to ILWIS data format, resampled to UTM at a 3 km. pixel resolution. The Vis006 and Vis008 channels are used to calculate NDVI or other related vegetation indices.

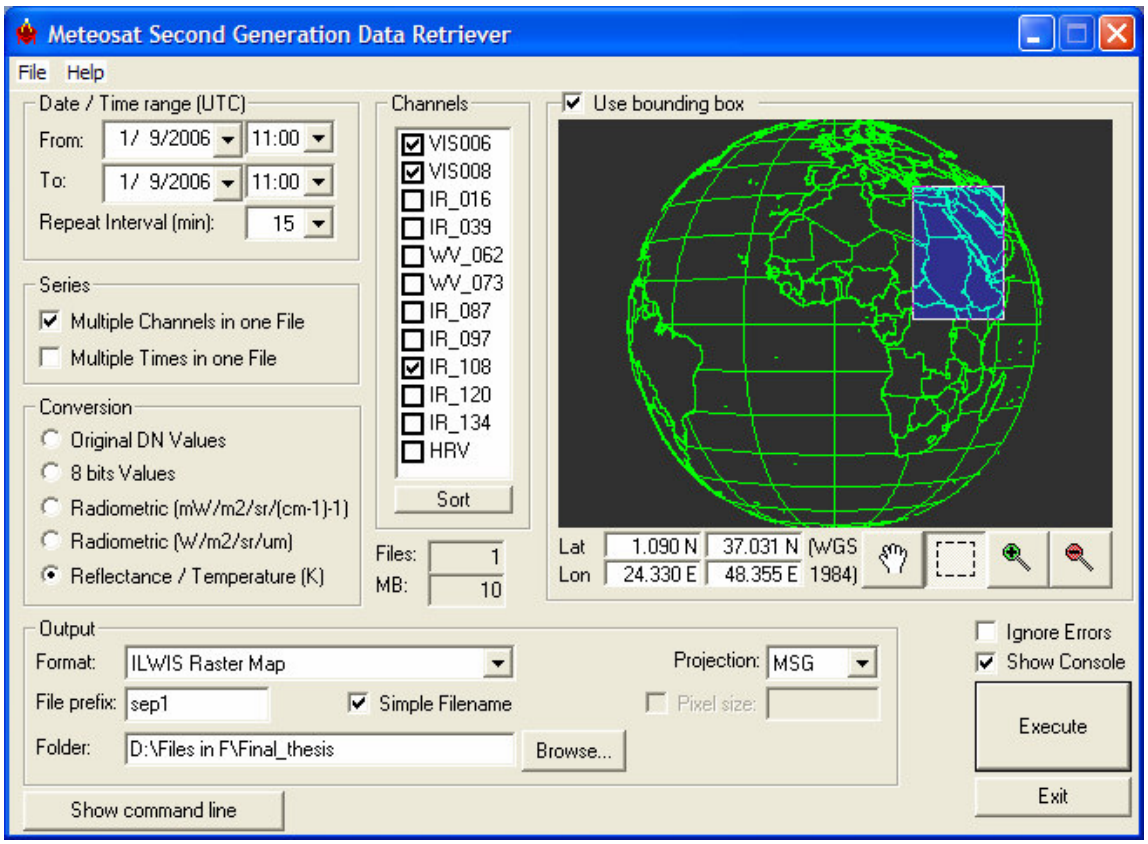

Figure 3-3: MSG Data Retriever

3.1.3.3. SPOT Vegetation data

SPOT Vegetation NDVI products have also been downloaded for the continent Africa (1998-2005) and Nile Basin NDVI values are extracted out. The vegetation data contains all products, including high level products, derived from the vegetation instrument on board the SPOT satellite. The vegetation 10-day synthesis archive is freely accessible through the website of the vegetation programme directly via the free S10 distribution server: http://free.vgt.vito.be. The vegetation instrument is dedicated to the daily observation of terrestrial ecosystems and the biosphere, particularly for addressing global change and environmental issues. The vegetation instrument observes the whole earth every day because of its large field of view, and is an essential tool for

studies on global vegetation. Ten-day composite data were constructed by selecting pixels with the maximum NDVI during the period. Selecting pixels with the maximum NDVI reduces cloud cover and water vapour effects that strongly reduce NDVI. There are three 10-day composite per month in this data set, from the first of the month to the 10th, from the 11th to the20^{th}, and from the 21st to the end of the month. The last compositing period can vary from 8-11 days, depending upon the number of days in the month. The image projection is Albers Equal Area Conic.

VGT-S10 products (ten day synthesis) are compiled by merging segments acquired in ten days. All the segments of this period are compared again pixel by pixel to pick out the best reflectance values. These products provide data from all spectral bands, the NDVI and auxiliary data on image acquisition parameters. A MVC synthesis is delivered with spatial resolution of 1×1 km was selected. The relation between the digital numbers the real NDVI is expressed as:

Real NDVI=Coefficient a*Digital Number plus coefficient b.

=a*DN+b

Coefficient a= 0.004

Coefficient b= -0.1

The maximum pixel size for raw data across track is 1.7km. Attitude oscillations of the satellite, the earth's relief and non-perfect globular shape of the earth make that this approximate value. However, pixels in vegetation products are projected and interpolated, resulting in a constant pixel resolution of 1 km.

3.1.4. Ancillary data

3.1.4.1. Land cover map

A generalized land cover map of part of the upper Blue Nile Basin including the Amhara region was prepared. It is extracted from the land cover map of the Blue Nile Basin study. The generalized land cover map presents quite a large number of different land cover types: plantation, woodland, grass land, perennial crops, moderately and dominantly cultivated, irrigated and forest, etc. It is being used to extract cultivated areas of the Amhara region which is the main concern in computing the NDVI values.

Figure 3-4 shows a generalized land cover map of part of the "Amhara" region which is entirely found in the in the upper Blue Nile Basin. Then, it is reclassified in to cultivated and non-cultivated classes. Dominantly cultivated, moderately cultivated, irrigated, perennial crops and plantations land cover types are grouped in to cultivated land class and the rest land cover types in to non-cultivated class. The cultivated land is only considered in deriving the NDVI for the "Amhara" region. The reclassified land cover map for part of the upper Blue Nile Basin in "Amhara" region is shown in Figure 3-5.

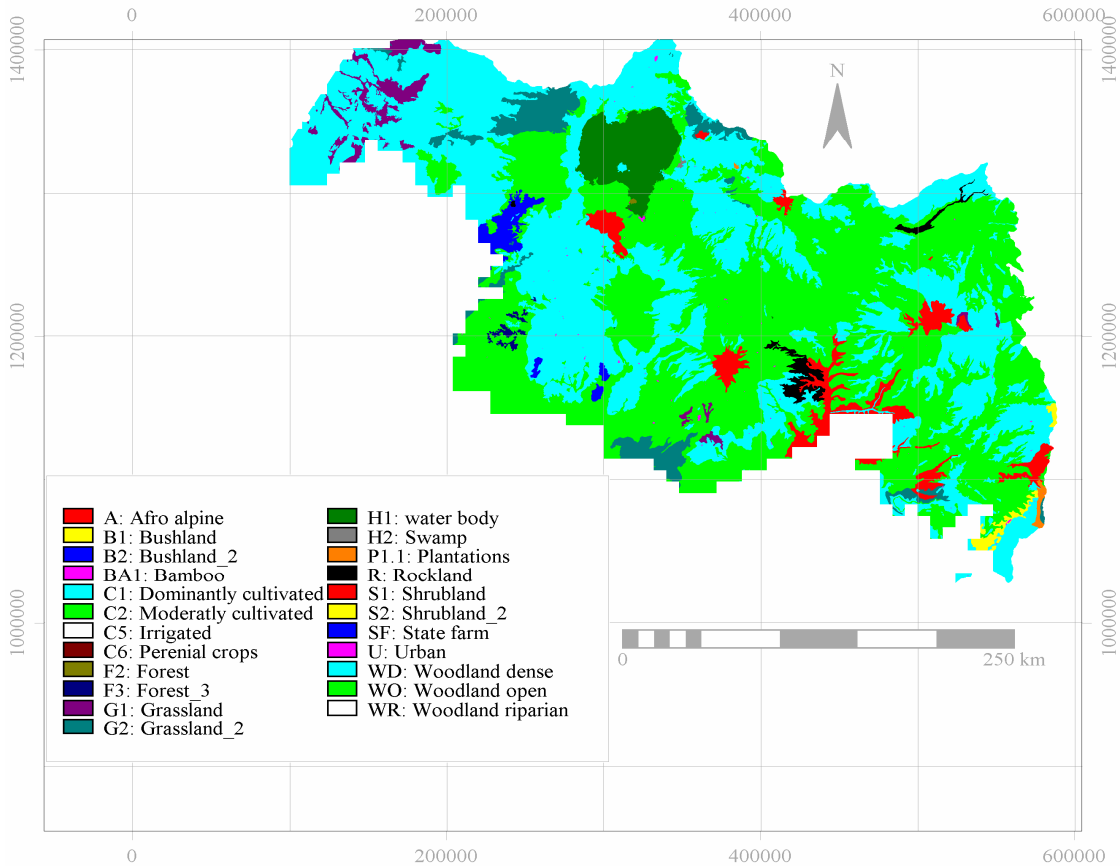

Figure 3-4: A Generalized land cover map of part of the Amhara region.

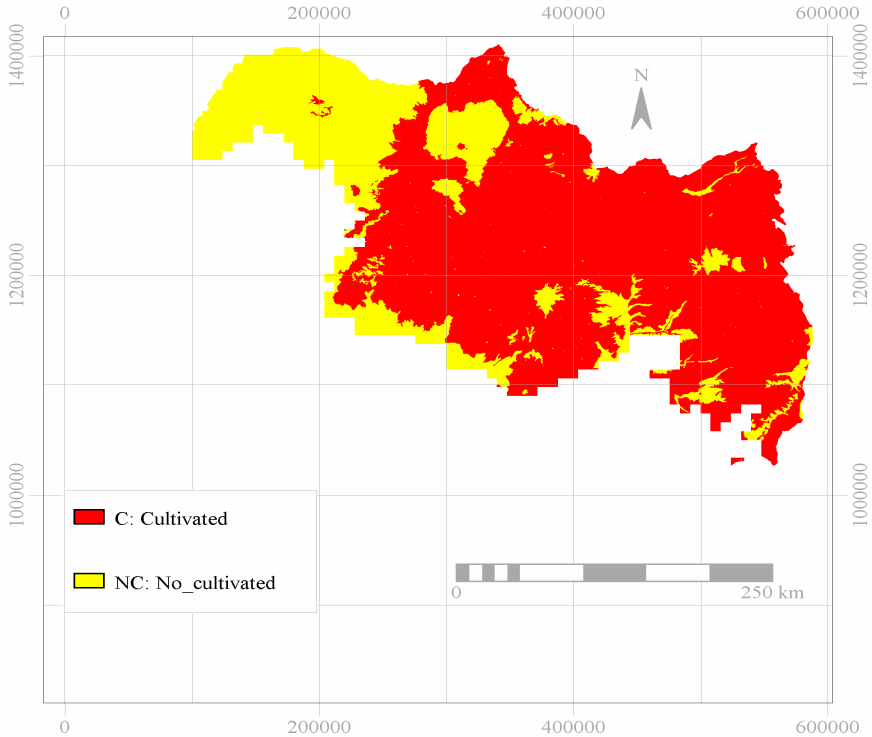

Figure 3-5: A Reclassified land cover map

3.2. Methods

The following diagram shows the overview of methods which are applied in this study.

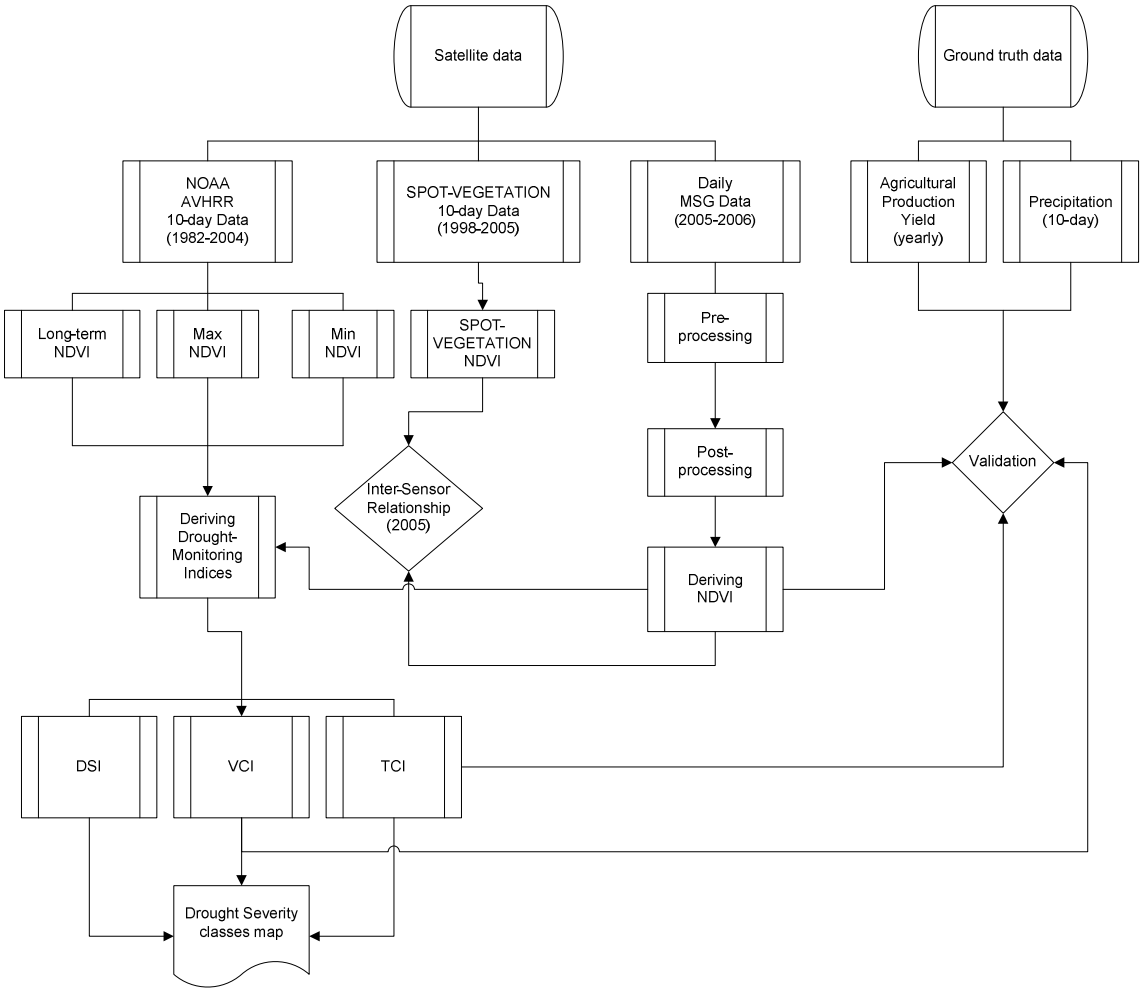

Figure 3-6: Schematic representation of the methodology

3.2.1. Pre-processing of satellite data

3.2.1.1. MSG image acquisition

SEVIRI radiometer is the main instrument on board MSG. The sensor has provided continuous acquisitions since January 2004, with 15-minutes repeat time cycle. It has an advantage as compared to other sensors which are available to provide near real time monitoring of vegetation changes at high temporal resolution. The higher temporal frequency allows for an improved removal of cloud contaminated pixels. The sensor provides 12 channels with two different resolutions over a swath width of half earth disk.

Channel number	Wave length region	Spectral band range(µm)	Sub Satellite Resolution(km)
1	VIS0.6	0.56-0.71	3
2	VIS0.8	0.74-0.88	3
3	NIR1.6	1.50-1.78	3
4	IR3.9	3.48-4.36	3
5	WV6.2	5.35-7.15	3
6	WV7.3	6.85-7.85	3
7	IR8.7	8.30-9.10	3
8	IR9.7	9.38-9.94	3
9	IR10.8	9.80-11.80	3
10	IR12.0	11.00-13.00	3
11	IR13.4	12.40-14.40	3
12	HRV	0.40-1.10	1

Table 3-2: Spectral characteristics of SEVIRI instrument.

Due to the fact that the file format of MSG data is not standard, the most commonly and widely used remote sensing packages can not able to open or process the raw compressed images (Maathuis and Retsios 2006). Use of MSG Data Retriever, a software developed at ITC as the most appropriate solution for reading MSG image files was adopted. By making an appropriate choice of spectral channels, area of interest, image acquisition date and time, a time series of MSG images has been constructed for the entire simulation period. Computation of Top of Atmosphere reflectance for the visible channels and Top of Atmosphere temperature (in Kelvin) for thermal channels is possible through the user interface adjustment of the relevant channels. After the MSG image file formats are converted into ILWIS raster format, the entire processing of the images has been done using ILWIS software package.

3.2.1.2. Cloud removal

Cloud contaminated pixels have been removed from each individual image by examining the histogram in such a way that eliminating pixels that have high reflectance and low temperatures. A cloud contaminated pixel will have a high reflectance in the visible channel and a low temperature in the thermal infrared channel. During the months where the cloud coverage is significant in most parts of the study area in rainy seasons, those images fully contaminated with cloud will be discarded and only those scenes which are at least partially free will be aggregated into decadal basis. Water pixels are also masked out in order to obtain only land responses representing vegetation cover.

The visible channels converted into reflectances allow easy computation of NDVI while the 10.8 micron channel converted to temperature has been used as a criterion to eliminate cloudy pixels from a time series of daily images. The temperature thresholds used for cloud removal varies for each day image and they are selected based on the argument that land surface pixels are slightly hotter than cloud contaminated and water pixels. If the pixel element is greater than this threshold temperature value, it is considered as a cloud-free land surface and otherwise it will be masked out. The temperature threshold ranges between 270 to 298 Kelvin. An ILWIS script showing a threshold values used in cloud removal algorithm is given in appendix-B.

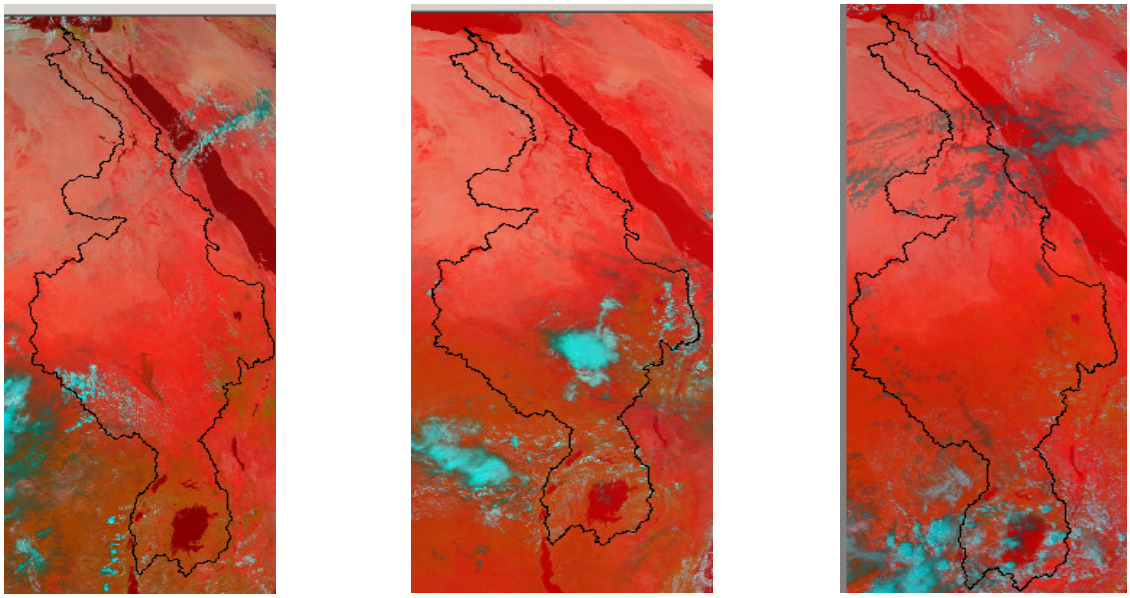

(a)April 1, 2005 at 11:00 UTC (b) June 1, 2006 at 11:00 UTC (C) November 1, 2006 at 11:00 UTC, at a colour composite of VIS 006, VIS 008 and IR 10.8 bands.

Figure 3-7: MSG images at different acquisition date and time for the study area.

The following diagram shows the procedure adopted for removing cloud contaminated pixels from the MSG images.

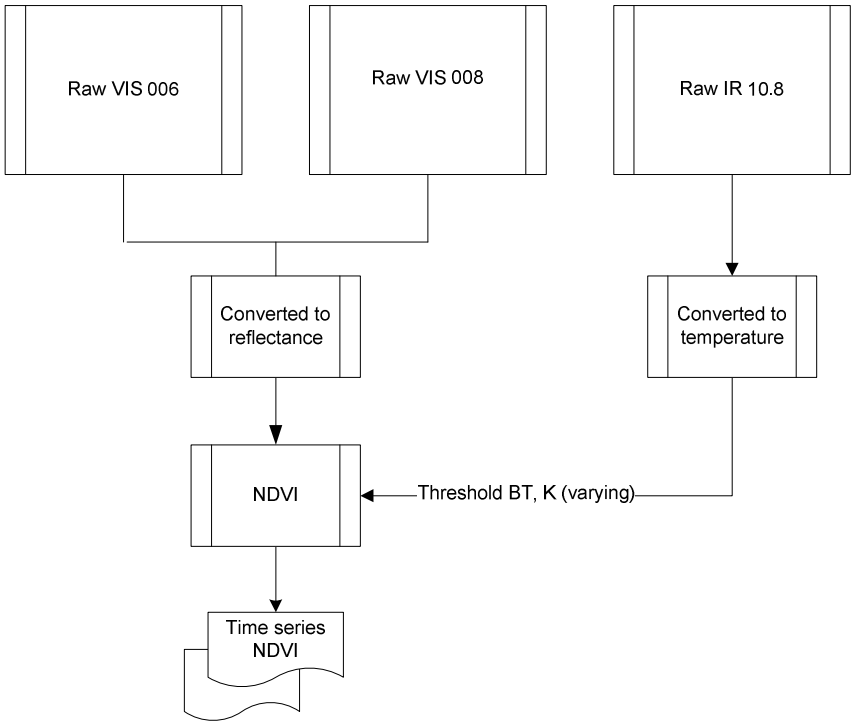

Figure 3-8: Cloud removal procedure.

3.2.2. Post-processing of satellite data to derive drought indices

After the clouds have been removed from each individual daily image and water pixels are masked out, daily NDVI values are computed from the reflectance of the visible and near-infra red bands by using the universally defined formula as follow:

$$NDVI = (NIR-VIS) / (NIR+VIS).$$

Then, daily NDVI's are aggregated into decadal basis. In this way 36 decadal NDVI maps per year are obtained. Finally, each decadal NDVI map is crossed with the cultivated land map of "Amhara" region and aggregation is made by grouping it with the districts in order to get the weighted average NDVI values for each district per decade.

In this study use of three different sensor data with different time series was applied: the NOAA-AVHRR data (1982-2004), SPOT Vegetation data (1998-2005) and Meteosat Second Generation data (2005-2006). Decadal long-term mean, absolute maximum and minimum NDVI value of 23-years was obtained from AVHRR sensor and used as input in computing the drought monitoring indices. Decadal NDVI values from 1998-2005 was obtained from the SPOT Vegetation sensor and current decadal NDVI values for 2005 and 2006 was derived from the Meteosat Second Generation data. The current NDVI values derived from the MSG data was used for computation of all the drought monitoring indices which are adopted in this study for assessment. However, the NDVI's obtained from the SPOT Vegetation are merely used as a surrogate the MSG data for validation of the NDVI with the available eight years agricultural production yield data because the MSG data are only available since 2004. Moreover, inter sensor relationship has been established between the two sensors by taking a time series NDVI data common to both sensors before using for validation. The inter sensor relationship results will be explained in the next chapter, section 4.1.2. The AVHRR and SPOT Vegetation data were prepared data and downloaded from their respective websites whereas the MSG data was entirely own processed for this study.

4. Data processing and results

4.1. Processing of satellite data

4.1.1. Computation of Drought-Monitoring Indices

Drought-monitoring indices are derived from Meteosat Second Generation (MSG) and AVHRR data. They are normally radiometric measures of vegetation condition and dynamics, exploiting the unique spectral signatures of canopy elements and are sensitive to vegetation type, growth stage, canopy cover and structure. They utilize reflectance data in two spectral bands, thus enhancing the vegetation signal and cancelling out the effects of topography, sun angle and atmosphere (Thenkabail 2004).

4.1.1.1. Computation of Drought Severity Index (DSI)

NDVI by itself does not reflect drought or non-drought conditions. Thus, the severity of a drought or the extent of wetness can be expressed by drought severity index. This index is defined as a measure of the deviation of the current NDVI values from their long term mean. In this study the current NDVI values are computed for year 2005 and 2006 on decadal basis, i.e. 36 decadal NDVI maps per year. Decadal long-term mean NDVI maps of 23-years (1982-2004) have been derived from NOAA-AVHRR results, which are freely accessible.

$$DEV_{NDVI} = NDVI_i - NDVI_{mean,\ m}.$$

Where:
$NDVI_i$ is the NDVI value for month i and $NDVI_{mean,\ m}$ is the long-term mean NDVI for the month m. for example; in AVHRR data record from 1982 to 2004, there has been 36 long-term decadal NDVI maps. When DEV_{NDVI} is negative, it indicates the below normal vegetation condition/health and, therefore suggests a prevailing drought situation.

An ILWIS script used for calculation of the severity index is found in appendix-B.

4.1.1.2. Computation of Water supply Vegetation Index (WSVI)

This index can be computed as follow:

$$WSVI = NDVI/T_b$$

Here, Decadal NDVI values are divided by their respective brightness temperature to obtain WSVI on decadal basis.

An ILWIS script used for calculation of this index is found in appendix-B.

4.1.1.3. Computation of Vegetation Condition Index (VCI)

$$VCI_j = \frac{(NDVI_j - NDVI_{min})*100}{(NDVI_{max} - NDVI_{min})}$$

Where, $NDVI_{max}$ and $NDVI_{min}$ are calculated from the long-term record for that month, and j is the index of the current month. Here, NDVImax and NDVImin are derived from NOAA-AVHRR data records of 23-years (1982-2004). There are 23 decadal NDVI values of the same decade. From these NDVI value sets it is possible to obtain the maximum and minimum values for each decade using map list statistics function.

Figure 4-5 shows the VCI that describes the moisture condition. The high value of VCI (the red area) corresponded to unstressed vegetation or undrought condition and the VCI close to zero percent reflects an extremely dry month. The duration of the successive months below normal conditions and magnitude of the deviation are two powerful indicators of drought severity. In this case, the VCI and DEVndvi have similar pattern, therefore it is expected they will have strong correlation that could be used to monitor the drought.

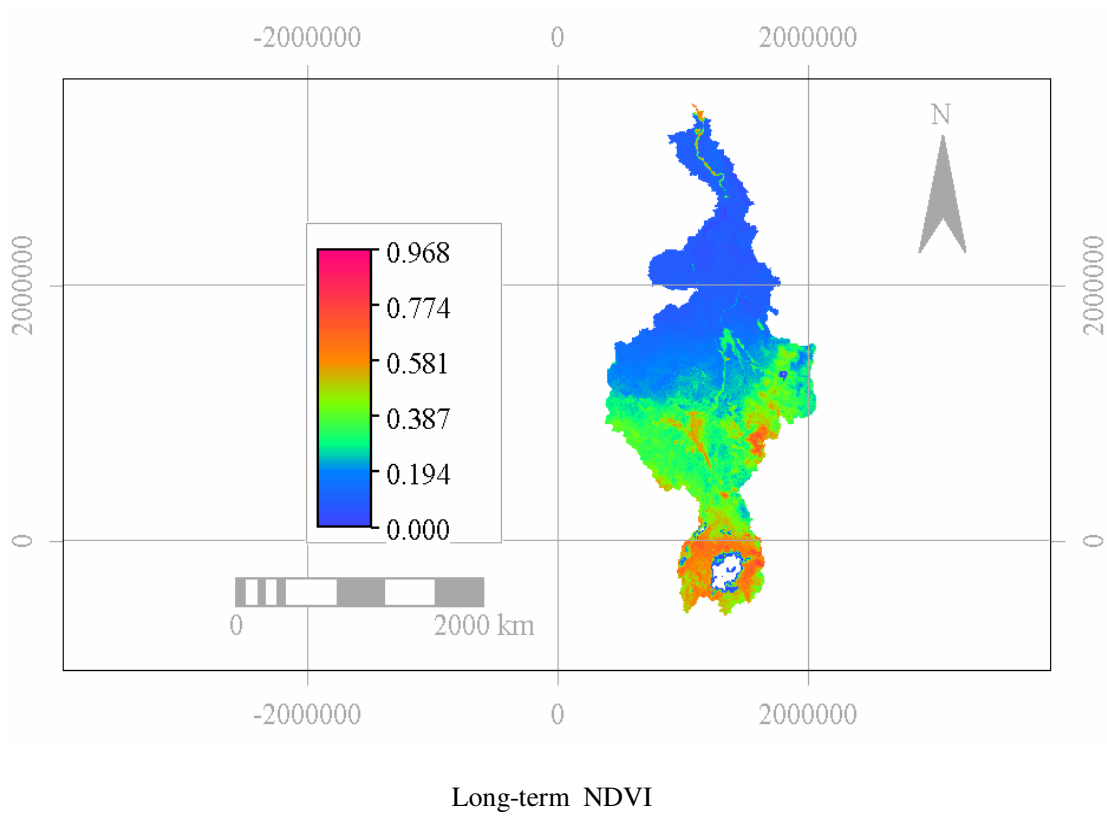

Long-term NDVI

Figure 4-1: Decadal long-term mean of NDVI map for the first decade of January.

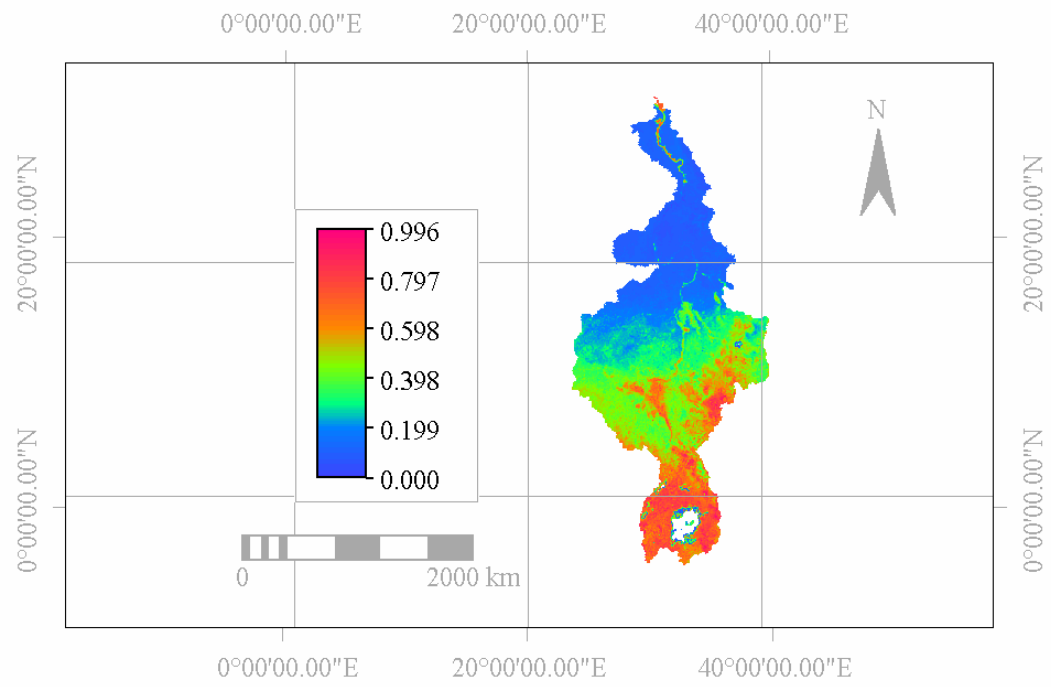

(a) Absolute maximum

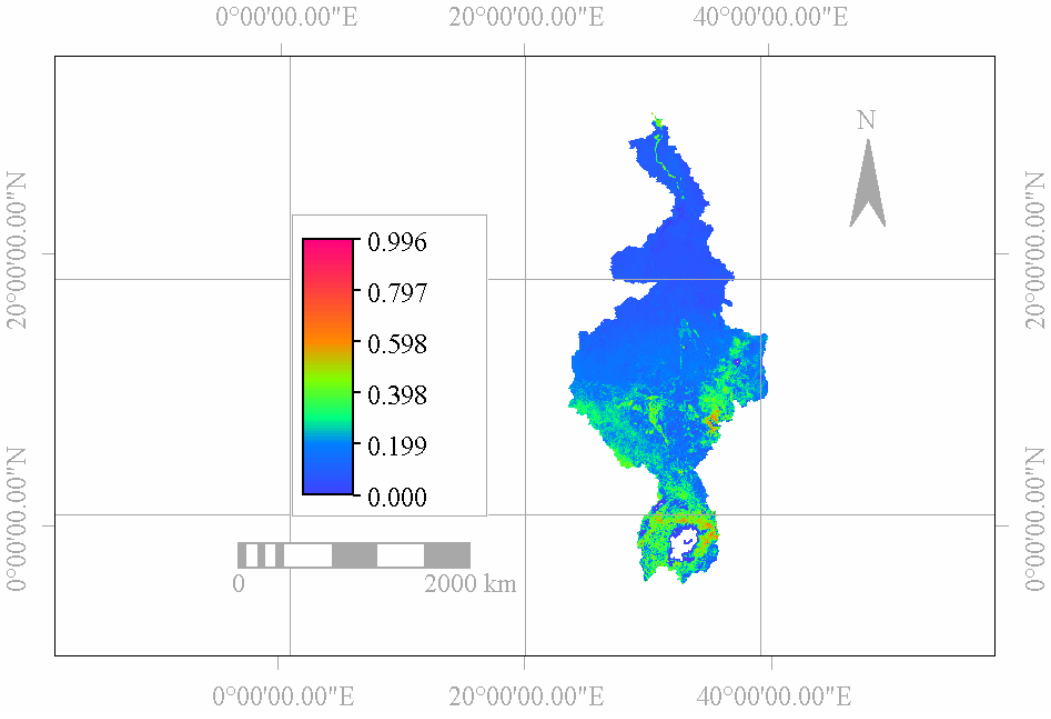

(b) Absolute Minimum

Figure 4-2: Maximum and Minimum NDVI maps derived from long records of remote sensing data for first decade of January.

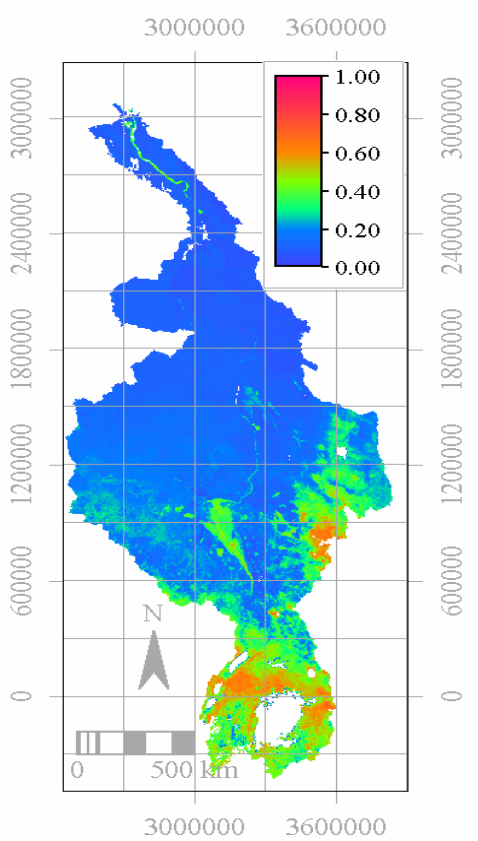

(a) Current NDVI of first decade of January, 2005.

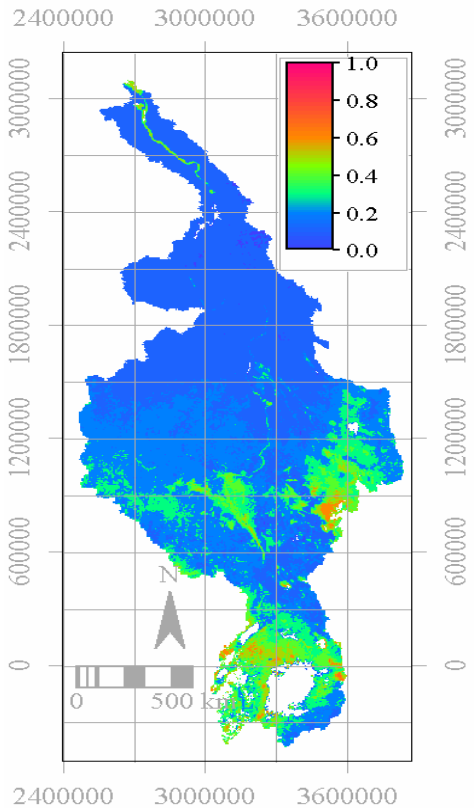

(b) Current NDVI of first decade of January, 2006.

Figure 4-3: Current NDVI maps computed from MSG images for first decade of January 2005 and 2006.

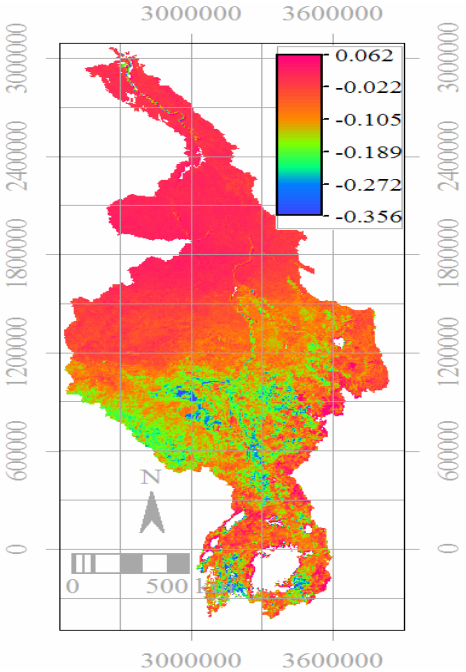

(b) DSI for first decade of January 2005.

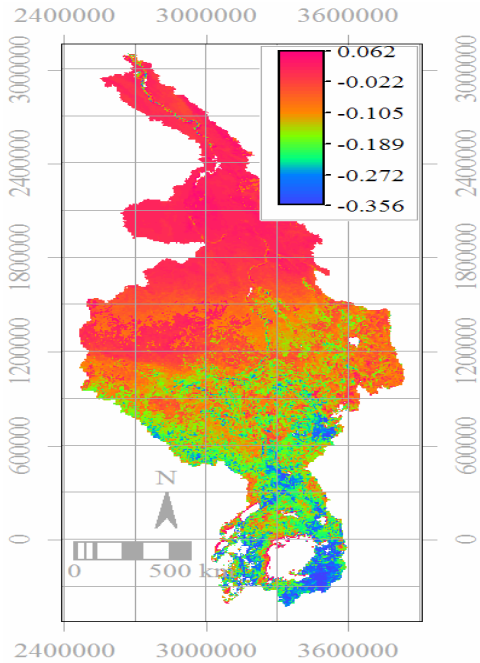

(b) DSI for first decade of January 2006.

Figure 4-4: Drought Severity Index (DSI) for first decade of January 2005 and 2006.

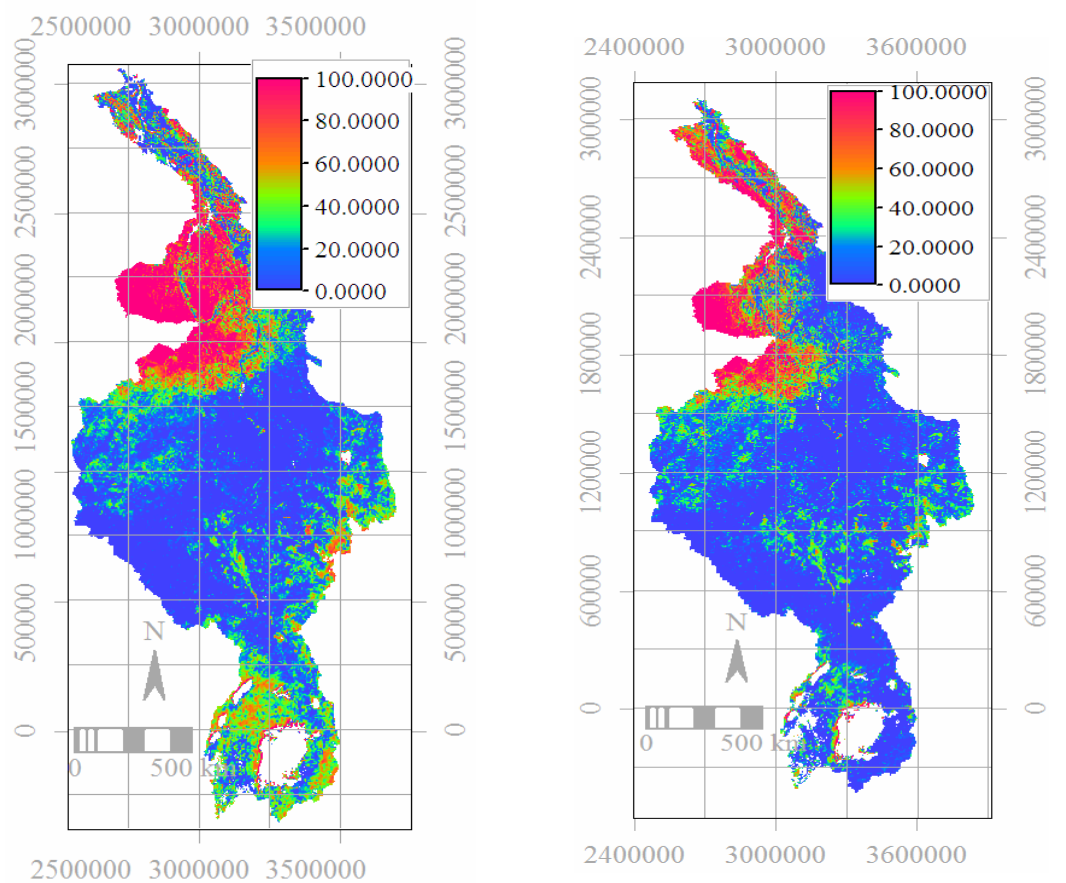

(a) VCI map of first decade of January, 2005.

(b) VCI map of first decade of January, 2006.

Figure 4-5: Vegetation Condition Index (VCI) for first decade of January 2005 and 2006.

4.1.1.4. Computation of Temperature Condition Index (TCI)

TCI is based on brightness temperature and represents the deviation of the current month's (decade's) value from the recorded maximum.

$$TCI_j = \frac{(BT_{max} - BT_j)*100}{(BT_{max} - BT_{min})}$$

Where, BT_j, BT_{max} and BT_{min} are the averaged decadal temperature, its multi-year absolute maximum and the absolute minimum respectively, and j defines the decade in each month. The TCI is similar to the VCI, except that the formula was modified to reflect the response of vegetation to temperature. Persistently, high temperatures (low TCI) during the rainy season are usually associated with drought condition. Here, the absolute maximum and minimum brightness was obtained from the daily brightness temperatures records for two year, 2005 and 2006.

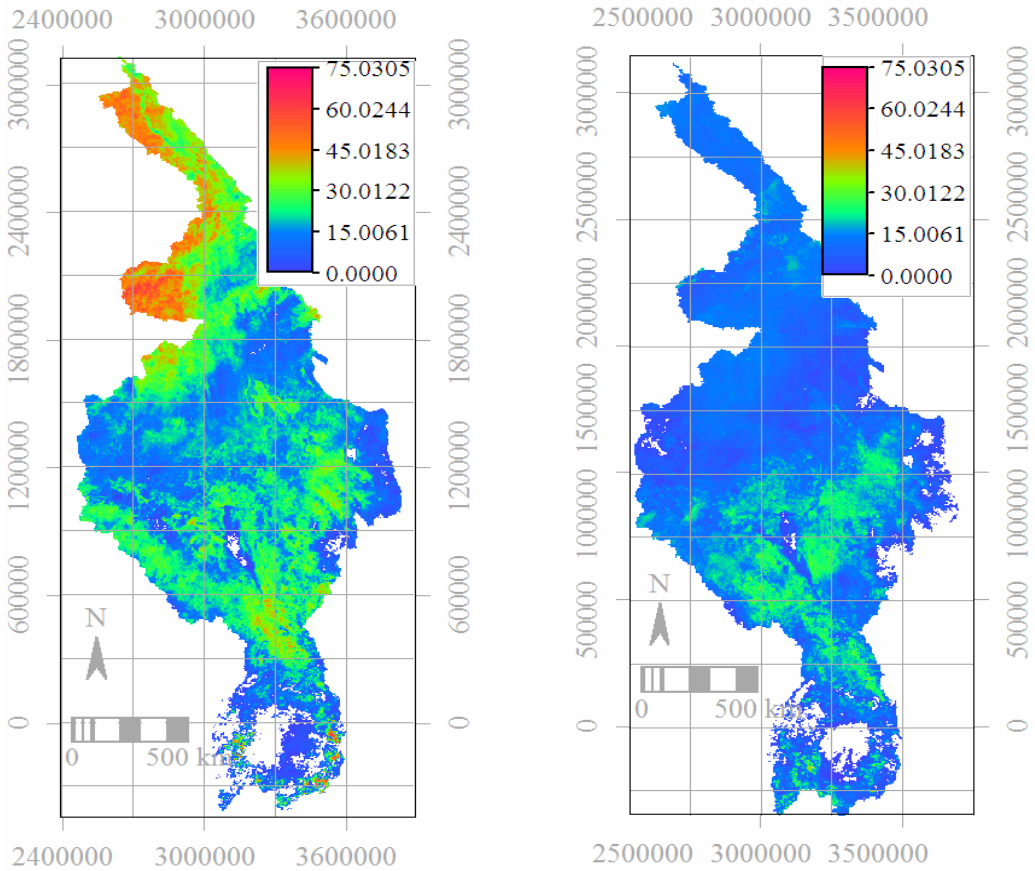

(a) TCI map of 1st decade of January, 2005 (b) TCI map of 1st decade of January, 2006

Figure 4-6 : Temperature Condition Index (TCI) for the first decades of January, 2005 and 2006.

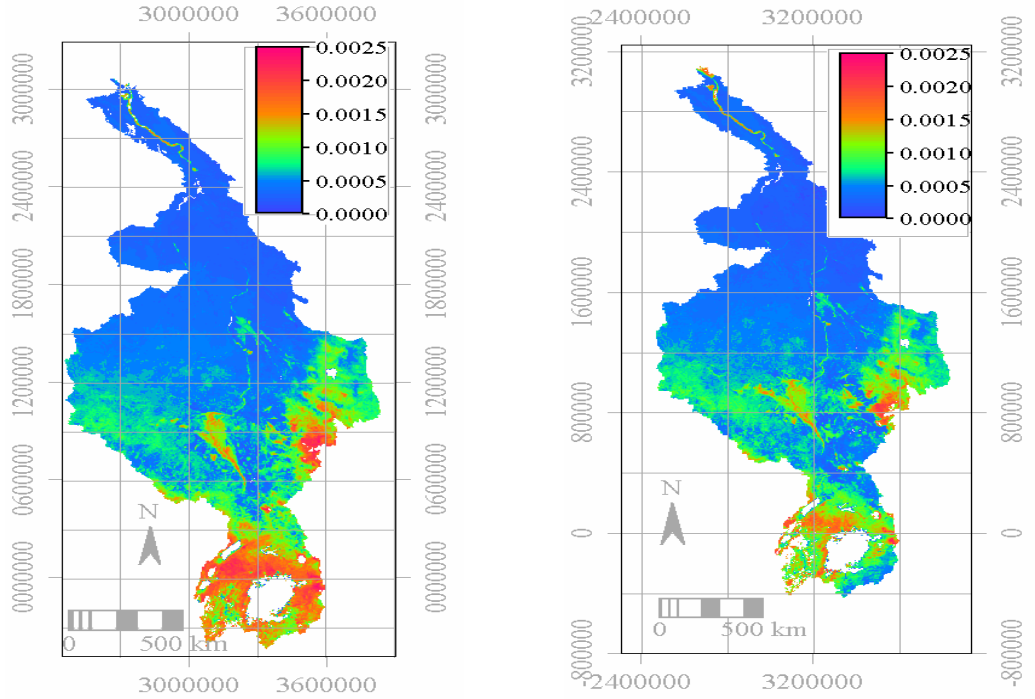

(a) WSVI map of 1st decade of January, 2005 (b) WSVI map of 1st decade of January, 2006

Figure 4-7: Water Supply Vegetation Index (WSVI) for the first decade of January, 2005 and 2006.

At the TCI of around 50%, the fair or normal temperature condition exists. When TCI values are close to 100%, the brightness temperature for this decade is equal to the long-term minimum for the pixel. Low TCI values (close to 0%) indicate very hot weather in that decade. When TCI is equal to zero percent, brightness temperature for the corresponding decade is equal to maximum long-term brightness temperature for the pixel. Consistently low TCI values over several consecutive time intervals may point to the drought development.

An ILWIS script used for calculation of the Temperature condition index is found in appendix-B.

4.1.2. Inter-Sensor relationship

4.1.2.1. Deriving NDVI from MSG data

Maximum value composite (MVC) technique for computation of maximum NDVI from a set of multi-temporal data can not be applied to MSG as NDVI exhibit variations which are not related with the ground cover, due to changes in solar zenith and azimuth angles (Lacaze and Berges 2005). Instead, the other way approach that employs the identification of maximum value during the day as an efficient mean to eliminate pixels contaminated with clouds or cloud-shadows, characterized by low temperature is used. This alternative technique applies a 2-step procedure, first daily compositing is implemented through analysis of thermal data (maximum surface temperature compositing) followed by decadal synthesis.

4.1.2.2. SPOT VEGETATION NDVI

Decadal NDVI data are freely available from SPOT VEGETATION distributor (VITO 2005). NDVI data can be obtained for the whole continent of Africa (38^0N to 35^0S, 26^0W to 60^0E) in a geographic projection, with a spatial resolution of 0.00892857 degree (i.e. approximately 1 km). The size of image is 9633 × 8177 pixels. NDVI data are given in byte format. Then, it has been converted into its normal NDVI range by the relationship mentioned earlier as:

$$NDVI = 0.004 * NDVI - 0.1$$

From these decadal NDVI values of the continent Africa, the values for the study area, Nile Basin, has been extracted. The SPOT VEGETATION NDVI is currently available since the first decade of April, 1998 to the third decade of December, 2005.

4.1.2.3. Correlation of MSG SEVIRI and SPOT data

As the data for MSG sensor is available since 2004 and only those data starting from the first decade of January, 2005 to the third decade of December 2006 has been processed in this study, use of the products from the other sensor, SPOT VEGETATION, is found important to validate the satellite derived results with the ground truth data: agricultural production yield and rainfall. In order to use the products of the two sensors data, first, comparison of the MSG derived products with the similar product obtained from the SPOT-VEGETATION shall be made by taking the same compositing period. Thus, the first decade of January, 2005 (January 1-10, 2005) has been taken to make such a comparison.

To compare with MSG data, SPOT VEGETATION NDVI image has been re-sampled at 0.025 degree which is the spatial resolution of the MSG sensor, because the spatial resolutions of the two sensors are different. Histograms of the re-sampled SPOT-VEGETATION NDVI and the derived MSG SEVERI NDVI are presented at Figure 4-8. One can notice the wider range of values of SPOT VEGETATION data, which can be explained by the fact that atmospheric corrections have been applied prior to computation of NDVI values (Lacaze and Berges 2005).

Finally, the two maps are crossed with each other to see the pattern of correlation between them and also correlation has been made by taking the aggregated decadal NDVI values of the two sensors for all districts in Amhara region in 2005. Then, the result showed that the correlation between SPOT VEGETATION NDVI and MSG SEVERI NDVI appears rather high (see, Figure 4-9), with a correlation coefficient r^2 = 0.92. Therefore, it looks reasonable to use the SPOT VEGETATION NDVI as a proxy of the MSG NDVI for validation purpose.

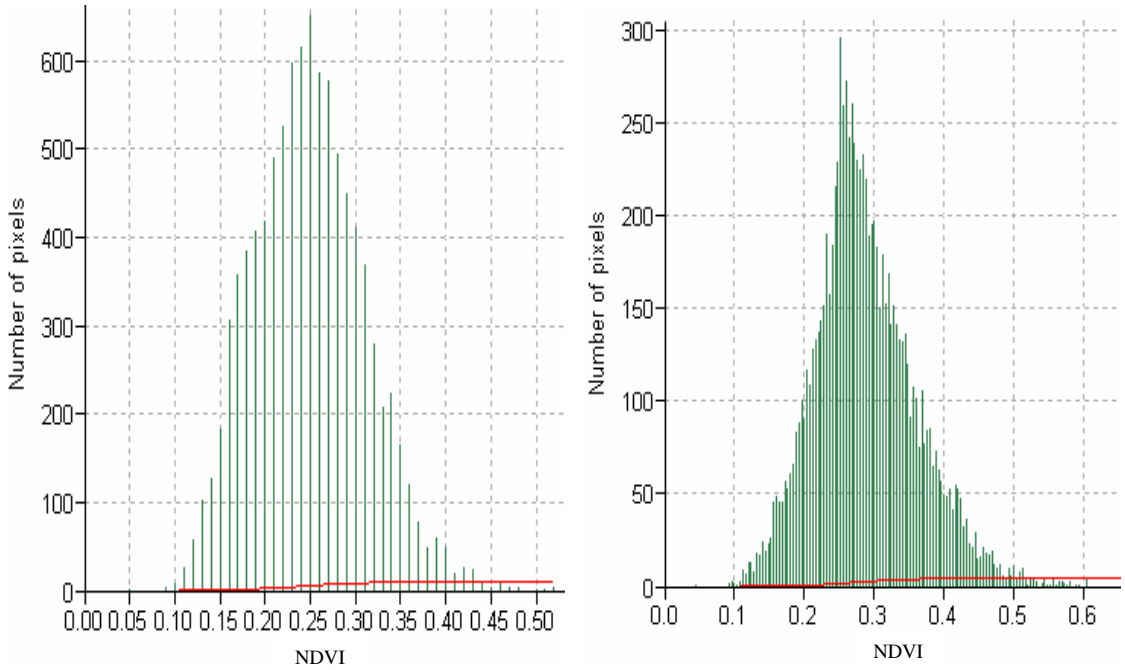

MSG NDVI

SPOT NDVI

Figure 4-8: Comparison of Histograms of MSG and SPOT VEGETATION NDVI

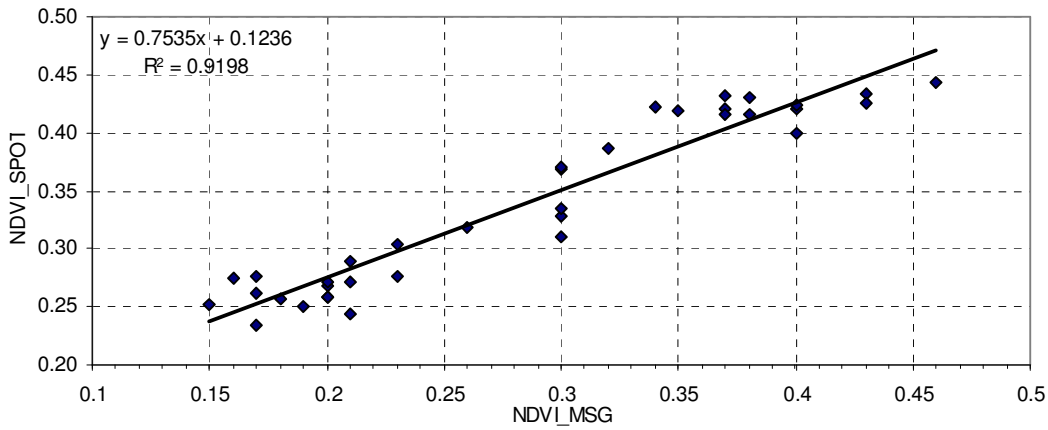

Figure 4-9: Graph showing the relation of MSG and SPOT NDVI for North Gondar

4.1.3. NDVI anomaly

To derive the seasonal pattern of NDVI for the period 1998-2005 which is the period agricultural production yield is available for this study, firstly, average NDVI for each year over the growing season was computed by using a map list stastics function in ILWIS GIS package. To derive NDVI anomaly it is also essential to get the maximum NDVI in all the growing season, which is June to October in this case. Thus, maximum NDVI has been computed for the growing season for each year from 1998-2005, so as to minimize effects of cloud contamination. NDVI composites using the maximum value compositing procedure minimises effects of cloud contamination, varying solar zenith angles and surface topography (Anyamba and Tucker 2005). Then, NDVI anomaly has been computed as:

$$\text{Anomaly NDVI}_{i} = ((\text{NDVI}_{max,\,i} - \text{mean NDVI}_{max}) / (\text{mean NDVImax}))*100$$

Where, Anomaly NDVI_{i} is NDVI anomaly in i^{th} year, NDVI_{max} is the maximum NDVI and mean NDVI_{max} is the average of maximum NDVI.

4.2. Processing of ground truth data

4.2.1. Production yield anomaly

Agricultural production yield is the main ground truth data used for validation of the satellite derived results. It is important to analyse the correlation between district level crop yields and NDVI to quantify the impact of drought on production of the major crops in the districts of the “Amhara” region. Since NDVI takes advantage of the reflective and absorptive characteristics of plants in the red and near-infra red portions of the electromagnetic spectrum, it can be used for assessment of weather impacts on vegetation and evaluation of vegetation health and productivity (Unganai and Kogan 1998). Yield trend have been computed on district basis and the yield anomaly has been calculated in the same fashion as the computation of NDVI anomaly.

4.2.2. Rainfall processing

Decadal (10-days) records of 18 stations found in the "Amhara" region which are spatially distributed over the districts are arranged into spreadsheets, provided by the Ethiopian Meteorological Service Agency. Rainfall data for the crop-growing season ranging from June to October have been summed up to get the total rainfall received during this period in each year (1996-2005). Since the rain gauge data are point measurements, use of inverse-distance moving average interpolation technique has been applied to obtain the contribution of each station over the areas. Inverse distance average technique is used because it better suits for interpolation of rainfall distribution over heterogeneous topographical terrain, as that of the "Amhara" region. Thus seasonal rainfall interpolated maps for 8-years have been prepared to establish relationship of rainfall variability with NDVI and agricultural yield production.

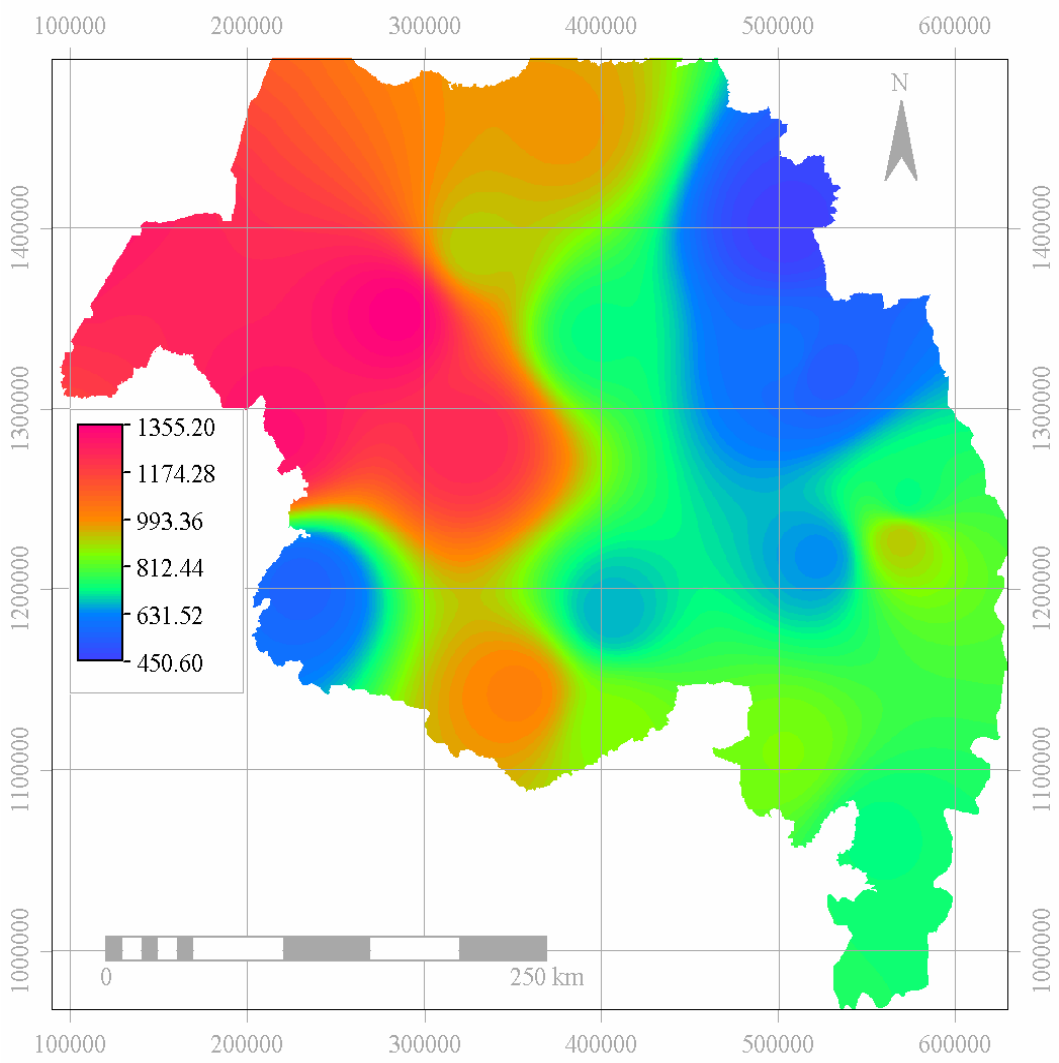

Figure 4-10: Total rain fall distribution of Amhara region for the growing season of 2005

5. Discussion and analysis of results

5.1. MSG data as a tool for a real time drought assessment

The decadal NDVI, VCI and TCI data have been deduced from MSG data for the period of 2005 and 2006. The NDVI has two components: the ecology and the weather. The estimate of the impact of weather on vegetation is possible only after separating the variability of NDVI which is related to the contribution of geographic resources. The ecosystem component is mainly controlled by slow changing environmental factors: climate, soil, topography and vegetation type, which determine the distribution of vegetation on land. The weather component of NDVI is controlled by weather parameters such as rainfall, which reflect the vegetation state and greenness. The weather component of NDVI is superimposed on the ecosystem component. Maximum vegetation is developed in years with optimal weather, since such weather stimulates efficient use of ecosystem resources. In contrast, minimum vegetation is developed in years with extremely unfavorable weather, which suppresses vegetation growth both directly and through a reduction in the rate of ecosystem resources. The absolute maximum and minimum NDVI calculated from several years' data that contain the extreme weather events can be used as a criterion for quantifying these extreme conditions. The highest and the lowest NDVI values during 1982-2004 for each of the 36 decades in a year and for each pixel have been obtained from NOAA-AVHRR data and downloaded from the Famine Early Warning System (FEWS-NET) site. The resulting maximum and minimum NDVI have been used as a criterion for estimating the upper favorable and the lower unfavorable limits of weather conditions.

Figure 5-1 shows the absolute maximum, minimum and the current NDVI curves of 2005 and 2006 for North Gondar districts. Similar curves for the other districts are given in appendix-C.

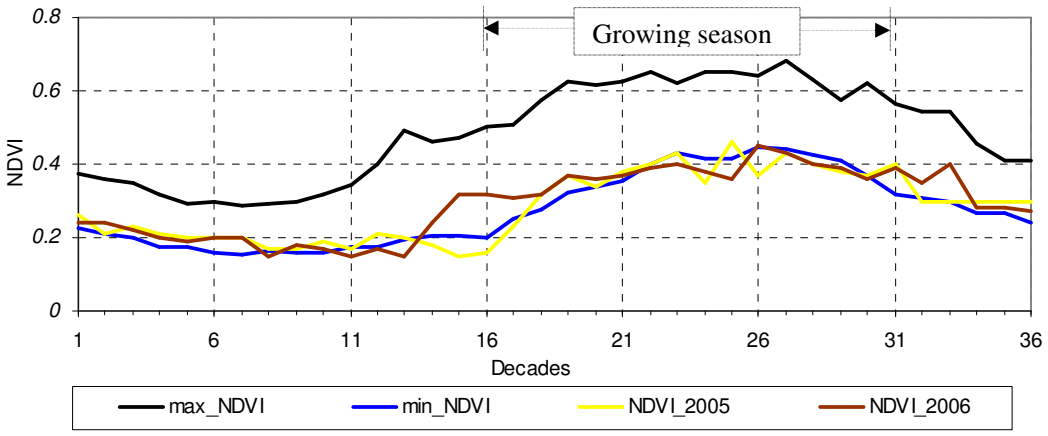

Figure 5-1: Absolute maximum and minimum, 2005 and 2006 NDVI curves for North Gondar district.

5.2. DSI, VCI and TCI as a tool for drought detection

5.2.1. Drought Severity Index (DSI)

As mentioned earlier the drought severity index (DSI) is an index which shows the deviation of the current NDVI from its long-term mean, accordingly it reveals the drought or non-drought condition based on the threshold value of the deviation, which is zero. Thus, in the periods where the difference of the current NDVI from its long-term is negative, it means that there is a prevailing of the drought situation though its severity varies on the magnitude of the deviation. So, the results obtained in this study indicate an existence of drought condition for all the decades of the year 2005 and 2006 in accordance with the criteria of the Drought Severity Index (DSI). Here under, the temporal profiles of the drought severity index for two districts (North Gondar and West Gojam) in 2005 are shown.

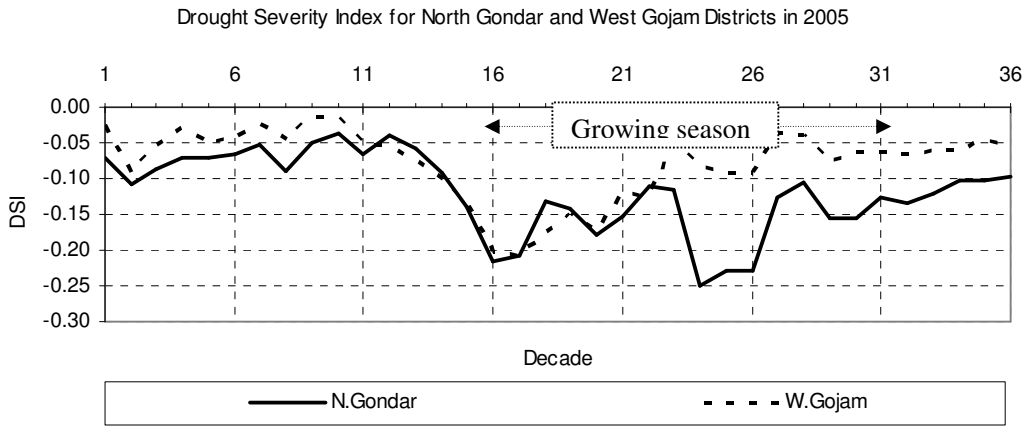

Figure 5-2: Temporal profile of Drought Severity Index for North Gondar and West Gojam Districts in 2005.

From the plot of temporal profile, it can be seen that the deviation of the current NDVI values from their respective long-term mean is higher in the decades from 15 to 27, which are the main rainy season in the demonstration region of the study area and less in the other decades, especially for the North Gondar district. This could indicate existence of a drought condition during the main growing season of the districts, which implies unfavourable vegetation condition of the area and hence implies reduction of the production yield from the long-term yield trend. Similar temporal profiles of the drought severity condition can be observed for all of the districts in the “Amhara” region.

Since the deviation is less than 0.10 for the consecutives decades ranging between 4-12 and 33-36, the drought severity condition in these decades of the year can be categorized as mild drought. In the decades between 12-14 and 27-33 the deviation ranges between 0.1 and 0.15, this shows a moderate drought severity condition and the deviation is above 0.15 for the consecutive decades between 15 to 27, which prevails a severe drought situation that can possibly lead to a substantial yield reduction below average yield in the area.

In the same way the temporal profile of the Drought Severity Index (DSI) has been constructed for the year 2006 for the above-mentioned districts is presented in Figure 5-3.

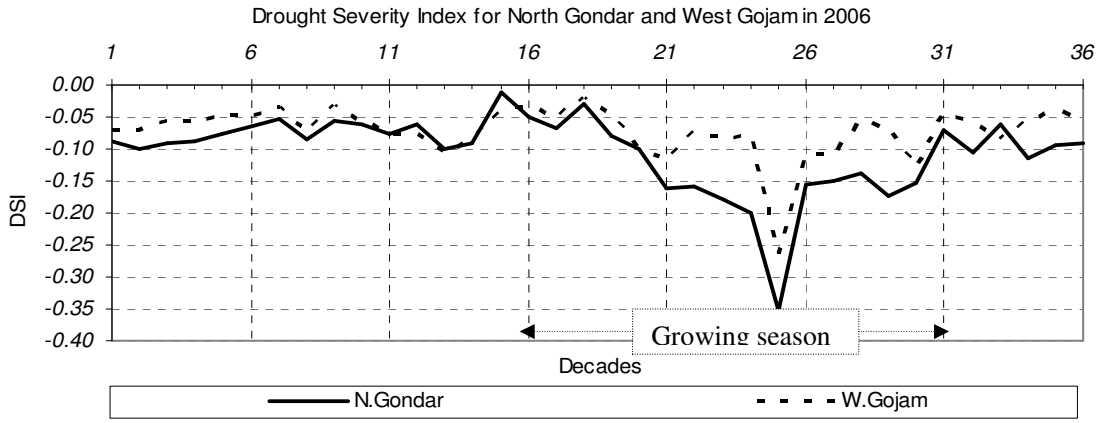

Figure 5-3: Temporal profile of Drought Severity Index for North Gondar and West Gojam Districts in 2006.

However, the drought severity class situation in 2006 is somewhat different from the previous year in that the deviation below 0.1 extends from the first decade up to 21st and between decades 31-36, that can be categorized under mild drought severity class. The deviation is between 0.10 to 0.15 for the decades ranging 22-24 and 27-30, and above 0.15 for the decades between 24 to 27 which show a moderate and severe drought condition respectively. Here the severe drought condition is reduced and restricted in only one month of the growing season. So that a better yield production is expected than the former year 2005. Furthermore, a mild drought condition prevailed during most of the other decades of the year. The results explained so far can be supplemented by the precipitation variation in 2005.

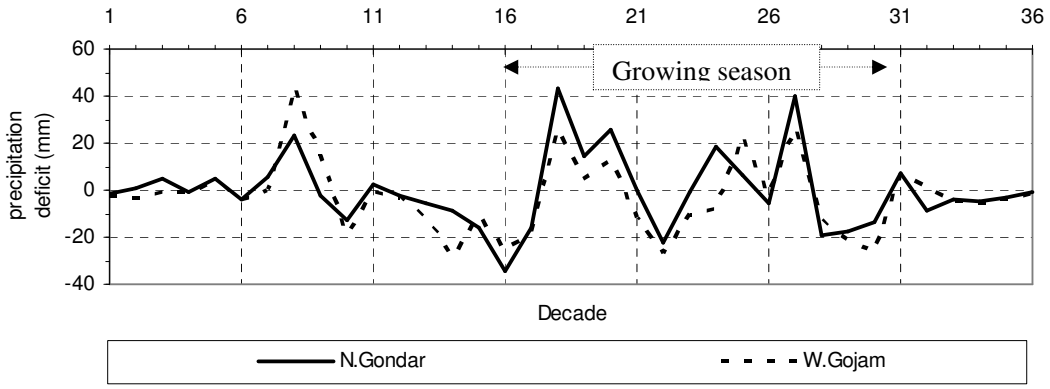

Figure 5-4: Temporal profile of precipitation deviation from the long-term mean for North Gondar and West Gojam districts in 2005.

The temporal profile precipitation variation in 2005 for the two districts shows a deficiency of the current precipitation from their respective long-term mean in most of the decades, which coincides with the result obtained by the drought severity index (DSI). The total yearly precipitation deficit of 2005 for North Gondar and West Gojam districts is found to be 8.65mm and 10.38 mm respectively. Therefore, this also supplements the existence of drought condition in the districts.

5.2.2. Vegetation Condition Index (VCI)

In order to reflect the ecosystem's features and separate the weather signal from the ecological signal, using multiyear observations, the NDVI was converted into the Vegetation Condition Index (VCI), which was applied successfully for drought monitoring and assessment of vegetation condition over most parts of the globe. It has become clear that no single indicator or index is adequate for monitoring drought on a regional scale; instead, a combination of monitoring tools integrated together is preferable for producing regional or national drought maps (MARTINI, SOUMARE et al. 2004).

In this study the Vegetation Condition Index (VCI) has been computed for the year 2005 and 2006 from MSG images. The results obtained clearly show that there is an existence of drought situation in both years. The temporal variation of the VCI values for the two districts, North Gondar and West Gojam, is shown in Figure 5-5.

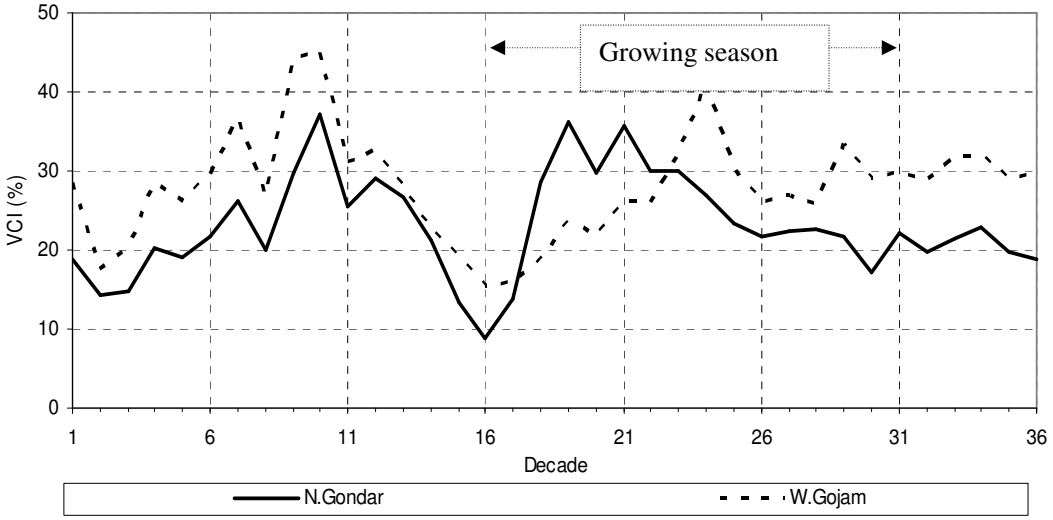

Figure 5-5: Temporal variation of VCI for North Gondar and West Gojam in 2005.

It can be seen from this figure that the Vegetation Condition Index (VCI) values are below 50% for all the decades of the year for both districts. In general, this indicates the occurrence of drought situation in this year. However, the VCI values are different from decade to decade ranging between 8-48%, which indicates that the drought severity condition is different over all the decades. At the start of the growing season, that is June (decade16) the values goes beyond 20% up to 10% and then grows slowly up to 40%, indicating an improvement of drought severity condition in the rest of the growing season. But, the VCI values are fairly above 20% in most of the decades other than the growing season. In general, the VCI values falls below 35% for most of the decades in the year that reveals an existence of drought severity according to the recommendation suggested by the developer of the Vegetation Condition Index (VCI). Furthermore, the result obtained by this index is complementary with results obtained by the other index, the drought severity index. Also the temporal profile of the Vegetation Condition Index (VCI) is constructed for the year 2006 for the above mentioned districts and shown in Figure 5-6.

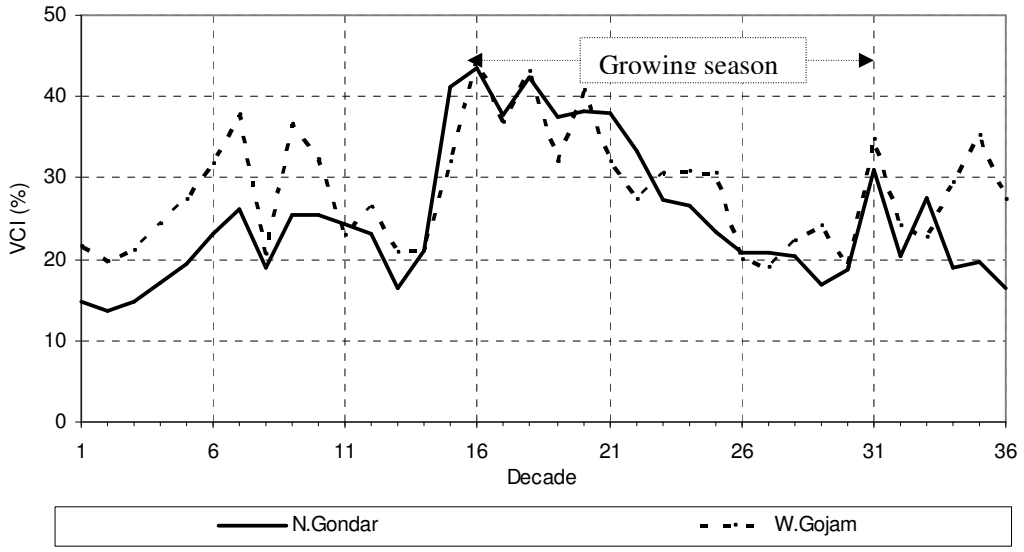

Figure 5-6: Temporal variation of VCI for North Gondar and West Gojam in 2006.

The Vegetation Condition Index (VCI) in 2006 has been improved at the beginning of the growing season and starts to decrease slowly thereafter. In this year also the Vegetation Condition Index is below 35% for most of the decades, indicating existence of drought for all the districts in the region. As VCI values for the growing season is fairly high during the growing season compared to that of the previous year, it is expected that a better agricultural production yield will be obtained in 2006. Here also the results obtained from the Vegetation Condition Index show similarities with the results of the other index, the Drought Severity Index (DSI). These results can be verified by in situ data of precipitation and crop yield collected from the "Amhara" region. The relation of the VCI and precipitation for the growing season of 2005 for one of the districts is given in Figure 5-7 and similar graphs for the other districts are given in appendix-D. There exists a fairly good relationship between the Vegetation Condition Index (VCI) and precipitation.

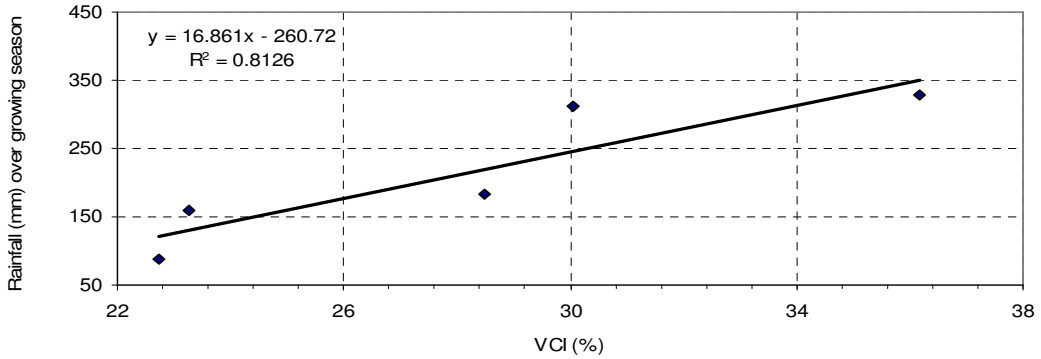

Figure 5-7: Correlation between the Vegetation Condition Index (VCI) and precipitation for North Gondar district

Moreover, the Vegetation Condition Index has been correlated with the total production yield of all the districts in 2005 and has shown a strong correlation. As satellite based radiative indices are a good

indicator of leaf area index, therefore the NDVI was found to correlate with agricultural production yield (Unganai and Kogan 1998), it is expected here also to find a good relation between the agricultural production yield of administrative region and the developed drought indices like the Vegetation Condition Index (VCI). A plot showing correlation of the VCI with yield is shown in Figure 5-8.

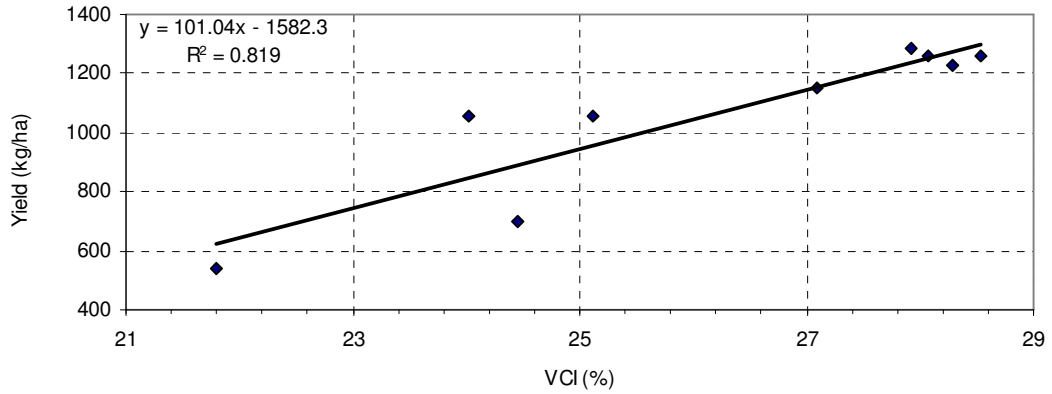

Figure 5-8: Correlation between the Vegetation Condition Index (VCI) and agricultural production yield in 2005.

5.2.3. Temperature Condition Index (TCI)

The Temperature Condition Index (TCI) is based on the thermal band converted to Top of Atmosphere Brightness Temperature (BT). TCI is used to determine temperature-related vegetation stress and also stress caused by excessive wetness. In combination with meteorological observations, the relationship between surface temperature and the moisture regime on the ground will detect drought-affected areas before biomass degradation occurs and hence TCI can play an important role in drought monitoring (Thenkabail 2004). The Temperature Condition Index (TCI) reflects different response of vegetation to temperature. High temperatures in the middle of the growing season indicate unfavorable conditions for drought, while low temperatures indicate favorable conditions. The TCI has been computed for 2005 and 2006 and their temporal variation is shown for the two districts.

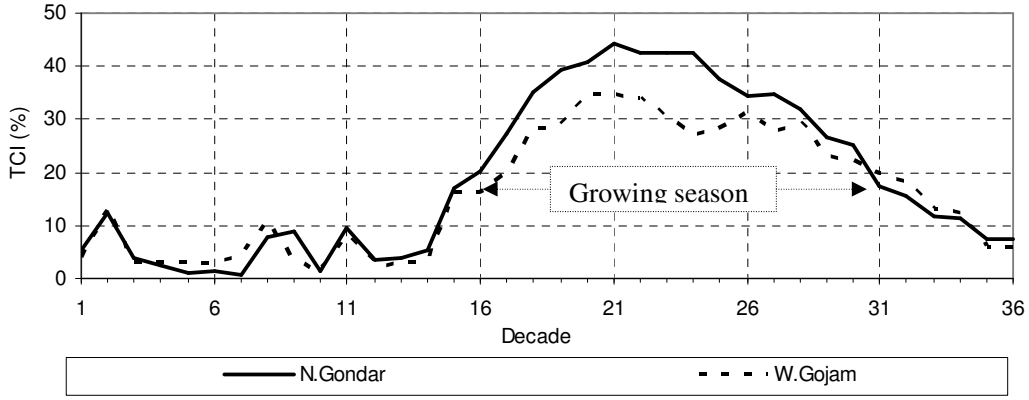

Figure 5-9: Temporal variation of TCI for North Gondar and West Gojam in 2005.

The result shows a TCI value of below 50% for all the decades in 2005 for all the districts in the region. The value is above 35% in the middle of the growing season and below 35% for all the rest decades of the year. Hence, it shows existence of drought condition in all the decades which is consistent to the results revealed by the other drought-monitoring indices. Also, the TCI variation for 2006 has been given below in Figure 5-10.

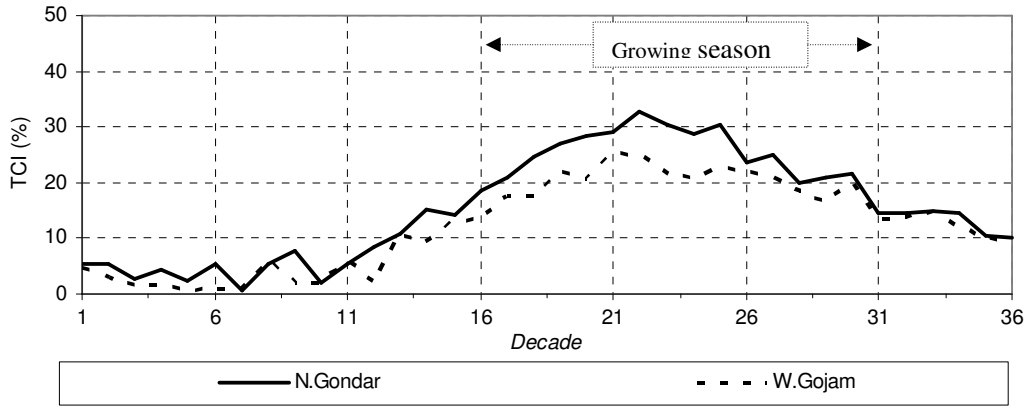

Figure 5-10: Temporal variation of TCI for North Gondar and West Gojam in 2006.

The Temperature Condition Index (TCI) indicates similar pattern of seasonal variation in 2006 except all the values falls below 35% for all the decades in the year. Since the TCI values are very low for the consecutive decades, it shows the on-set of severe drought development.

The satellite-derived TCI values have been verified by correlating with the ground truth data of both precipitation and total agricultural yield of the districts. There exists a good relationship between the TCI values and the rainfall as it is shown in Figure 5-10.

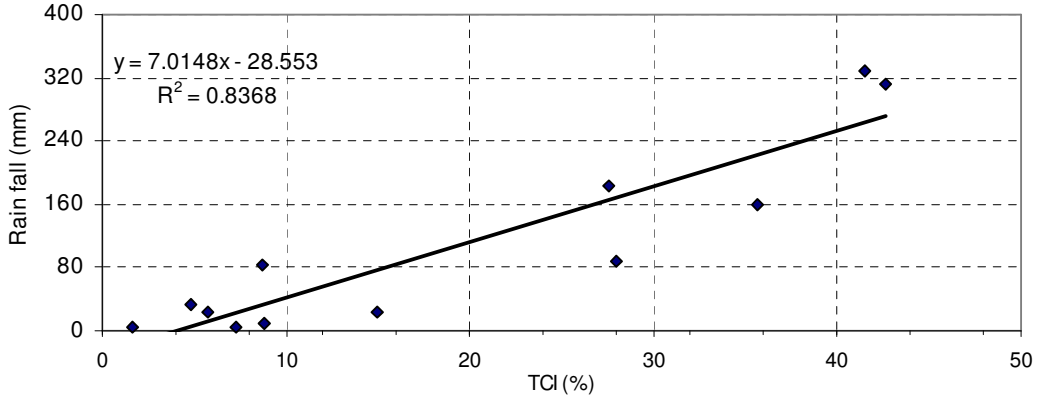

Figure 5-11: Correlation between the Temperature Condition Index (TCI) and precipitation for North Gondar district.

Moreover, the Temperature Condition Index is fairly correlated with the agricultural production yield for the year 2005. So, the satellite-derived results can be used for the assessment of drought development and monitoring in the region.

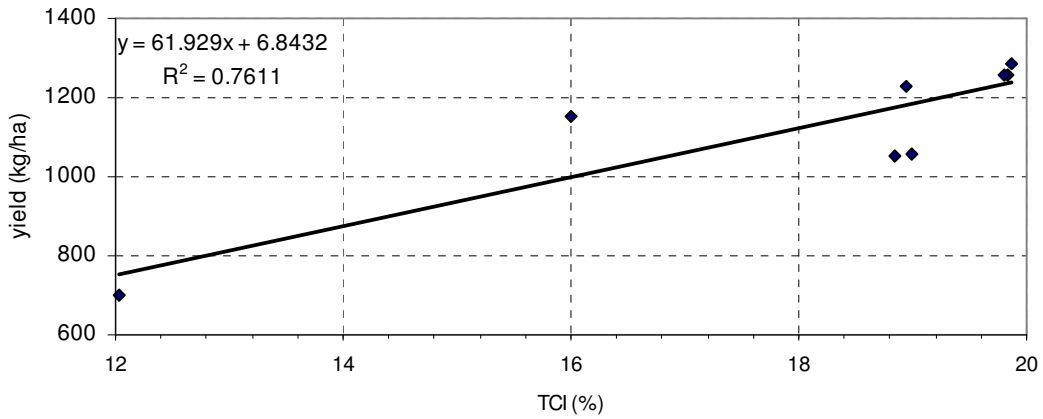

Figure 5-12: Correlation between the Temperature Condition Index (TCI) and agricultural production yield in 2005.

5.3. Validation

5.3.1. Relationship between NDVI and precipitation

Theoretically, NDVI can be considered as a climatic recorder mainly rainfall. According to studies of (Henericksen 1986) cited in (Y.Richard and I.Poccard 1998), it has been shown that NDVI was highly sensitive to an extended rainfall anomaly, the 1984 Ethiopian drought. Moreover, a study by (Anyamba and Tucker 2005) concluded that there exists strong correlation between NDVI and rainfall. In this study, the monthly NDVI was calculated as the average of consecutive three decades in each month, whilst the sum of the rainfall in the three decades of the same month was assigned as the monthly rainfall. The correlation between NDVI and rainfall was computed for all the districts and maximum correlation is obtained for a lag time of three months. The districts under study have varying proportions of vegetated and non-vegetated areas. Different classes of vegetated area are forest and agricultural areas. Non-vegetated area includes bare soil and land reserved to non agricultural use. The graph below shows the correlation of monthly NDVI and rainfall for North Gondar district in 2005. Graphs for other districts are presented in the appendix-F.

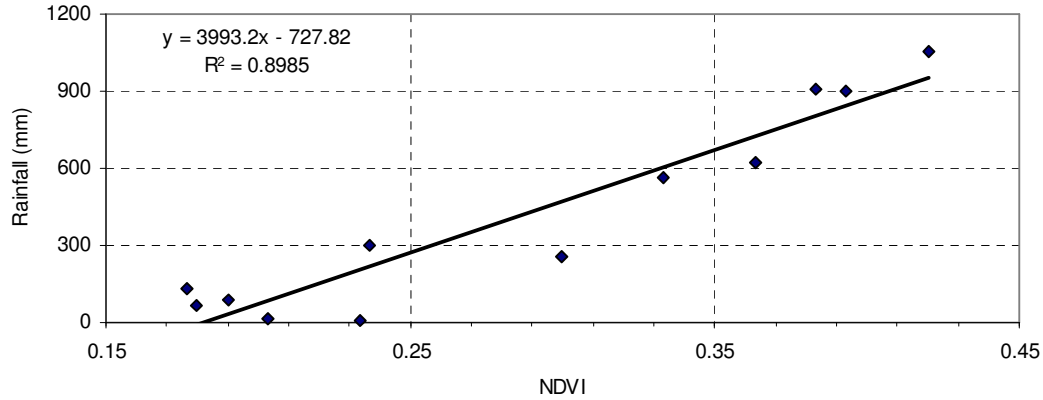

Figure 5-13: Graph showing the relationship between monthly NDVI and 3-months lag time precipitation for North Gondar district in 2005.

Table 5-1 gives the correlation coefficients for all the districts in Amhara region for 10-day and monthly NDVI with average decadal and monthly rainfall respectively.

District	Correlation coefficient	
	Monthly NDVI	Decadal NDVI
N.Gondar	0.8985	0.7633
W.Gojam	0.8926	0.8234
S.Gondar	0.7655	0.6584
E.Gojam	0.7582	0.5434
W.Hamera	0.7337	0.6151
N.Wollow	0.6992	0.4889
Awi	0.6487	0.6498
S.Wollow	0.5785	0.3567

Table 5-1: Correlation coefficients showing the relationship between monthly and decadal NDVI and rainfall for all the districts.

Rainfall is an important meteorological parameter which influences the type of vegetation in a region. As NDVI is effectively used for monitoring crop yield and drought, use of NDVI is well established in assessing the vigour and productivity (Chandrasekar, Sai et al. 2006). In this study an attempt has been also made to find the relation between rainfall and decadal NDVI in all the districts of the "Amhara" region. Monthly district-wise average rainfall data for all the districts were used.

The rainfalls lag period shows up to nine 10-day periods, i.e., three months. This indicates the maximum time period for which an influence of rainfall on NDVI could be observed. The study shows that series of 10-day and monthly MSG NDVI are related to lagged rainfall in the "Amhara" region of the upper Blue Nile basin, depicting changes in soil moisture and vegetation development. The relation is stronger when NDVI is aggregated into monthly composites. In the analysis of the relationship of NDVI with rainfall, it is found that low NDVI occurs in low rainfall regions and high NDVI occurs in high rainfall regions. The average NDVI response from the districts will be influenced by land use and cropping pattern of the district under study.

The weakest relation between NDVI and rainfall occurs at 10-day resolution for North and South Wollow districts. It is likely that the lack of strength of the relations could be partly explained by lack of detailed ground information. These ground information are important to delineate agricultural and non-agricultural land more precisely. However, such data was not available. Besides, these districts are the major producers of "Belg" season, secondary rain which is over the period of March-May. Also, there are unaccounted differences in rainfall intensity, duration and soil properties which may have a negative effect on the relations (Wang, K.P.Price et al. 2001). Figure 5-14 shows the correlation of decadal NDVI and rainfall for North Gondar district. Graphs showing Decadal NDVI and rainfall for other districts are given in the appendix-F.

It can be observed from Table 5-1 that most of the districts have a strong correlation (>0.5) except North and South Wollow districts. These two districts fall in the low rainfall zone of the region. Most

of the agricultural activity is carried out in the "Belg" season (March-May). Hence, the correlation of the NDVI with the rainfall over the main growing season is poor.

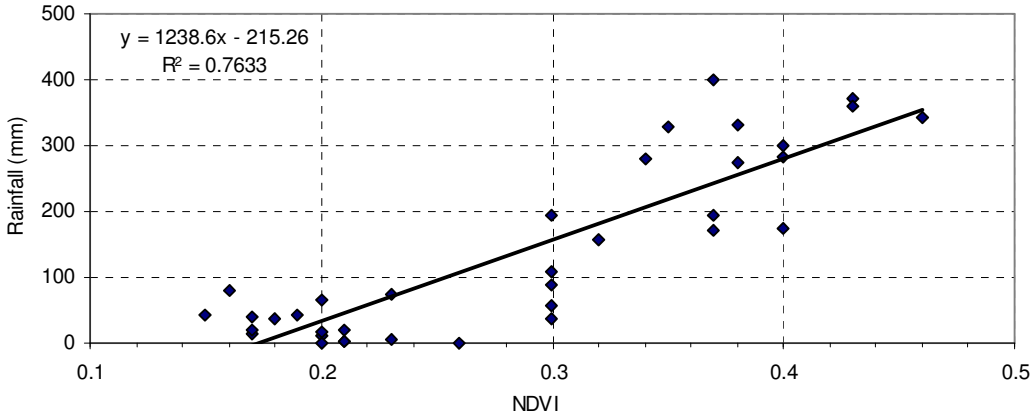

Figure 5-14: Graph showing the relationship between Decadal NDVI and precipitation for North Gondar district in 2005.

5.3.2. Relationship between NDVI and production yield

Correlation between NDVI and annual crop production yield for all the districts of the "Amhara" region is examined based on the masks that delineate patterns of where these crops are produced. Relations between NDVI and annual production yield were analyzed using maximum NDVI over the growing season. There exists a strong correlation between maximum NDVI over the growing season and the total production yield for most of the districts in "Amhara" region. Table 5-2 shows the correlation coefficients for all the districts in the region.

Districts	correlation coefficients
North Gondar	0.823
South Gondar	0.8449
West Gojam	0.8175
East Gojam	0.7813
Awi	0.7061
North Wollow	0.6456
South Wollow	0.6688
North Shoa	0.5319

Table 5-2: Correlation coefficients between maximum NDVI and total production yield.

The relationship was established between maximum NDVI over the growing season and total production yield. In doing so, outliers values of agricultural statistics for North Gondar district in 2000 and Awi district in 1999 has been first discarded from the list. Also, the NDVI values are obtained only for cultivated lands of each district. While extracting the cultivated map for Amhara region from the land cover map of the Blue Nile basin, significant portions of the cultivated land for few districts such as the North Shoa district was ignored as the entire area of these districts doesn't

fully encompassed by the Blue Nile basin. Hence, it is likely to obtain less reliable maximum NDVI values and thereby it would have been the cause for obtaining a lower correlation between NDVI and agricultural production yield in these districts. As North and South Wollow districts fall under low rainfall zones in the region and significant amount of agricultural production is obtained from the so-called "Belg" season or the secondary rain season (march-may), it also will have a negative impact on the relation. Herewith a graph showing the relationship between Maximum NDVI and total agricultural yield for North Gondar district is shown and such graphs for the other districts are presented in the appendix-G.

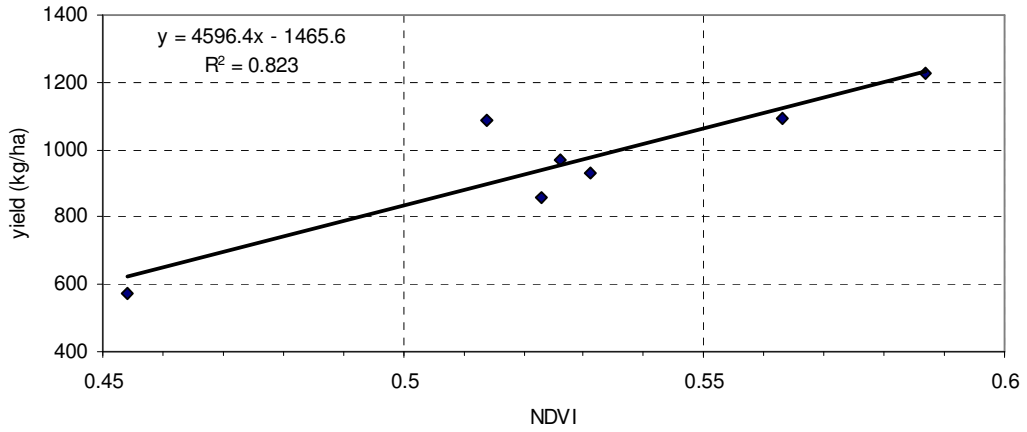

Figure 5-15: Graph showing the relationship between NDVI and Agricultural yield for the North Gondar district.

Furthermore, relationship between NDVI anomaly and total agricultural production yield anomaly was done and it has been found that NDVI anomaly and total agricultural yield anomaly is giving a good correlation identical as the correlation between maximum NDVI and production yield. Thus, this represents that as NDVI anomaly increases so do the total agricultural yield which means that when NDVI anomaly is above normal total agricultural production is also on a higher side, whereas when NDVI anomaly is on a negative side gross production yield anomaly also follows a negative tendency which indicates that a district wise agricultural yield can be assessed by analyzing NDVI anomaly. The following graph gives the relationship between NDVI anomaly and production yield anomaly for one of the districts in the Amhara region and other similar graphs have been depicted in the appendix.

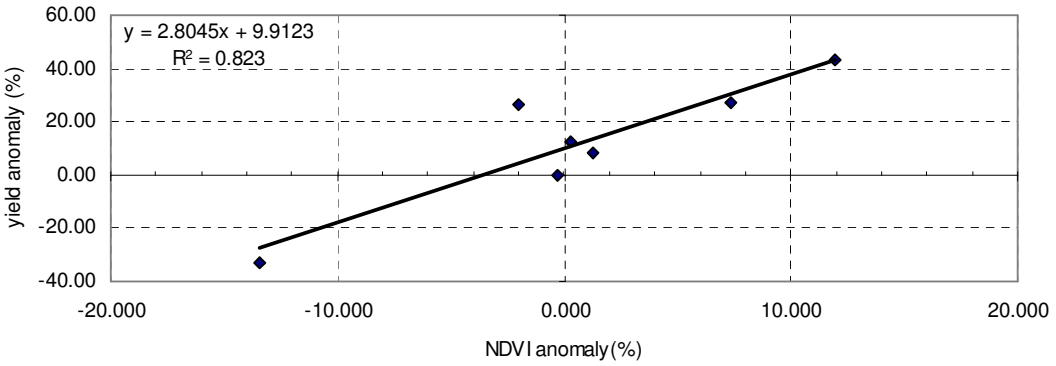

Figure 5-16: NDVI anomaly versus yield anomaly for North Gondar district.

5.4. Classification of drought severity classes.

Finally, the drought map for the central Nile Basin in 2005 and 2006 has been obtained on decadal basis by integrating all the drought-monitoring indices: Drought Severity Index (DSI), Vegetation Condition Index (VCI) and Temperature Condition Index (TCI), as this portion of the basin has a more or less similar agro-climatology as the "Amhara region" where the ground truth data were obtained to validate the satellite derived results. To do so, first drought classification has been made based on the criterion suggested threshold values of each drought-index on decadal basis. Then, these maps were aggregated by summing up the decadal maps of each drought indices and merged into one decadal map using the map calculation function in ILWIS GIS software package. Decadal maps obtained by integrating the three drought-monitoring indices over the growing season are grouped in a map list and summed up to merge again into one drought map over a year. However, those decadal maps which have a significant number of undefined pixels have been ignored before merging in order to avoid unclassified pixels from the final map.

The final map was classified into non drought, sporadic drought, moderate drought and drought classes based on the argument that a pixel has a drought and/or non drought condition for either of one, two or all the three drought-monitoring indices. The intermediate drought classification into, sporadic and moderate drought, was some how a difficult task and was entirely based on the judgment that how many number of pixels are under drought condition in accordance with only one index or two indices. The thresholds used for classification are 0-10: no drought, 10-20: sporadic drought, 20-30: moderate drought and 30-45: severe drought. Similar methodology could also be applied to obtain a classified drought map for other parts of the basin which has a different agro-climatology than the region where ground truth data that was used in this study. Figure 5-18 shows the final drought map for the central part of the Nile Basin in 2005 and 2006.

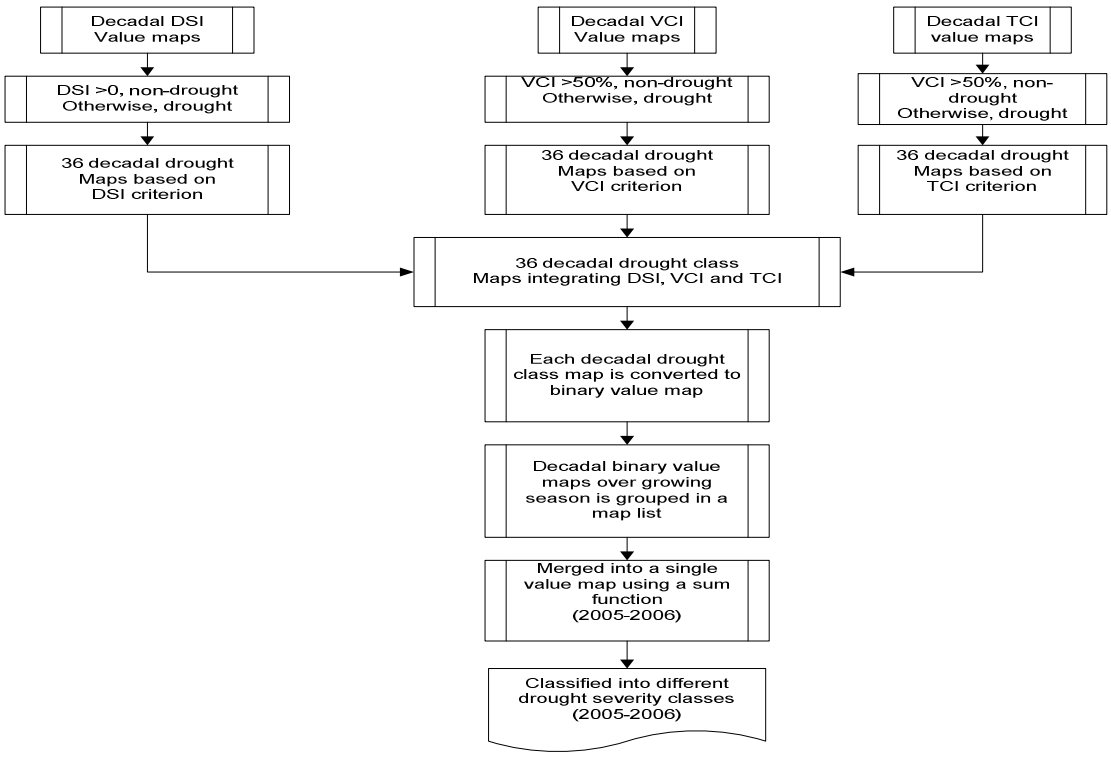

Figure 5-17: Flow chart showing classification of drought severity classes

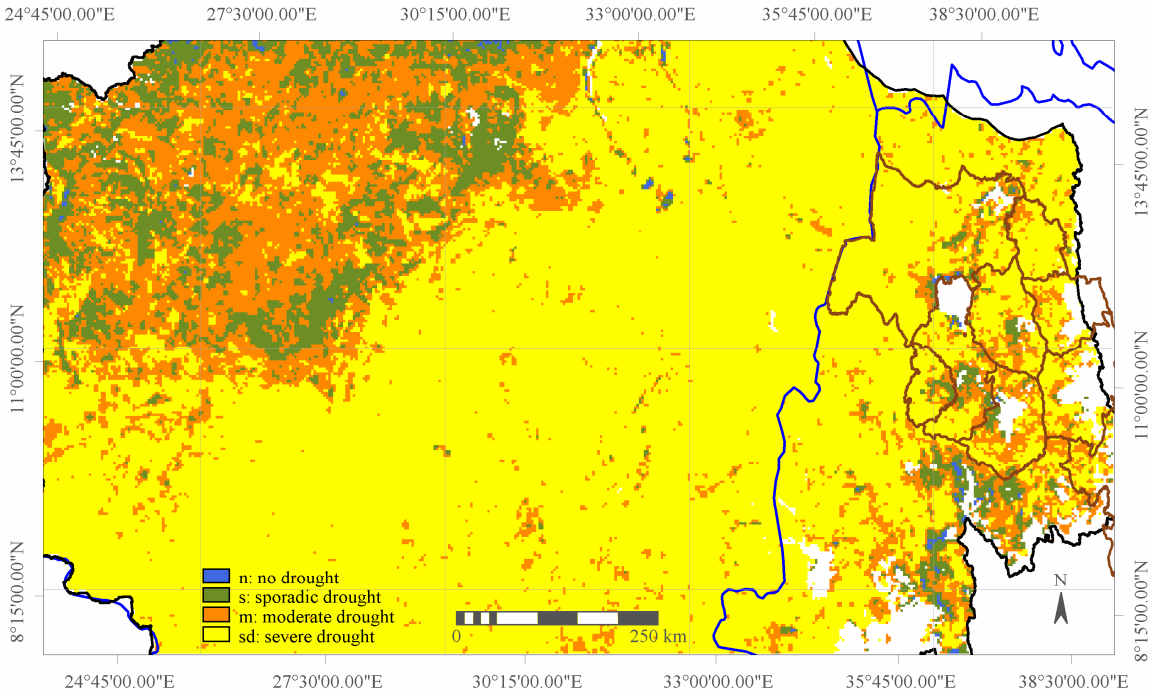

2005

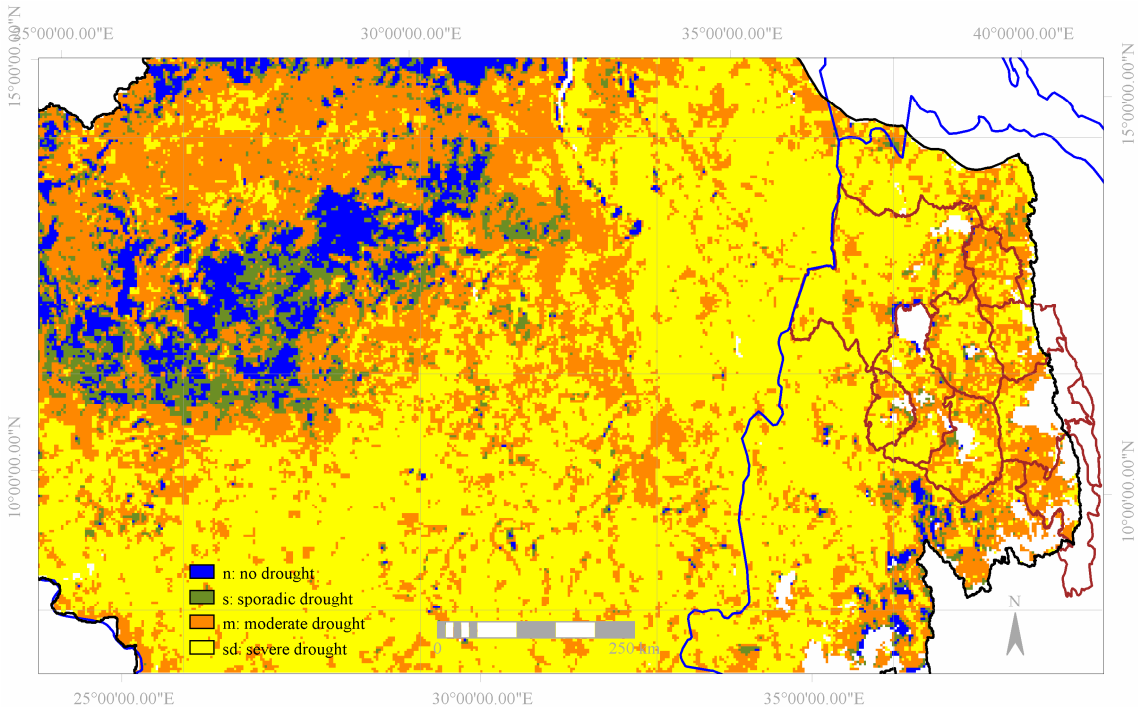

2006

Figure 5-18: Drought map for central part of the Nile Basin in 2005 and 2006.

6. Conclusion and recommendations

6.1. Conclusion

The temporal and spatial characteristics of drought can be detected, tracked and mapped from satellite data particularly that obtained from the Meteosat Second Generation (MSG) data at basin-wise level. Based on the analysis for the "Amhara" region which is found in the upper part of the Blue Nile Basin, this study shows the drought condition scenario can be constructed from the deviation of Normalized Difference Vegetation Index (NDVI) from its long-term mean, the Vegetation Condition Index (VCI) and the Temperature Condition Index (TCI). The same methodology can be adopted for other parts of the basin and similar results could be obtained. Despite the promising results, there is still need to improve on the quality of satellite data for current application, especially in cloud removal algorithm. Besides, satellite data is affected by various sources of errors such as, sensor degradation and atmospheric agitation due to aerosols.

A strong correlation has been observed between NDVI and agricultural production yield and between NDVI anomaly and agricultural production yield anomaly for most of the districts in "Amhara" region. Since the Vegetation Condition Index (VCI) is derived from NDVI, it is therefore not surprising to obtain a good relationship between agricultural yield and VCI over the growing season. As crop (plant) biological processes such as photosynthesis, respiration, plant growth and development are temperature dependent, it is also reasonable to find a significant relation between agricultural yield and TCI.

The satellite derived drought-monitoring indices have also been correlated with precipitation to see how vegetation stresses condition and consequently agricultural production yield is changing with the variability of rainfall. The result showed that the existence of a reasonably good relation between NDVI and rainfall variability over the growing season. A maximum correlation has been observed between NDVI and precipitation with a lag time of three months (Nine decades). Furthermore, a strong correlation also exists between the Vegetation Condition Index (VCI) and precipitation, and the Temperature Condition Index (TCI) and precipitation for most of the districts in "Amhara" region. These validation results of the satellite developed indices based on the ground data is vital for successful application of MSG data for near real-time drought assessment and detection of vegetation stress resulting from drought in different parts of the basin and this analysis can be continued using new ground truth data and new areas.

Thus, the satellite derived drought-indices can sufficiently identify and characterize the onset and severity of drought condition for different agro-climatologically homogeneous regions of the basin in combination with respective in situ ground data. The results obtained from the satellite derived indices in this research are found to be complementary with each other, especially over the growing season and their deviation from the long-term mean can be used as a good indicator for identifying the drought and non-drought condition for near real time drought assessment. However, all the derived

indices have a bottle-neck in differentiating intermediate drought and non-drought conditions (classes) as there is no a clear cut threshold values suggested so far for such distinction.

6.2. Recommendations

As mentioned above drought severity classes had been classified in to non-drought and different drought conditions. However, the magnitude of drought severity varies within these categories and hence strategies for mitigation of its adverse impacts are different for different magnitude of drought severity. Therefore, it is essential to quantify the magnitude of drought severity into various degrees of drought classes.

For developing a toolbox based on the MSG-indicators linked with agricultural statistics for drought prediction and loss of agricultural production as an early warning system, detailed information on the crop calendar is required. As such information was not available for the “Amhara” region; it is recommended that other parts of the basin can be taken to develop such a toolbox.

Moreover, drought analysis from socio-economic point of view had not been seen in this study. In addition to identifying the drought affected areas in the basin, the study could be more meaningful if effects of drought on human and livestock population were assessed.

As products of Meteosat Second Generation image data are delivered via EUMETCast through an African service in C-band via AtlanticBird-3 and has a near real time monitoring capability, installation of a ground receiving stations for Africa is very important and recommendable for the near real time drought monitoring. This station’s requirement comprises only a standard PC and a digital Video Broad-cast (DVB) card inserted and a satellite off-set antenna. Besides, these products are cloud masked and hence improve the quality of satellite derived results significantly. In addition, Vegetation Instrument data can be delivered via EUMETCast.

Reference:

Anyamba, A. and C. J. Tucker (2005). "Analysis of Sahelian vegetation dynamics using NOAA-AVHRR NDVI data from 1981-2003." Journal of Arid Environments **63**: 596-614.

Chandrasekar, K., M. V. R. S. Sai, et al. (2006). "Vegetation response to rainfall as monitored by NOAA–AVHRR." National Remote Sensing Agency, Hyderabad 500 037, India **CURRENT SCIENCE, VOL. 91, NO. 12**.

Chopra, P.,2006,Drought risk assessment using remote sensing and GIS : a case study of Gujarat,Msc thesis,ITC,Enschede,67 p.

EKLUNDH, L. (1997). "Estimating relation between AVHRR NDVI and rainfall in East Africa at 10-day and monthly time scales."

Fensholt, R., I. Sandholt, et al. (2005). "Analysing NDVI for the African continent using the geostationary meteosat second generation SEVIRI sensor." Remote Sensing of Environment **101**(2): 212-229.

Gieske, A. S. M., J. H. M. Hendrikse, et al. (2005). "Processing of MSG-1 SEVIRI data in the thermal infrared-algorithm development with the use of the SPARC2004 data set." Presented at the ESA proceedings WPP-250 : SPARC final workshop, 4-5 July, 2005. Enschede : ESA, 2005. 8 p.

Hounam, C. E. (1975). Drought and agriculture : report of the CAgM working group on the assessment of drought. Geneva, World Meteorological Organization (WMO).

IWMI (2006) Drought Assessment and Mitigation In South West Asia.2006, http://www.iwmi.cgiar.org, October 2006,

Jiren, L. and Y. Musul (2002). "Application of Temote Sensing to Water Resources management in Arid Regions of China." Remote Sensing Technology Application centre, Ministry of water Resources, China, 20 West Chengongzhuang Road, Beijing 100044, China1,12.

Kassa, A.,1999,DROUGHT RISK MONITORING FOR THE SUDAN USING NDVI,Msc thesis University College London,47

Kogan, F. N. (1997). "Global Drought Watch from Space." Bulletin of the American meteorological society **78**(4): 621-621.

Kogan, F. N. (2000). "Contribution of Remote sensing to Drought Early Warning." National Oceanic and Atmospheric (NOAA), National Environmental Satellite Data and Information Services (NESDIS), Washington DC, U.S.A: 15.

Kogan, N. F. (1995). "Application of Vegetation Index and Brightness Temperature for Drought Detection." Advances in Space Research **15, pp.91-100**.

Lacaze, B. and J.-C. Berges (2005). "Contribution of Meteosat Second Generation (MSG) to drought early warning." Proceedings of the International conference: Remote Sensing and Geoinformation

Processing in the Assessment and Monitoring of Land Degradation and Desetification: State of the Art and Operational Perspectives, September 7th to 9th, Trier, Germany.

Maathuis, B. H. P., A. S. M. Gieske, et al. (2006). "Meteosat - 8 : from temperature to rainfall." In: ISPRS 2006 : ISPRS mid-term symposium 2006 remote sensing : from pixels to processes, 8-11 May 2006, Enschede, the Netherlands. Enschede : ITC, 2006. 5 p.

Maathuis, B. H. P. and V. Retsios (2006). "Installation, setup and use of a low cost c - band meteosat - 8 ground receiving station in Rwanda." In: AARSE 2006 : Proceeding of the 6th AARSE international conference on earth observation and geoinformation sciences in support of Africa's development, 30 October - 2 November 2006, Cairo, Egypt. Cairo : The National Authority for Remote Sensing and Space Science (NARSS), 2006. ISBN 1-920-01710-0. 8 p.

MARTINI, M., P. B. SOUMARE, et al. (2004). "Crops and rangeland monitoring in senegal using SPOT 4/5 VEGETATION data." http://www.vgt.vito.be/vgtapen/pages/fullpapers/Martini_full_long.pdf.

Mazzanti, S. G. a. M. (1996). "Pixel-by-Pixel Classification for Zoning and Monitoring."

McVicar, T. R. and D. L. B. Jupp (1998). "The current and potential operational uses of remote sensing to aid decisions on drought exceptional circumstances in Australia: a review." Agricultural Systems **57**(3): 399-468.

Mohamed, Y. A. (2005). "Hydroclimatology of the Nile : results from a regional climate model." Hydrology and earth system sciences (HESS) **9**(3).

Narasimhan, B. and R. Srinivasan (2005). "Development and evaluation of Soil Moisture Deficit Index (SMDI) and Evapotranspiration Deficit Index (ETDI) for agricultural drought monitoring." Agricultural and Forest Meteorology **133**: 69-88.

Pinzon, J., et al., Brown M.E., Tucker C.J. (2004). "Satellite time series correction of orbital drift artifacts using emoerical mode decomposition. Hilbert-Huang Transform: Introduction and Applications. N.Huang: Chapter 10, part II. Applications."

Quiring, S. M. and T. N. Papakryiakou (2003). "An evaluation of agricultural drought indices for the Canadian prairies." Agricultural and Forest Meteorology **118**(1-2): 49-62.

Su, Z. and G. J. Roerink (2004). Drought risk reduction. Alterra-rapport. Wageningen, Alterra**:** 87 p.

Team, U. C. R. S. P. (2000). "Amhara National regional State Food security Research Assessment report."

Thenkabail, P. S., Gamage, M. S. D. N. and Smakhtin, V. U. (2004). The Use of Remote Sensing Data for Drought Monitoring in Southwest Asia. Geneva.

Tucker, C. J., compton J, Choudhury, Bhaskar J. (1987). "Satellite remote sensing of drought conditions." Remote Sensing of Environment (ISSN 0034-4257), vol 23, p. 243-251. **23**.

Tucker, C. J., Pinzon J.E., Brown M.E., Slayback D., Pak E.W., Mahoney R., Vermote E., EL Saleous N. (2005). ""An Extended AVHRR 8-km NDVI Data Set Comaptible with MODIS and SPOT Vegetation NDVI Data.'" International Journal of Remote Sensing, in press.

Unganai, L. S. and F. N. Kogan (1998). "Drought Monitoring and Corn Yield Estimation in Southern Africa from AVHRR Data." Remote Sensing of Environment **63**(3): 219-232.

Unganai, L. S. and F. N. Kogan (1998). "Southern Africa's recent droughts from space." Advances in Space Research **21**(3): 507-511.

VITO (2005). "Free Vegetation products. cf. Internet address http://free.vgt.bito.be/."

Wang, J., K.P.Price, et al. (2001). "Spatial patterns of NDVI in response to precipitation and temperature in the central Great Plains." International Journal of Remote sensing **22, NO.18,3827-3844**.

Wang, J., P. M.Rich, et al. (2005). "Relations between NDVI, Grassland Production, and Crop Yield in the Central Great Plains." Geocarto International **20, No.3**.

Wilhite, D. A. (2000). "Drought preparedness and response in the context of Sub-Saharan Africa." In: Journal of contingencies and crisis management, 8(2000)2, pp. 81-92.

Y.Richard and I.Poccard (1998). "A Statistical study of NDVI densitivity to seasonal and interannual rainfall variations in Southern Africa." International Journal of Remote sensing, in press. **19, No. 15. 2907-2920**.

Appendices:

Appendix-A: Correlation graphs of yield versus culivated area.

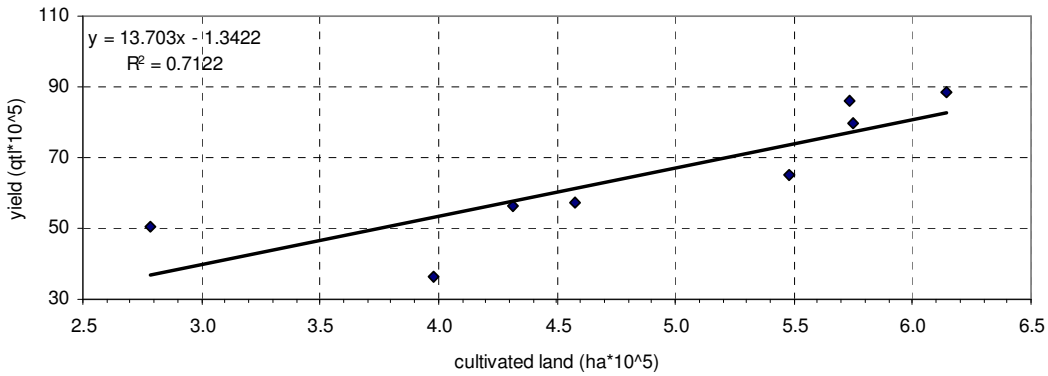

East Gojam

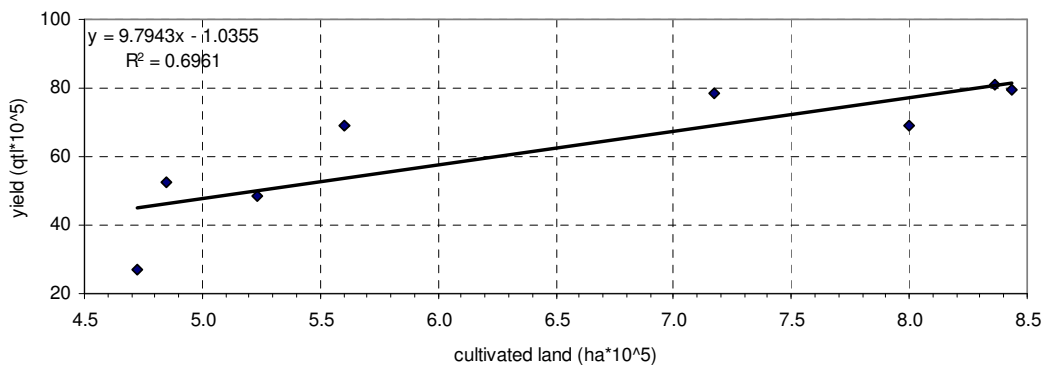

North Gondar

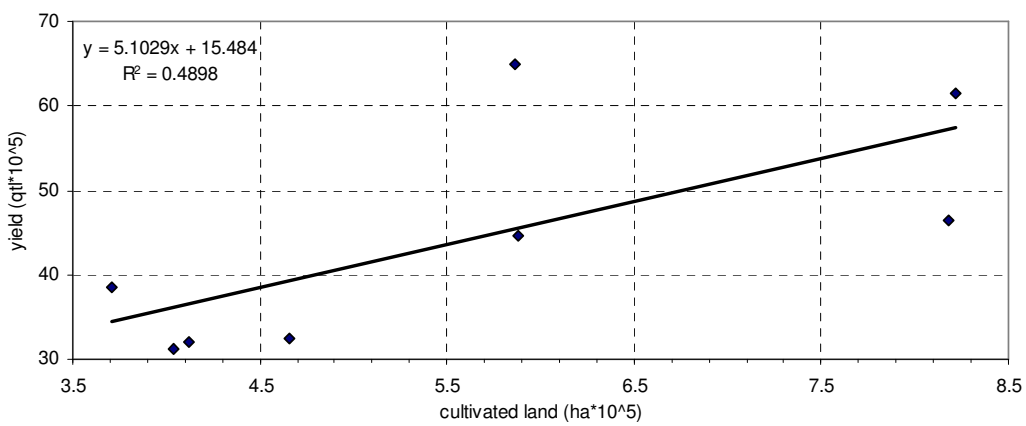

South Gondar

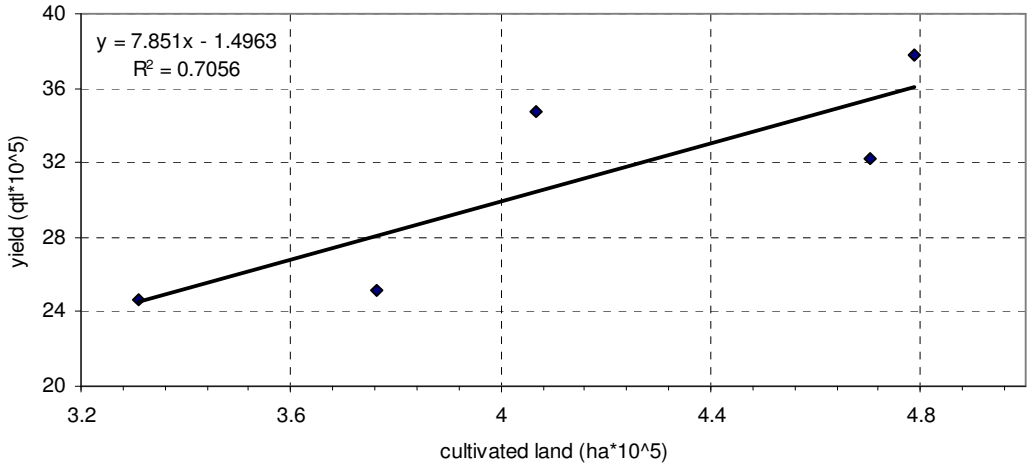

South Wollow

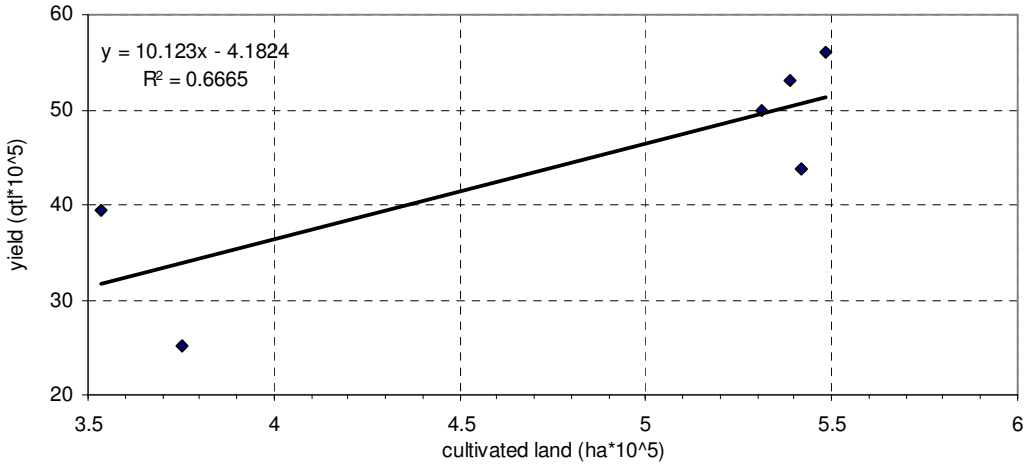

North Shoa

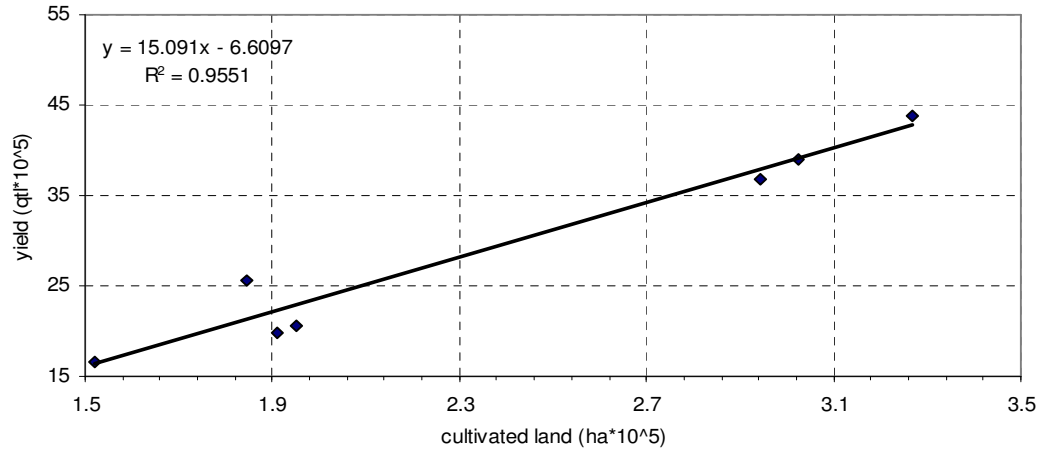

Awi

Appendix-B: ILWIS Scripts for Computation of drought monitoring indices

```
//Temperature thresholds used for cloud removal
mask_ndvi_jan1:=iff(jan1_200501011100_ch_1_2_9_band_3>295,ndvi_jan1,?)
mask_ndvi_jan2:=iff(jan2_200501021100_ch_1_2_9_band_3>296,ndvi_jan2,?)
mask_ndvi_jan3:=iff(jan3_200501031100_ch_1_2_9_band_3>294,ndvi_jan3,?)
mask_ndvi_jan4:=iff(jan4_200501041100_ch_1_2_9_band_3>295,ndvi_jan4,?)
mask_ndvi_jan5:=iff(jan5_200501051100_ch_1_2_9_band_3>295,ndvi_jan5,?)
mask_ndvi_jan6:=iff(jan6_200501061100_ch_1_2_9_band_3>294,ndvi_jan6,?)
mask_ndvi_jan7:=iff(jan7_200501071100_ch_1_2_9_band_3>293,ndvi_jan7,?)
mask_ndvi_jan8:=iff(jan8_200501081100_ch_1_2_9_band_3>294,ndvi_jan8,?)
mask_ndvi_jan9:=iff(jan9_200501091100_ch_1_2_9_band_3>294,ndvi_jan9,?)
mask_ndvi_jan10:=iff(jan10_200501101100_ch_1_2_9_band_3>293,ndvi_jan10,?)
mask_ndvi_jan12:=iff(jan12_200501121100_ch_1_2_9_band_3>295,ndvi_jan12,?)
mask_ndvi_jan13:=iff(jan13_200501131100_ch_1_2_9_band_3>295,ndvi_jan13,?)
mask_ndvi_jan14:=iff(jan14_200601141100_ch_1_2_9_band_3>294,ndvi_jan14,?)
mask_ndvi_jan15:=iff(jan15_200501151100_ch_1_2_9_band_3>290,ndvi_jan15,?)
mask_ndvi_jan16:=iff(jan16_200501161100_ch_1_2_9_band_3>289,ndvi_jan16,?)
mask_ndvi_jan17:=iff(jan17_200501171100_ch_1_2_9_band_3>292,ndvi_jan17,?)
mask_ndvi_jan18:=iff(jan18_200501181100_ch_1_2_9_band_3>293,ndvi_jan18,?)
mask_ndvi_jan19:=iff(jan19_200501191100_ch_1_2_9_band_3>292,ndvi_jan19,?)
mask_ndvi_jan20:=iff(jan20_200501201100_ch_1_2_9_band_3>286,ndvi_jan20,?)
mask_ndvi_jan21:=iff(jan21_200501211100_ch_1_2_9_band_3>283,ndvi_jan21,?)
mask_ndvi_jan22:=iff(jan22_200501221100_ch_1_2_9_band_3>290,ndvi_jan22,?)
mask_ndvi_jan23:=iff(jan23_200501231100_ch_1_2_9_band_3>292,ndvi_jan23,?)
mask_ndvi_jan24:=iff(jan24_200501241100_ch_1_2_9_band_3>290,ndvi_jan24,?)
mask_ndvi_jan25:=iff(jan25_200501251100_ch_1_2_9_band_3>292,ndvi_jan25,?)
mask_ndvi_jan26:=iff(jan26_200501261100_ch_1_2_9_band_3>293,ndvi_jan26,?)
mask_ndvi_jan27:=iff(jan27_200501271100_ch_1_2_9_band_3>292,ndvi_jan27,?)
mask_ndvi_jan28:=iff(jan28_200501281100_ch_1_2_9_band_3>295,ndvi_jan28,?)
mask_ndvi_jan29:=iff(jan29_200501291100_ch_1_2_9_band_3>294,ndvi_jan29,?)
mask_ndvi_jan30:=iff(jan30_200501301100_ch_1_2_9_band_3>294,ndvi_jan30,?)
mask_ndvi_jan31:=iff(jan31_200501311100_ch_1_2_9_band_3>293,ndvi_jan31,?)

//masking water pixels
mask1_ndvi_jan1:=iff(ndvi_jan1>0,mask_ndvi_jan1,?)
mask1_ndvi_jan2:=iff(ndvi_jan2>0,mask_ndvi_jan2,?)
mask1_ndvi_jan3:=iff(ndvi_jan3>0,mask_ndvi_jan3,?)
mask1_ndvi_jan4:=iff(ndvi_jan4>0,mask_ndvi_jan4,?)
mask1_ndvi_jan5:=iff(ndvi_jan5>0,mask_ndvi_jan5,?)
mask1_ndvi_jan6:=iff(ndvi_jan6>0,mask_ndvi_jan6,?)
mask1_ndvi_jan7:=iff(ndvi_jan7>0,mask_ndvi_jan7,?)
mask1_ndvi_jan8:=iff(ndvi_jan8>0,mask_ndvi_jan8,?)
mask1_ndvi_jan9:=iff(ndvi_jan9>0,mask_ndvi_jan9,?)
```

```
mask1_ndvi_jan10:=iff(ndvi_jan10>0,mask_ndvi_jan10,?)
mask1_ndvi_jan12:=iff(ndvi_jan12>0,mask_ndvi_jan12,?)
mask1_ndvi_jan13:=iff(ndvi_jan13>0,mask_ndvi_jan13,?)
mask1_ndvi_jan14:=iff(ndvi_jan14>0,mask_ndvi_jan14,?)
mask1_ndvi_jan15:=iff(ndvi_jan15>0,mask_ndvi_jan15,?)
mask1_ndvi_jan16:=iff(ndvi_jan16>0,mask_ndvi_jan16,?)
mask1_ndvi_jan17:=iff(ndvi_jan17>0,mask_ndvi_jan17,?)
mask1_ndvi_jan18:=iff(ndvi_jan18>0,mask_ndvi_jan18,?)
mask1_ndvi_jan19:=iff(ndvi_jan19>0,mask_ndvi_jan19,?)
mask1_ndvi_jan20:=iff(ndvi_jan20>0,mask_ndvi_jan20,?)
mask1_ndvi_jan21:=iff(ndvi_jan21>0,mask_ndvi_jan21,?)
mask1_ndvi_jan22:=iff(ndvi_jan22>0,mask_ndvi_jan22,?)
mask1_ndvi_jan23:=iff(ndvi_jan23>0,mask_ndvi_jan23,?)
mask1_ndvi_jan24:=iff(ndvi_jan24>0,mask_ndvi_jan24,?)
mask1_ndvi_jan25:=iff(ndvi_jan25>0,mask_ndvi_jan25,?)
mask1_ndvi_jan26:=iff(ndvi_jan26>0,mask_ndvi_jan26,?)
mask1_ndvi_jan27:=iff(ndvi_jan27>0,mask_ndvi_jan27,?)
mask1_ndvi_jan28:=iff(ndvi_jan28>0,mask_ndvi_jan28,?)
mask1_ndvi_jan29:=iff(ndvi_jan29>0,mask_ndvi_jan29,?)
mask1_ndvi_jan30:=iff(ndvi_jan30>0,mask_ndvi_jan30,?)
mask1_ndvi_jan31:=iff(ndvi_jan31>0,mask_ndvi_jan31,?)

//Extracting NDVI for Nile Basin only (study Area)
nile_mask1_ndvi_jan1:=ifnotundef(nile_basin,mask1_ndvi_jan1,?)
nile_mask1_ndvi_jan2:=ifnotundef(nile_basin,mask1_ndvi_jan2,?)
nile_mask1_ndvi_jan3:=ifnotundef(nile_basin,mask1_ndvi_jan3,?)
nile_mask1_ndvi_jan4:=ifnotundef(nile_basin,mask1_ndvi_jan4,?)
nile_mask1_ndvi_jan5:=ifnotundef(nile_basin,mask1_ndvi_jan5,?)
nile_mask1_ndvi_jan6:=ifnotundef(nile_basin,mask1_ndvi_jan6,?)
nile_mask1_ndvi_jan7:=ifnotundef(nile_basin,mask1_ndvi_jan7,?)
nile_mask1_ndvi_jan8:=ifnotundef(nile_basin,mask1_ndvi_jan8,?)
nile_mask1_ndvi_jan9:=ifnotundef(nile_basin,mask1_ndvi_jan9,?)
nile_mask1_ndvi_jan10:=ifnotundef(nile_basin,mask1_ndvi_jan10,?)
nile_mask1_ndvi_jan12:=ifnotundef(nile_basin,mask1_ndvi_jan12,?)
nile_mask1_ndvi_jan13:=ifnotundef(nile_basin,mask1_ndvi_jan13,?)
nile_mask1_ndvi_jan14:=ifnotundef(nile_basin,mask1_ndvi_jan14,?)
nile_mask1_ndvi_jan15:=ifnotundef(nile_basin,mask1_ndvi_jan15,?)
nile_mask1_ndvi_jan16:=ifnotundef(nile_basin,mask1_ndvi_jan16,?)
nile_mask1_ndvi_jan17:=ifnotundef(nile_basin,mask1_ndvi_jan17,?)
nile_mask1_ndvi_jan18:=ifnotundef(nile_basin,mask1_ndvi_jan18,?)
nile_mask1_ndvi_jan19:=ifnotundef(nile_basin,mask1_ndvi_jan19,?)
nile_mask1_ndvi_jan20:=ifnotundef(nile_basin,mask1_ndvi_jan20,?)
nile_mask1_ndvi_jan21:=ifnotundef(nile_basin,mask1_ndvi_jan21,?)
nile_mask1_ndvi_jan22:=ifnotundef(nile_basin,mask1_ndvi_jan22,?)
nile_mask1_ndvi_jan23:=ifnotundef(nile_basin,mask1_ndvi_jan23,?)
```

```
nile_mask1_ndvi_jan24:=ifnotundef(nile_basin,mask1_ndvi_jan24,?)
nile_mask1_ndvi_jan25:=ifnotundef(nile_basin,mask1_ndvi_jan25,?)
nile_mask1_ndvi_jan26:=ifnotundef(nile_basin,mask1_ndvi_jan26,?)
nile_mask1_ndvi_jan27:=ifnotundef(nile_basin,mask1_ndvi_jan27,?)
nile_mask1_ndvi_jan28:=ifnotundef (nile_basin,mask1_ndvi_jan28,?)
nile_mask1_ndvi_jan29:=ifnotundef(nile_basin,mask1_ndvi_jan29,?)
nile_mask1_ndvi_jan30:=ifnotundef(nile_basin,mask1_ndvi_jan30,?)
nile_mask1_ndvi_jan31:=ifnotundef(nile_basin,mask1_ndvi_jan31,?)

//Computation of DSI
DSI_jan1_05:=nile_jan1_ndvi_max_05-nile_ndvi_jan1_res
DSI_jan2_05:=nile_jan2_ndvi_max_05-nile_ndvi_jan2_res
DSI_jan3_05:=nile_jan3_ndvi_max_05-nile_ndvi_jan3_res

//Computation of VCI
VCI_jan1_05.mpr{dom=value.dom;vr=0.0000:100.0000:0.0001}:=(((Nile_jan1_max_ndv-
jan1_min_res))/((jan1_max_res-jan1_min_res)))*100
VCI_jan2_05.mpr{dom=value.dom;vr=0.0000:100.0000:0.0001}:=(((Nile_jan2_max_ndv-
jan2_min_res))/((jan2_max_res-jan2_min_res)))*100
VCI_jan3_05.mpr{dom=value.dom;vr=0.0000:100.0000:0.0001}:=(((Nile_jan3_max_ndv-
jan3_min_res))/((jan3_max_res-jan3_min_res)))*100

//Computation of TCI
TCI_jan1_05.mpr{dom=value.dom;vr=0.0000:100.0000:0.0001}:=(((nile_BT_max_05-
nile_BT_jan1_05))/((nile_BT_max_05-nile_BT_min_05)))*100
TCI_jan2_05.mpr{dom=value.dom;vr=0.0000:100.0000:0.0001}:=(((nile_BT_max_05-
nile_BT_jan2_05))/((nile_BT_max_05-nile_BT_min_05)))*100
TCI_jan3_05.mpr{dom=value.dom;vr=0.0000:100.0000:0.0001}:=(((nile_BT_max_05-
nile_BT_jan3_05))/((nile_BT_max_05-nile_BT_min_05)))*100

//Computation of WSVI
wsvi_jan1_05:=nile_mask1_ndvi_jan1/jan1_200501011100_CH_1_2_9_band_3
wsvi_jan2_05:=nile_mask1_ndvi_jan2/jan2_200501021100_CH_1_2_9_band_3
wsvi_jan3_05:=nile_mask1_ndvi_jan3/jan3_200501031100_CH_1_2_9_band_3
wsvi_jan4_05:=nile_mask1_ndvi_jan4/jan4_200501041100_CH_1_2_9_band_3
wsvi_jan5_05:=nile_mask1_ndvi_jan5/jan5_200501051100_CH_1_2_9_band_3
wsvi_jan6_05:=nile_mask1_ndvi_jan6/jan6_200501061100_CH_1_2_9_band_3
wsvi_jan7_05:=nile_mask1_ndvi_jan7/jan7_200501071100_CH_1_2_9_band_3
wsvi_jan8_05:=nile_mask1_ndvi_jan8/jan8_200501081100_CH_1_2_9_band_3
wsvi_jan9_05:=nile_mask1_ndvi_jan9/jan9_200501091100_CH_1_2_9_band_3
wsvi_jan10_05:=nile_mask1_ndvi_jan10/jan10_200501101100_CH_1_2_9_band_3
wsvi_jan12_05:=nile_mask1_ndvi_jan12/jan12_200501121100_CH_1_2_9_band_3
wsvi_jan13_05:=nile_mask1_ndvi_jan13/jan13_200501131100_CH_1_2_9_band_3
wsvi_jan14_06:=nile_mask1_ndvi_jan14/jan14_200601141100_CH_1_2_9_band_3
wsvi_jan15_05:=nile_mask1_ndvi_jan15/jan15_200501151100_CH_1_2_9_band_3
```

```
wsvi_jan16_05:=nile_mask1_ndvi_jan16/jan16_200501161100_CH_1_2_9_band_3
wsvi_jan17_05:=nile_mask1_ndvi_jan17/jan17_200501171100_CH_1_2_9_band_3
wsvi_jan18_05:=nile_mask1_ndvi_jan18/jan18_200501181100_CH_1_2_9_band_3
wsvi_jan19_05:=nile_mask1_ndvi_jan19/jan19_200501191100_CH_1_2_9_band_3
wsvi_jan20_05:=nile_mask1_ndvi_jan20/jan20_200501201100_CH_1_2_9_band_3
wsvi_jan21_05:=nile_mask1_ndvi_jan21/jan21_200501211100_CH_1_2_9_band_3
wsvi_jan22_05:=nile_mask1_ndvi_jan22/jan22_200501221100_CH_1_2_9_band_3
wsvi_jan23_05:=nile_mask1_ndvi_jan23/jan23_200501231100_CH_1_2_9_band_3
wsvi_jan24_05:=nile_mask1_ndvi_jan24/jan24_200501241100_CH_1_2_9_band_3
wsvi_jan25_05:=nile_mask1_ndvi_jan25/jan25_200501251100_CH_1_2_9_band_3
wsvi_jan26_05:=nile_mask1_ndvi_jan26/jan26_200501261100_CH_1_2_9_band_3
wsvi_jan27_05:=nile_mask1_ndvi_jan27/jan27_200501271100_CH_1_2_9_band_3
wsvi_jan28_06:=nile_mask1_ndvi_jan28/jan28_200601281100_CH_1_2_9_band_3
wsvi_jan29_05:=nile_mask1_ndvi_jan29/jan29_200501291100_CH_1_2_9_band_3
wsvi_jan30_05:=nile_mask1_ndvi_jan30/jan30_200501301100_CH_1_2_9_band_3
wsvi_jan31_05:=nile_mask1_ndvi_jan31/jan31_200501311100_CH_1_2_9_band_3
```

Appendix-C: Graphs showing absolute maximum, minimum and current NDVI curves for 2005 and 2006

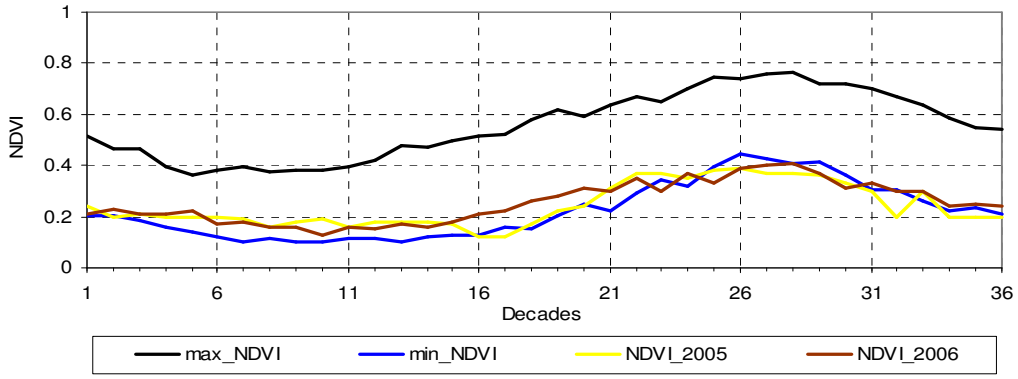

South Gondar

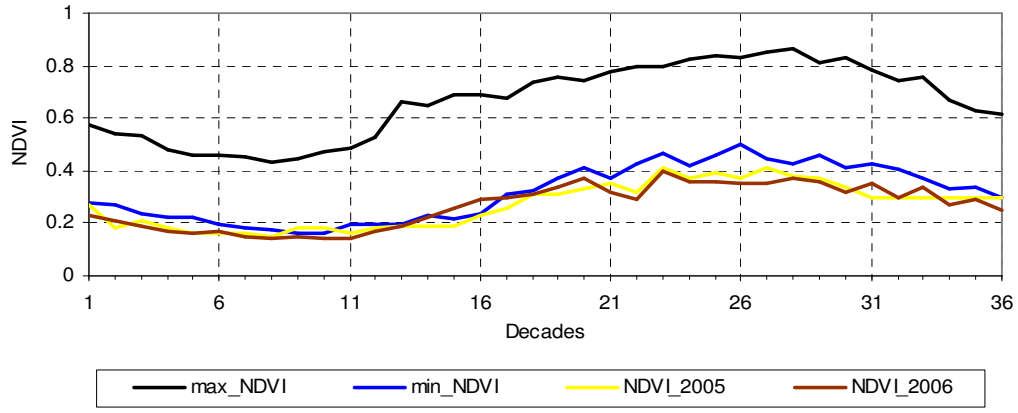

West Gojam

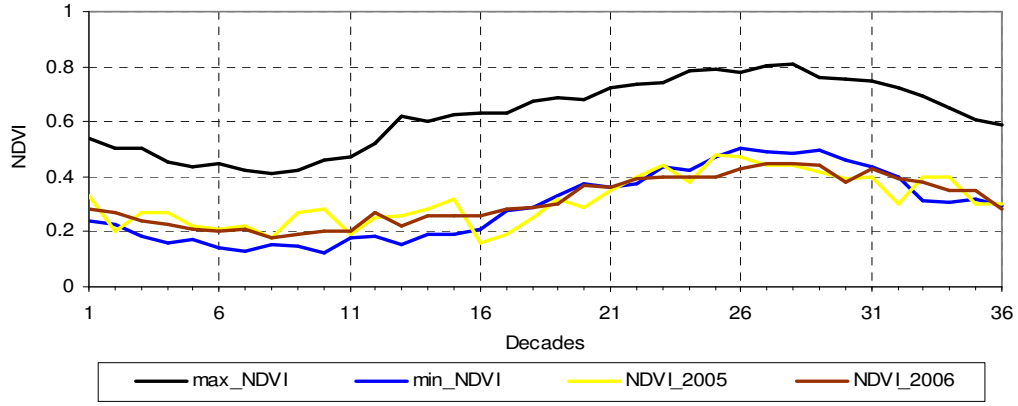

East Gojam

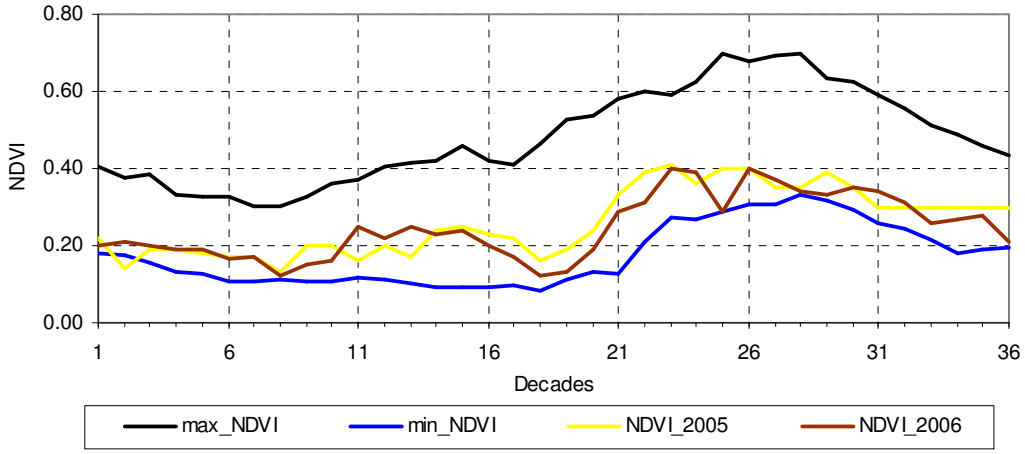

North Wollow

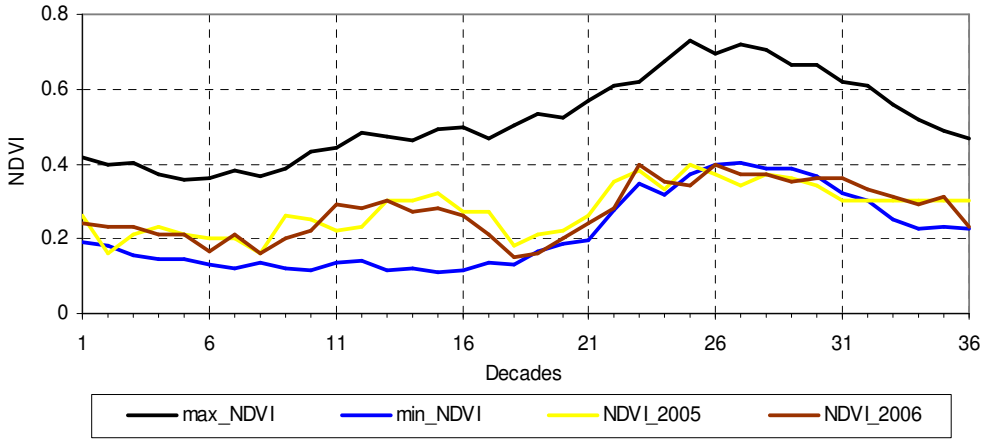

South Wollow

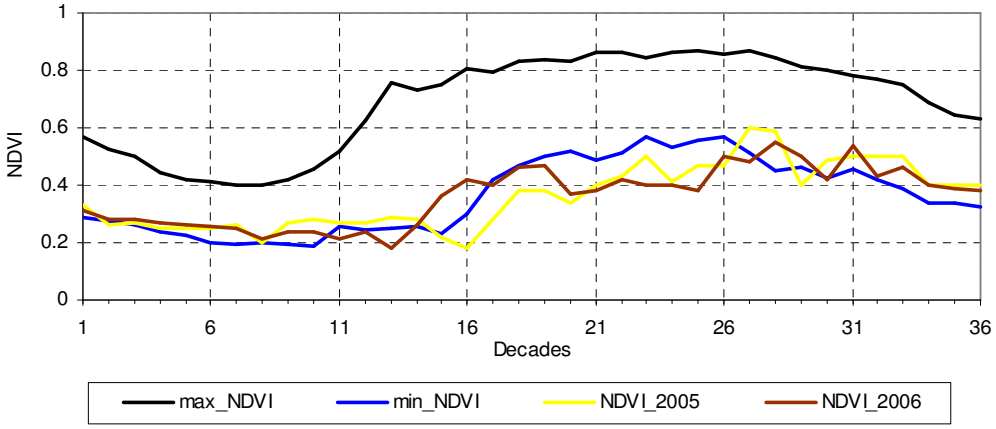

Awi

Appendix-D: Graphs showing correlation between VCI and precipitation

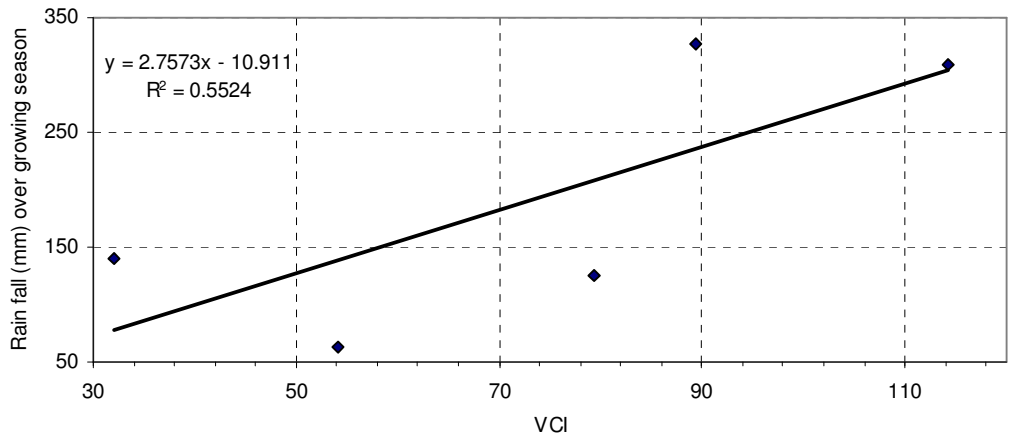

South Gondar

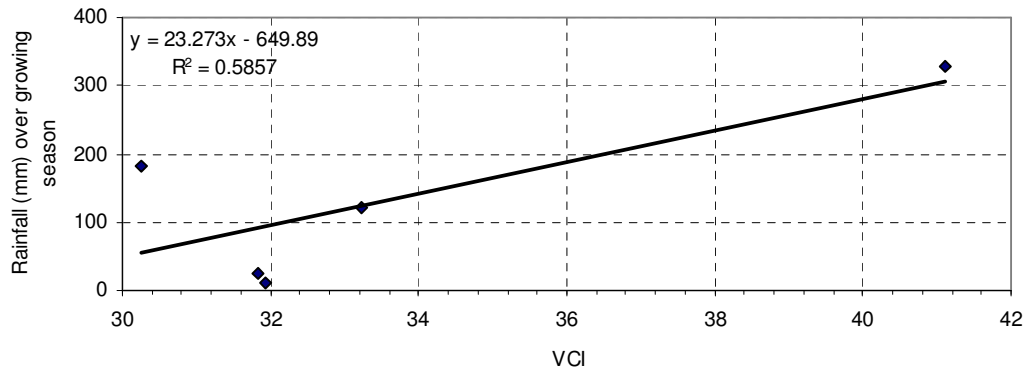

West Gojam

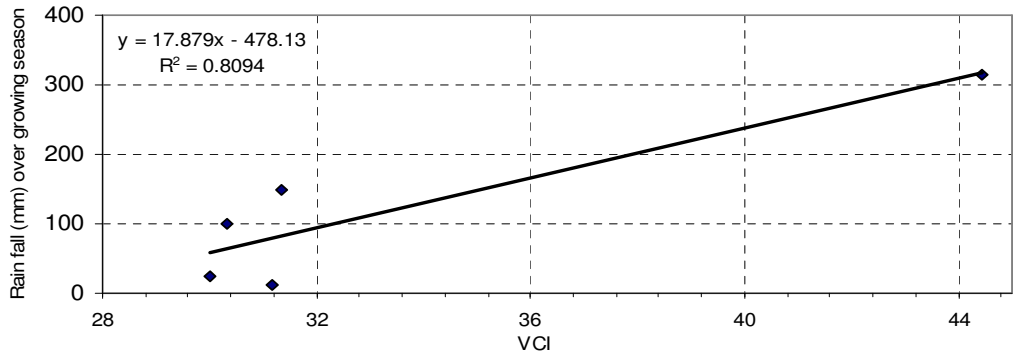

East Gojam

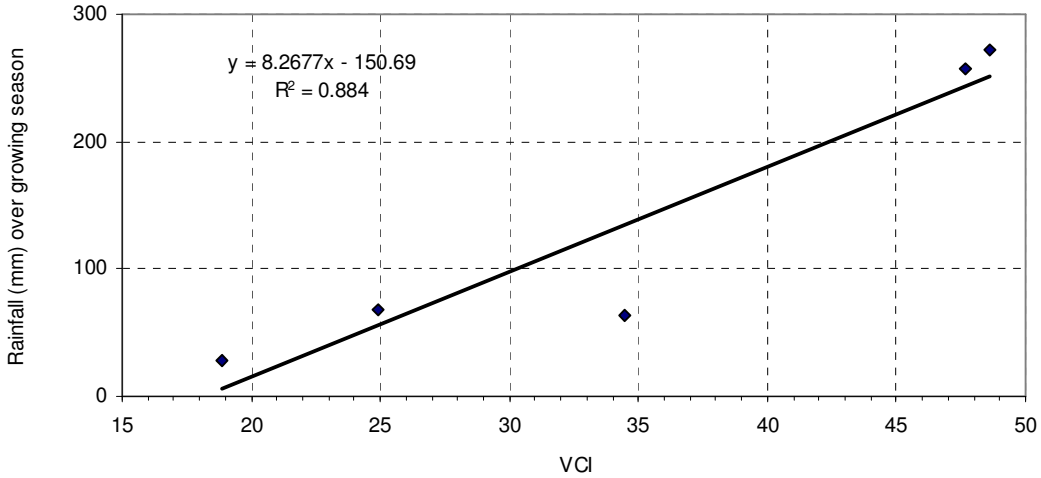

North Wollow

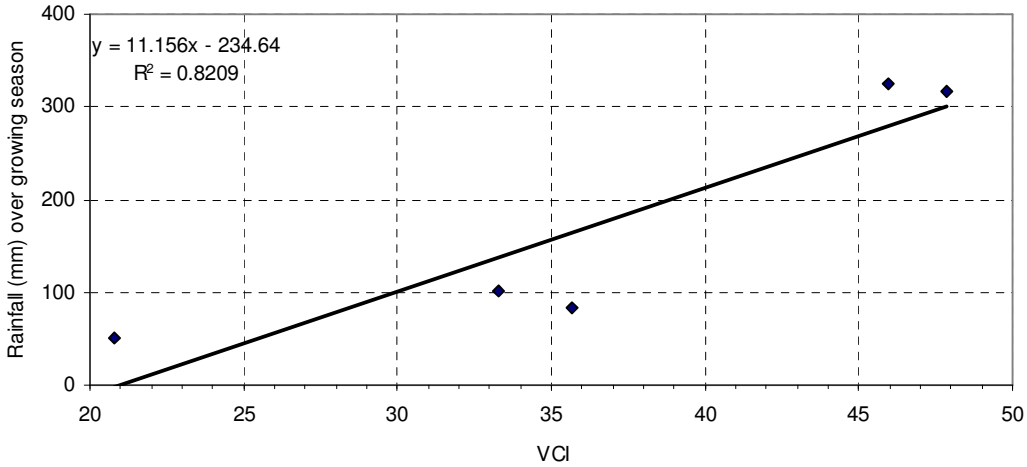

South Wollow

Appendix-E: Graphs showing correlation between TCI and precipitation

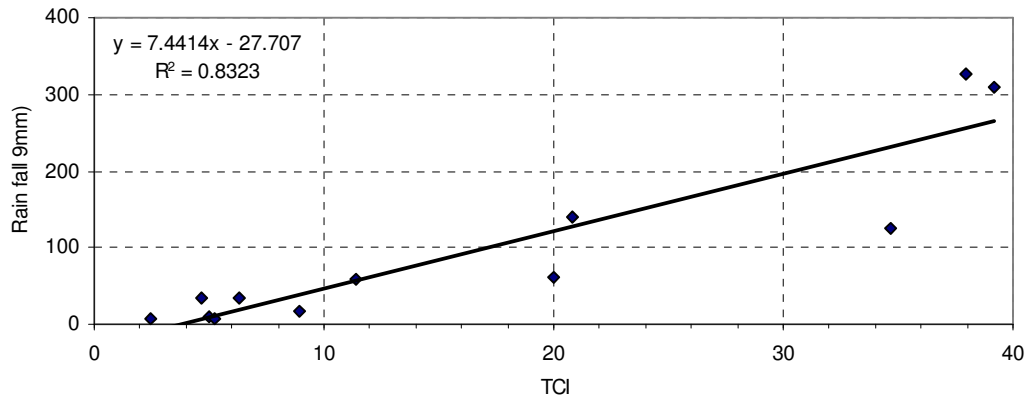

South Gondar

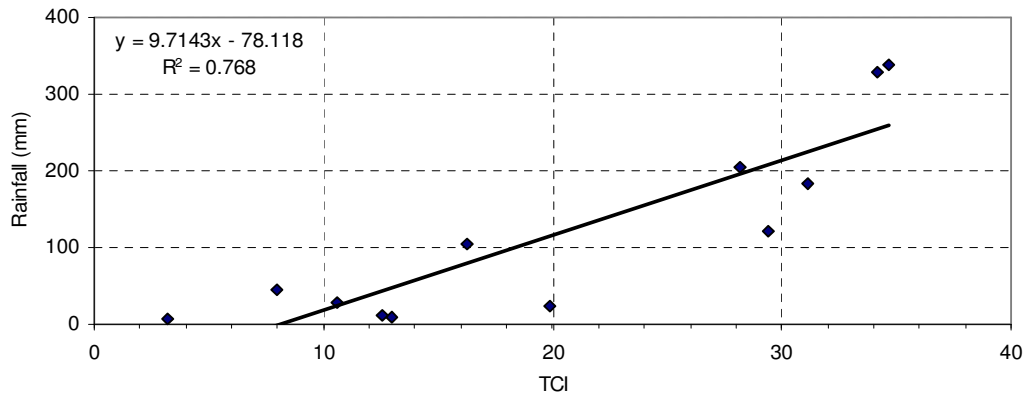

West Gojam

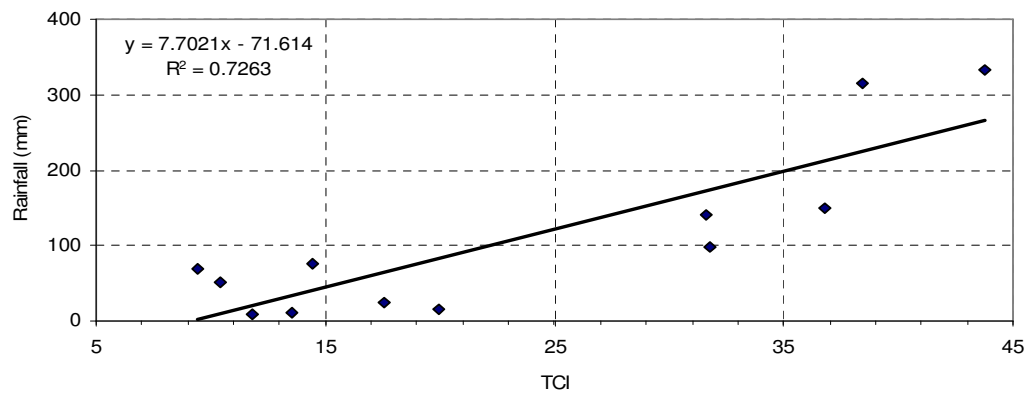

East Gojam

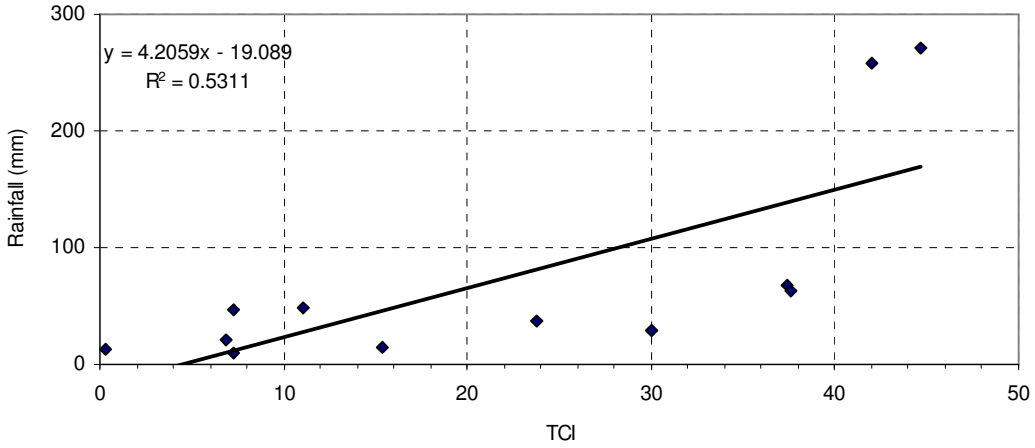

North Wollow

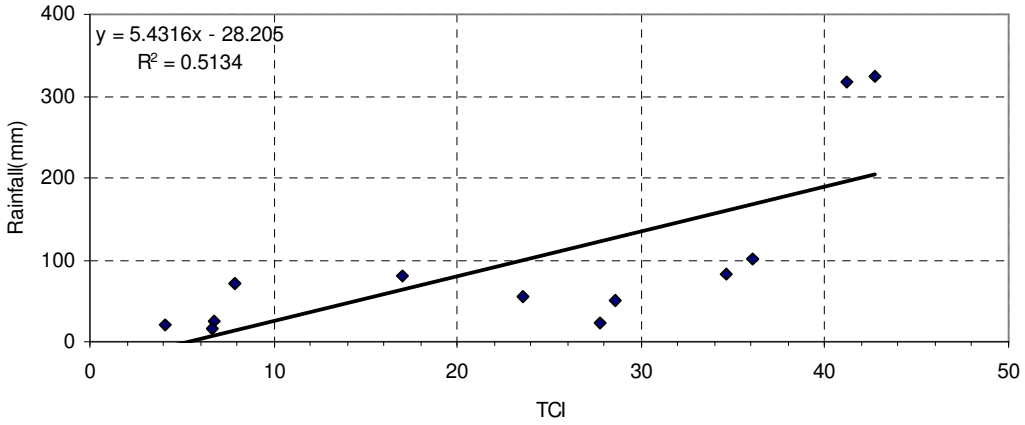

South Wollow

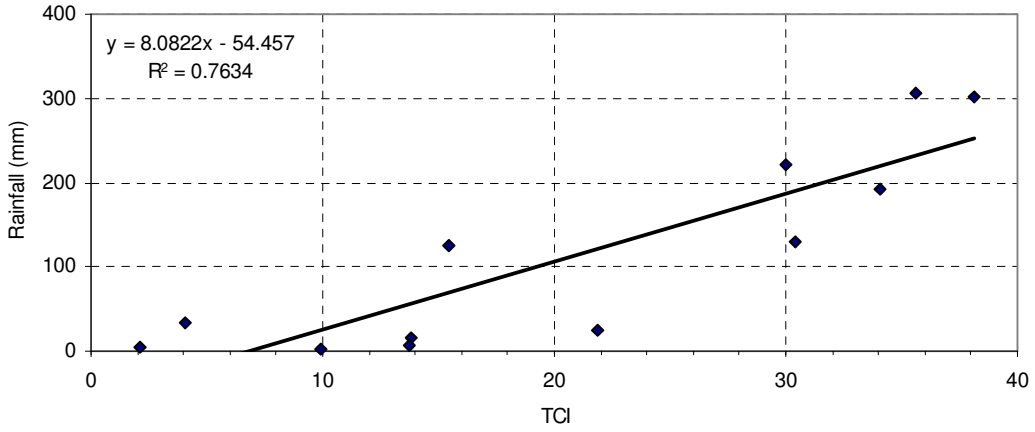

Awi

Appendix-F: Graphs showing relationship between NDVI and precipitation

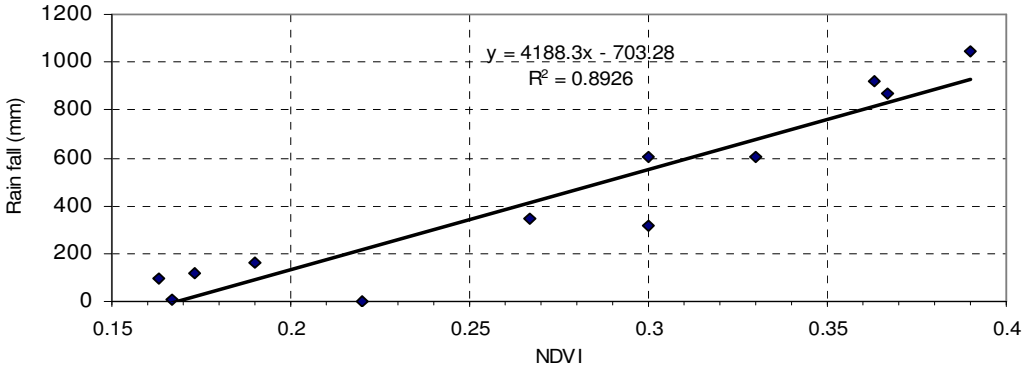

West Gojam

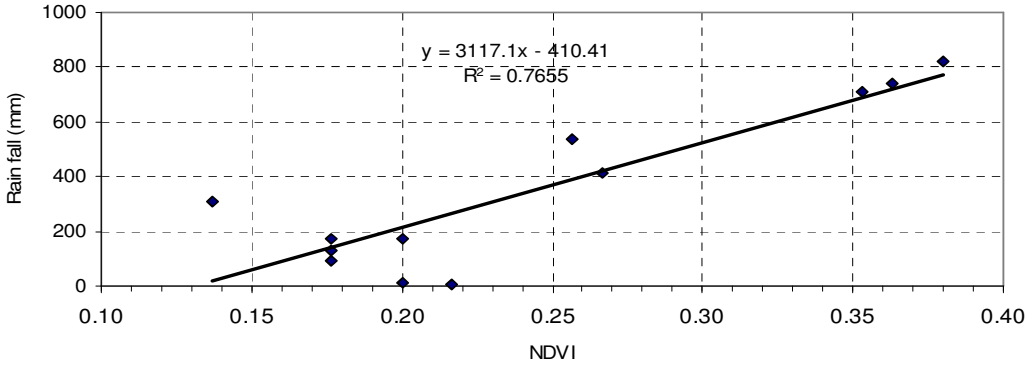

South Gondar

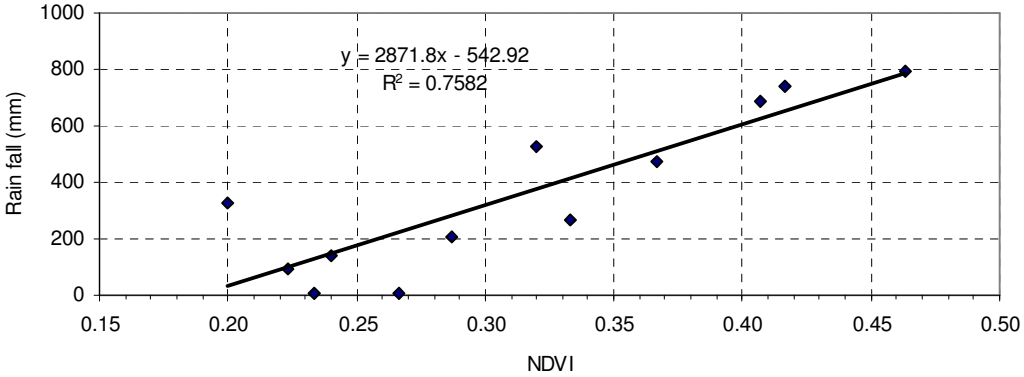

East Gojam

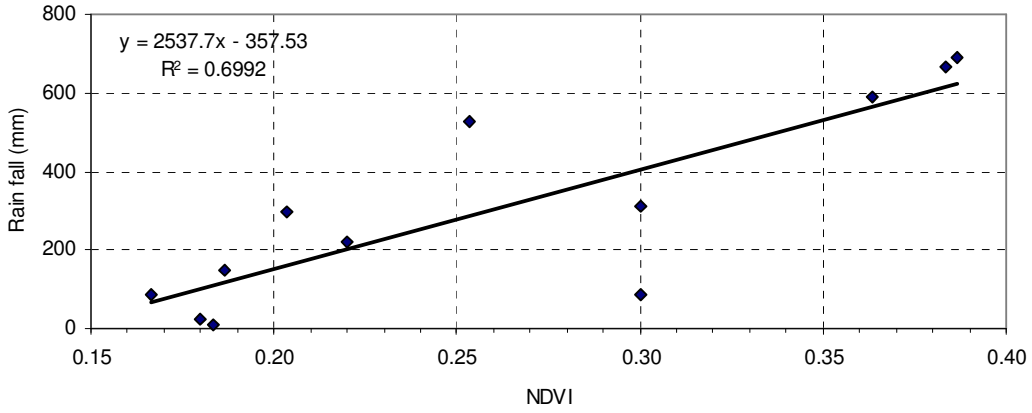

North Wollow

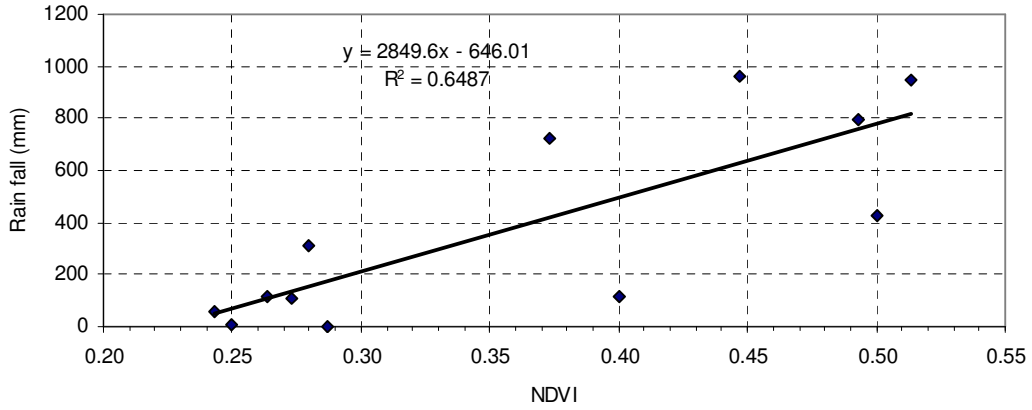

Awi

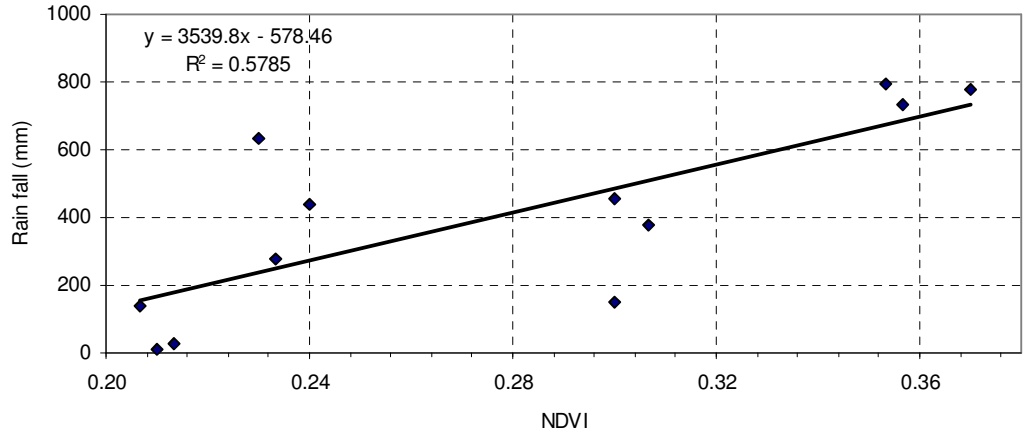

South Wollow

Appendix-G: Graphs showing relationship between NDVI and production yield

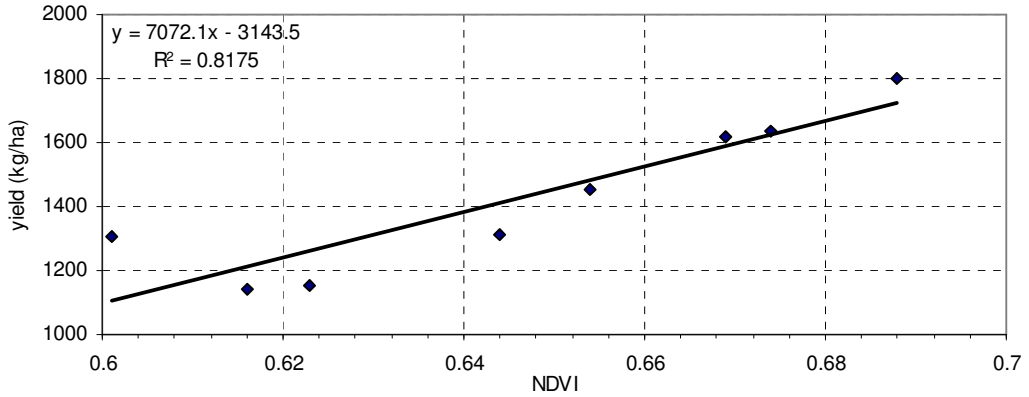

West Gojam

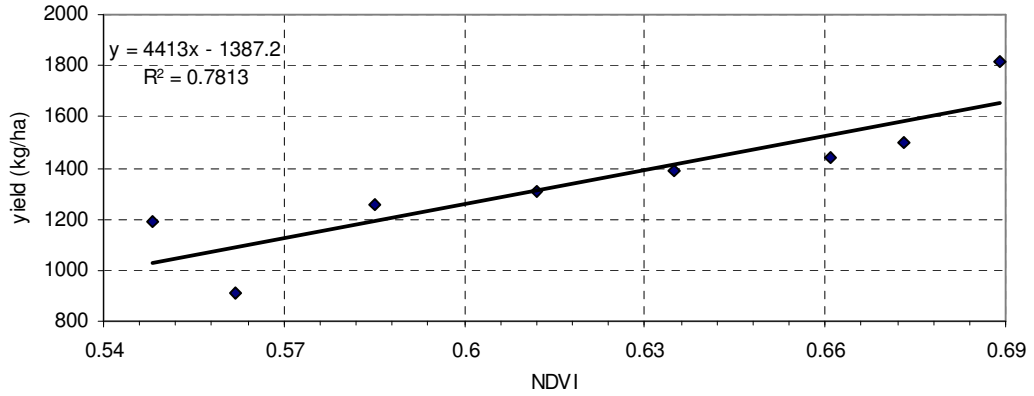

East Gojam

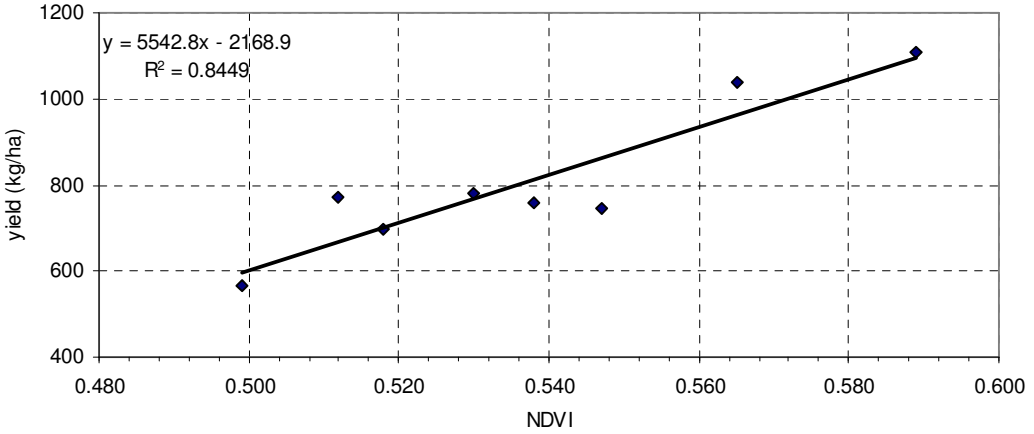

South Gondar

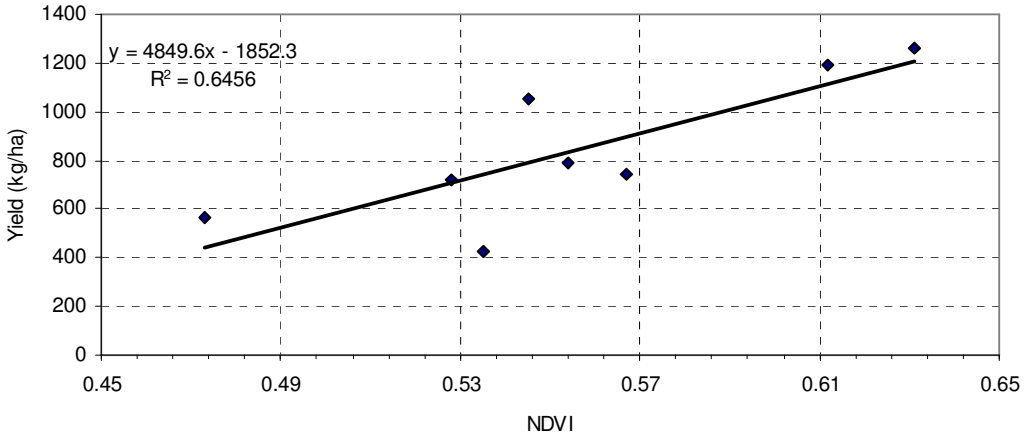

North Wollow

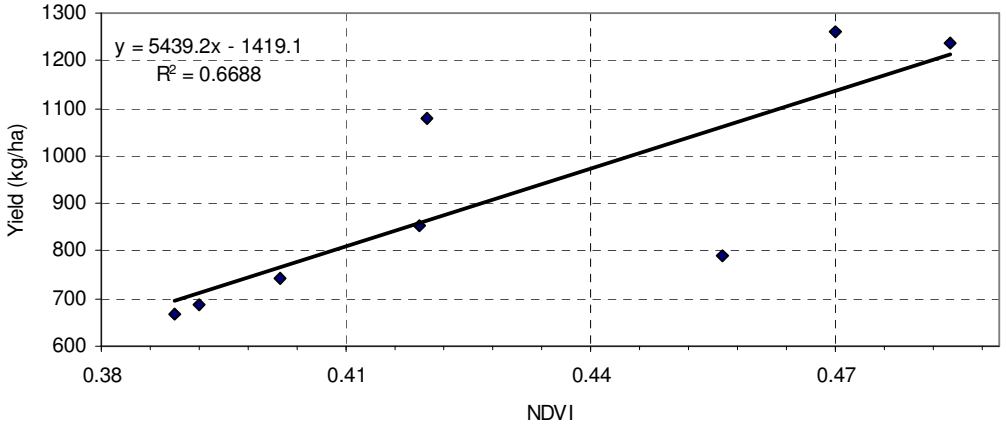

South Wollow

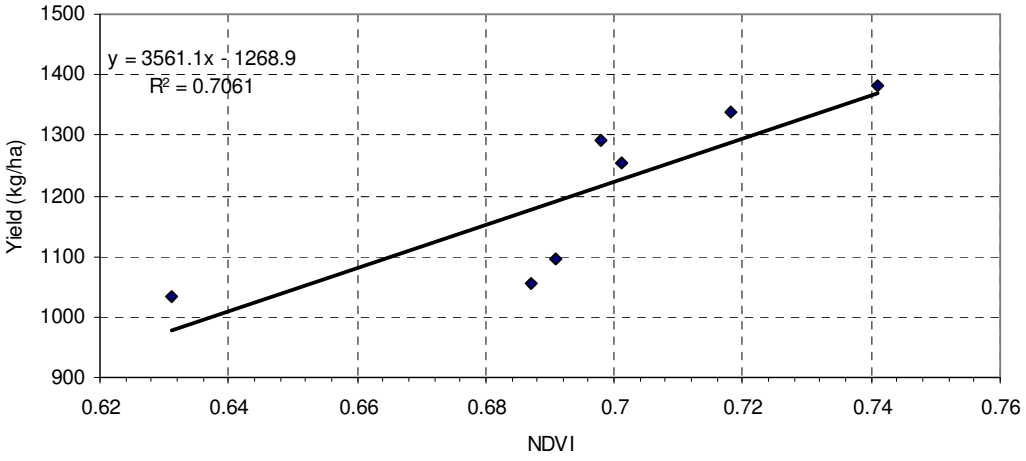

Awi